1978

Determination of nitrosamines by a photo-electrochemical method

Bobby G. Snider
Iowa State University

7813247

SNIDER, BOBBY G.
DETERMINATION OF NITROSAMINES BY A PHOTO-ELECTROCHEMICAL METHOD.

IOWA STATE UNIVERSITY, PH.D., 1978

Determination of nitrosamines by a photo-electrochemical method

by

Bobby G. Snider

A Dissertation Submitted to the
Graduate Faculty in Partial Fulfillment of
The Requirements for the Degree of
DOCTOR OF PHILOSOPHY

Department: Chemistry
Major: Analytical Chemistry

Approved:

Signature was redacted for privacy.

In Charge of Major Work

Signature was redacted for privacy.

For the Major Department

Signature was redacted for privacy.

For the Graduate College

Iowa State University
Ames, Iowa

1978

TABLE OF CONTENTS

LIST OF FIGURES

LIST OF TABLES

I. ELECTROCHEMICAL REDUCTION OF NITROGEN(II,III,IV)

A. Introduction

Considerable disagreement exists in the chemical literature concerning the electrochemical reaction of oxides of nitrogen(II,III,IV); namely, NO, HNO_2 and NO_2 in acidic solutions. Elucidation of these electrochemical reactions is of importance in several areas: (i) the understanding of chemical reactions occurring on absorption of nitrogen oxides in acidic solutions; (ii) the electroanalytical determination of nitrogen oxides as air pollutants (1) and (iii), as presented in this thesis, the indirect determination of nitrosamines on the basis of the photolytic decomposition of nitrosamines to produce NO_2^-.

The research described in this thesis is limited to the study of the reduction waves obtained at a platinum electrode for NO, HNO_2 and NO_2 dissolved in solutions containing 1 M to 10 M acid. Of primary interest are the chemical reactions occurring prior to the electron transfer, the electrochemical processes corresponding to the observed reduction waves and the parameters which affect the analytical sensitivity of the electroanalytical determination of NO_2^-.

B. Literature Review

1. Chemistry of nitrogen(II,III,IV)

The complexity of the chemistry of nitrogen results partly from the fact that stable compounds have been found for nitrogen in oxidation states from -3 to +5. Adding to the complexity is the fact that reaction products often cannot be predicted solely on the basis of thermodynamic considerations. William L. Jolly has summarized this fact in his text "Inorganic Chemistry of Nitrogen" (2): "... the chemical reactions of nitrogen are seldom thermodynamically controlled. ... Whenever a nitrogen compound can react to form several alternative compounds, it is quite commonly observed that the most thermodynamically stable compound does not form at all, or that several products form simultaneously." The chemistry of some nitrogen compounds is considered in this thesis. The discussions are limited to those aspects of nitrogen chemistry directly related to this research. For a more detailed discussion of nitrogen chemistry, the reader is directed to one of several scholarly works (3, 4, 5, 6, 7).

a. Chemistry of nitrogen(II) The compounds of nitrogen(II) which are of interest in this thesis are derived from the diatomic compound with oxygen. This compound, nitric oxide (NO), is a colorless gas at room temperature and has an odd number of electrons. Unlike

other compounds with an odd number of electrons, such as NO_2, NO is colorless, chemically inactive and does not dimerize in the gas phase. An explanation for the lack of dimerization is that there is no increase in the bond order resulting from dimerization. Despite the absence of dimerization in the gas phase, the dimer has been proposed as an intermediate in chemical (8) and electrochemical reactions (9) in aqueous solvents.

Nitric oxide is not readily reduced; the standard reduction potential is -0.30 V vs. NHE. However, stannous ion (Sn^{2+}) does reduce NO to hydroxylamine (NH_2OH) and N_2. Stannite ion ($HSnO_2^-$) reduces NO to hyponitrite ion ($N_2O_2^{2-}$) in alkaline media (10).

Disproportionation of NO occurs in concentrated acids and at a variety of surfaces. Topol, Oldham and Adler (11) studied the disproportionation of NO in concentrated sulfuric acid. The NO disproportionates according to Equation I.1. Despite the large equilibrium constant for

$$4NO + 2H^+ \rightleftarrows 2NO^+ + N_2O + H_2O;\ K = 2 \times 10^{50} \qquad (I.1)$$

the reaction, the reaction does not reach equilibrium even after several days. The reaction is heterogeneous in nature, being dependent upon the area of the gas-liquid interface. Chien-Chung and Lunsford (12) adsorbed NO on various zeolites and detected N_2O_2, NO, NO^+ and NO^- at the surface by infrared spectroscopy. Kasai and Bishop (13) found that

NO^+ and NO_2^- are produced when NO was allowed to interact with Linde Type Y zeolites. Swartz and Youssefi (14) noted that NO dissociatively adsorbs on Ni and the products NO_3^-, NO_2^-, N_2 and NO were found by X-ray photoelectron spectroscopy.

b. Chemistry of nitrogen(III) Oxygen compounds of nitrogen(III) can exist in a variety of ionic and molecular forms in acidic solutions depending upon acid activity, water activity and the anions present. Nitrite ion (NO_2^-), nitrous acid (HNO_2), nitrosonium ion (NO^+), nitrous acidium ion ($H_2NO_2^+$), nitrosyl salts (XNO, where X represents the associated anion) and dinitrogen trioxide (N_2O_3) are the species of nitrogen(III) which are commonly known. Nitrite anion is produced from the dissociation of the weak acid HNO_2 (pK_a = 3.4) and is not present in solutions with an acid concentration greater than 0.1 M. The chemical reactions which interrelate the formation of these N(III) species are shown in Equation I.2. The $H_2NO_2^+$ ion

$$\begin{array}{ccccc} & & NO_2^- + H^+ \rightleftarrows HNO_2 & & \\ & & \uparrow\downarrow{\scriptstyle +H^+ \atop -H_2O} & & \\ H^+ + N_2O_3 & \underset{}{\overset{+HNO_2}{\rightleftharpoons}} & NO^+ & \overset{+H_2O}{\rightleftharpoons} & H_2NO_2^+ \\ \downarrow{\scriptstyle H_2O} & & \uparrow\downarrow{\scriptstyle X^-} & & \\ 2HNO_2 & & XNO & & \end{array} \qquad \text{(I.2)}$$

is important as an intermediate in chemical reactions (15) but does not exist in any significant concentration (16). The fraction of nitrogen(III) existing as N_2O_3 ($X_{N_2O_3}$) is given in Figure I.1 for an analytical concentration of 10^{-3} M for nitrogen(III) and does not exist at any significant concentration for concentrations of nitrogen(III) below 10^{-3} M. The fraction of nitrogen(III) not existing as HNO_2 is considered to be $X_{NO^+ + XNO}$ and is shown in Figure I.1 as a function of acid concentration for $HClO_4$ (16). The values shown in Figure I.1 for $X_{NO^+} + XNO$ and $X_{N_2O_3}$ were determined or calculated from data obtained spectroscopically (16, 17). Although not shown in Figure I.1, the fraction of nitrogen(III) existing as HNO_2 (X_{HNO_2}) is $1-X_{NO^+} + XNO$ for any acid concentration shown in Figure I.1. Thus, the predominant nitrogen(III) species is HNO_2 for concentrations of $HClO_4$ below 7 M, and the predominant species are NO^+ and XNO at concentrations of $HClO_4$ larger than 8 M.

The existence of NO^+ in acidic solutions was confirmed by UV-VIS and Raman spectra. Raman lines attributable to NO^+ increase in intensity as the $HClO_4$ concentration is increased from 6.5 M to 9.0 M (18, 19). In this same range of acid concentration, an absorption peak ($\lambda_m \approx 250$ nm) increases in absorbance, and a set of absorption bands (330 nm to 390 nm) due to HNO_2 decreases in absorbance (16).

Figure I.1. Correlation of various parameters with acid concentration

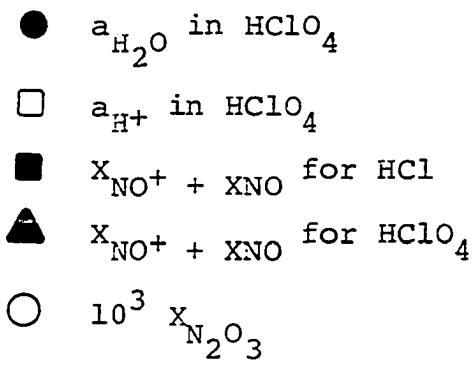

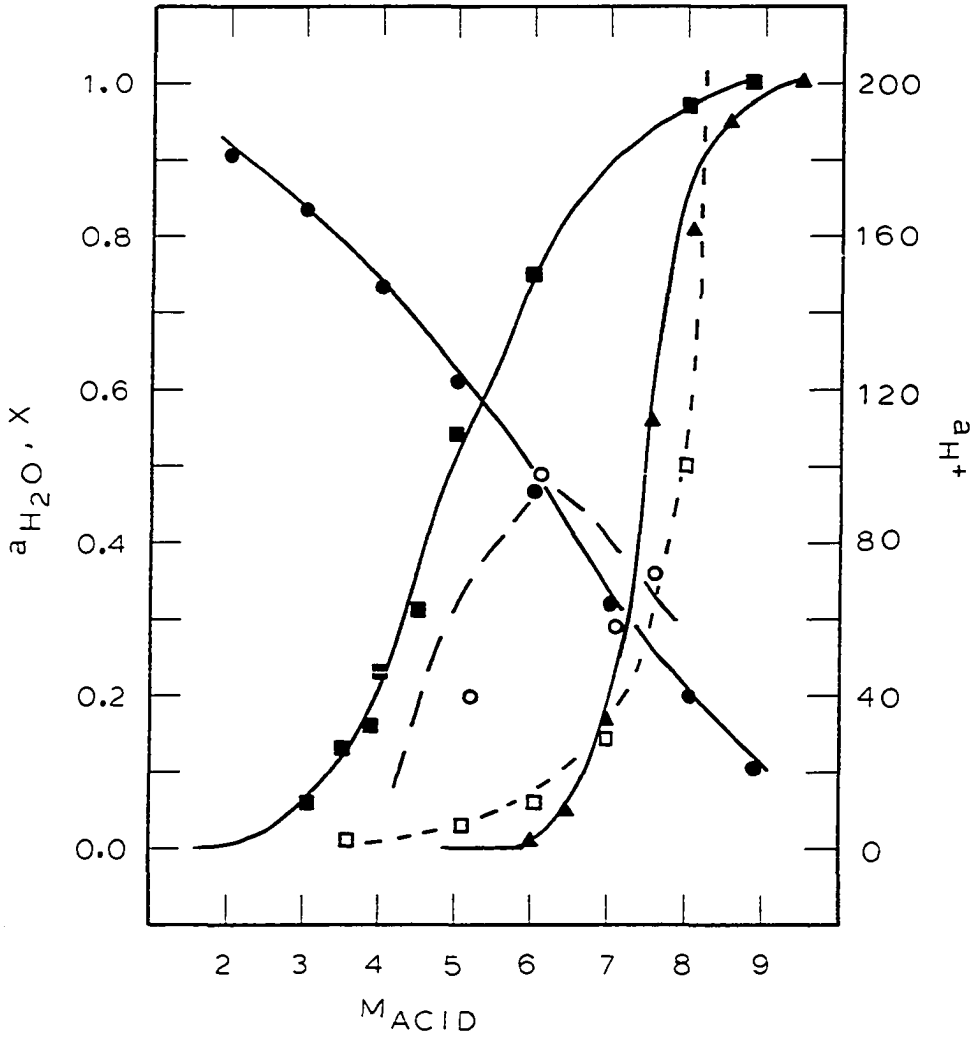
1.0
0.8
0.6
0.4
0.2
0.0
a_{H_2O}, X
200
160
120
80
40
0
a_{H^+}
2
3
4
5
6
7
8
9
M_{ACID}

Nitrous acid is best regarded as the hydroxylated form of NO^+. Other nucleophiles can replace OH^- to give compounds of the type XNO, referred to as nitrosyl compounds, as depicted in Equation I.3.

$$HNO_2 + HX \rightleftarrows XNO + H_2O \qquad (I.3)$$

$$K = [XNO]a_{H_2O}/[HNO_2]a_{HX} \qquad (I.4)$$

In Equation I.4:

a_{H_2O} = activity of water

a_{HX} = activity of acid

Equilibrium constants for Equation I.3 are given for various anions in Table I.1 (20). The calculated equilibrium

Table I.1. Equilibrium constants for Equation I.3

X	XNO	$K_{calc'd}$	$K_{exp't}$
ClO_4^-	NO^+	7×10^{-5}	2×10^{-7}
HSO_4^-	$NOHSO_4$	9×10^{-6}	3×10^{-5}
NO_3^-	N_2O_4	4×10^{-5}	3×10^{-3}
Cl^-	ClNO	6×10^{-4}	1×10^{-3}
Br^-	BrNO	9×10^{-2}	5×10^{-2}
NO_2^-	N_2O_3	18	---

constants were evaluated from thermodynamic considerations. High acid activity and low water activity promote the formation of the nitrosyl compounds. The correlation between the activity of acid and the concentration of NO^+ is shown

in Figure I.1. The change in acid activity (21) is larger than the change in water activity (22) for an increase in acid concentration. Hence, the acid activity is the predominant cause for the increase in the NO^+ concentration at higher acid concentrations. Thus, $X_{NO^+} + XNO$ for HCl (23) is larger than $X_{NO^+} + XNO$ for $HClO_4$ as shown in Figure I.1 because of the larger formation constant for ClNO.

Solutions of HNO_2 decompose at a rate dependent on several factors. The decomposition is often stated as occurring according to Equation I.5. Several researchers

$$3HNO_2 \rightleftarrows HNO_3 + 2NO + H_2O \qquad (I.5)$$

have reported that the rate of the decomposition depends on the rate of solution agitation (24, 25). Kobayaski, Nobutsune, Hara, Niki and Kitano (24) have proposed that the rate of decomposition is controlled by the rate of diffusion of HNO_2 to the liquid-gas interface in quiescent solutions. Several researchers have determined that the rate of decomposition of HNO_2 is at a maximum when the acid concentration is 7 M (16, 25, 26). At this concentration of acid, both HNO_2 and NO^+ exist in significant concentrations as is seen in Figure I.1. Bayliss and Watts (25) have proposed the reactions given by Equations I.6-I.9 as a mechanism of the decomposition of HNO_2.

$$HNO_2 + H^+ \rightleftarrows H_2NO_2^+ \quad (I.6)$$

$$H_2NO_2^+ \rightleftarrows NO^+ + H_2O \quad (I.7)$$

$$NO^+ + HNO_2 \rightleftarrows N_2O_3 + H^+ \quad (I.8)$$

$$2N_2O_3 \rightleftarrows 2NO_2 + 2NO$$
$$\downarrow H_2O$$
$$\rightarrow HNO_2 + HNO_3 \quad (I.9)$$

c. Chemistry of nitrogen(IV) The principal compound of nitrogen(IV) is NO_2. Nitrogen dioxide (NO_2) dimerizes to N_2O_4 in the liquid and gas state as shown in Equation I.10 (27). The predominant species produced on dissolution

$$2NO_2 \rightleftarrows N_2O_4;\ K = 8.8\ atm^{-1} \text{ at } 25°C \quad (I.10)$$

of NO_2 in acidic solutions depends upon the concentration of the acid. Three distinct regions are observable. In solutions containing less than 6 M acid, HNO_2 and HNO_3 are the predominant species. Nitrogen dioxide is the predominant species in solutions containing 6 M to 12 M acid. Nitric acid and NO^+ are the predominant species in solutions containing 12 M to 18 M acid.

Nitrous acid and HNO_3 are produced by disproportionation of NO_2 in aqueous solutions as described by Equation I.11

$$2NO_2 + H_2O \rightleftarrows HNO_2 + HNO_3 \quad (I.11)$$

(28). The equilibrium constant for the reaction can be calculated from thermodynamic data given for the reactions in Equations I.12 and I.13 (29). The calculation is

$$N_2O_4 + 2H^+ + 2e^- \rightleftarrows 2HNO_2;\ E° = 1.07 \qquad (I.12)$$

$$HNO_3 + 2H^+ + 2e^- \rightleftarrows NO_2 + H_2O;\ E° = 0.803 \qquad (I.13)$$

summarized by Equations I.14-I.16. Because of the large value of K given in Equation I.16, the reaction of NO_2

$$Rx_{I.11} = Rx_{I.12} - Rx_{I.13} \qquad (I.14)$$

$$K = 10^{\{(+n_{I.12}FE°_{I.12} - n_{I.13}FE°_{I.13})/RT\}} \qquad (I.15)$$

$$K = 10^{8.93} \qquad (I.16)$$

with water is expected to proceed quantitatively. If a large concentration of HNO_2 is produced, significant decomposition of the HNO_2 occurs as described by Equations I.6-I.9. The series of reactions is reviewed by Equations I.17-I.19, and Equation I.20 describes the net reaction.

$$2(2NO_2 + H_2O \rightleftarrows HNO_2 + HNO_3) \qquad (I.17)$$

$$2HNO_2 \rightleftarrows N_2O_3 + H_2O \qquad (I.18)$$

$$N_2O_3 \rightleftarrows NO + NO_2 \qquad (I.19)$$

$$3NO_2 + H_2O \rightleftarrows 2HNO_3 + NO \qquad (I.20)$$

The predominant nitrogen(III) species is NO^+ in $HClO_4$ greater than 7 M in acid concentration. Hence, the reaction of NO_2 with H_2O changes from that of Equation I.11 to that of Equation I.21 (22, 29). The equilibrium constant for

$$2NO_2 + H^+ \rightleftarrows NO^+ + HNO_3 \qquad (I.21)$$

the reaction in Equation I.21 is calculated from

thermodynamic data given for Equations I.22-I.24. The calculation is summarized in Equations I.25-I.27. Because of

$$HNO_2 + H^+ \rightleftarrows NO^+ + H_2O;\ K = 2 \times 10^{-7} \quad \text{(I.22)}$$

$$2HNO_3 + 2H^+ + 2e^- \rightleftarrows N_2O_4 + 2H_2O;\ E° = 0.803 \quad \text{(I.23)}$$

$$N_2O_4 + 2H^+ + 2e^- \rightleftarrows 2HNO_2;\ E° = 1.07 \quad \text{(I.24)}$$

$$Rx_{I.21} = Rx_{I.24} + 2Rx_{I.22} - Rx_{I.23} \quad \text{(I.25)}$$

$$\log K_{I.21} = [n_{I.24}F(E°_{I.24} - E°_{I.23}) + (2)\ 2.3RT \log K_{I.22}]/RT \quad \text{(I.26)}$$

$$K = 3.5 \times 10^{-5} \quad \text{(I.27)}$$

the small value of the equilibrium constant for the reaction in Equation I.21, the predominant species is NO_2 for acid concentrations from 6 M to 12 M. However, the high activity of the acid promotes the formation of NO^+ and HNO_3 for acid concentrations in the range 12 M to 18 M, and NO^+ and HNO_3 are the predominant species in concentrated HNO_3 and H_2SO_4 (30). The equilibrium constant in Equation I.26 is given for solutions of $HClO_4$. The equilibrium constant for solutions of other acids is obtained by substituting the appropriate equilibrium constant from Table I.1 in Equation I.22.

2. Electrochemistry of nitrogen(II,III,IV)

The emphasis of this review is on the electrochemistry of N(II,III,IV) at Pt electrodes in acidic media with acid

concentrations greater than 0.01 M. Electrochemical studies reported in the literature for conditions different than this are not discussed.

Bianchi, Mussini and Traini investigated the electrochemistry of NO, HNO_2, N_2O_4 and N_2O_5 at a Pt electrode in H_2SO_4 (31). The electrochemical reactions were observed to depend on the concentration of the H_2SO_4, the stability of the NO^+ and the presence of other nitrogen oxides. The electrochemical reactions, the corresponding values of E° and the range of acid concentration involved are summarized in Table I.2. The identification by Bianchi, et al., of

Table I.2. Electrochemical reactions proposed by Bianchi, et al. (31)

Electrochemical Reaction	E° (V vs. NHE)	Range of Concentration	
$2NO + 2H^+ + 2e^- \rightleftarrows H_2N_2O_2$	0.700	H_2SO_4 < 73%	(I.28)
$HNO_2 + H^+ + e \rightleftarrows NO + H_2O$	0.990	H_2SO_4 < 73%	(I.29)
$NO^+ + e^- \rightleftarrows NO$	0.990	H_2SO_4 > 73%	(I.30)
$N_2O_4 + 2H^+ + 2e^- \rightleftarrows 2HNO_2$	1.09	H_2SO_4 < 73%	(I.31)
$N_2O_4 + 2H^+ + 2e^- \rightleftarrows 2NO^+ + 2H_2O$	1.27	H_2SO_4 > 73%	(I.32)
$N_2O_5 + 2H^+ + 2e^- \rightleftarrows N_2O_4 + H_2O$	1.58	H_2SO_4 > 73%	(I.33)

products from electrode reactions was based on thermodynamic considerations rather than direct chemical evidence.

Mussini and Casarini (32) performed additional studies on the electrochemistry of NO, NO^+, HNO_2 and N_2O_4 at a Pt

electrode in H_2SO_4. The potential of a Pt electrode in a solution of NO and H_2SO_4 was observed to be independent of the concentration of H_2SO_4. With a mixture of N_2O_3 and N_2O_4 in H_2SO_4, the electrode potential increased as the concentration of the H_2SO_4 was increased from 58% to 73%. This observation was concluded to result from the hydrolysis reaction given by Equation I.34. Electrochemical reactions

$$NO^+ + H_2O \rightleftarrows HNO_2 + H^+ \qquad (I.34)$$

were proposed by Mussini and Casarini for two cases: 50% H_2SO_4, where HNO_2 is the predominant species, and 80% H_2SO_4, where NO^+ is the predominant species. The electrochemical reactions, the corresponding values of E° and the reaction orders are given in Table I.3. The reaction order, as evaluated by Mussini and Casarini, should be interpreted as the apparent value of n calculated from exhaustive electrolysis of the analyte as given in the corresponding reaction.

Topol, Osteryoung and Christie (33) investigated the electrochemistry of HNO_3, NO_2, HNO_2 and NO at a Pt electrode in concentrated H_2SO_4. They proposed that the nitronium ion (NO_2^+) is formed according to Equations I.40 and I.41 when HNO_3 and NO_2 are dissolved in concentrated H_2SO_4.

$$HNO_3 + 2H_2SO_4 \rightleftarrows NO_2^+ + H_3O^+ + 2HSO_4^- \qquad (I.40)$$

$$2NO_2 + 3H_2SO_4 \rightleftarrows NO_2^+ + NO^+ + 3HSO_4^- + H_3O^+ \qquad (I.41)$$

Table I.3. Electrochemical reactions proposed by Mussini and Casarini (32)

Electrochemical Reaction	E° V vs. NHE	Reaction Order	Concentration of H_2SO_4	
$NO + H_2O - e^- \rightleftarrows HNO_2 + H^+$	0.99	0.5	50%	(I.35)
$NO - e^- \rightleftarrows NO^+$	0.97	0.5	80%	(I.36)
$NO^+ + e^- \rightleftarrows NO$	0.97	1.0	80%	(I.37)
$N_2O_4 + 4H^+ + 2e^- \rightleftarrows 2NO^+ + 2H_2O$	1.25	0.5	80%	(I.38)
$2NO^+ + 2H_2O - 2e^- \rightleftarrows N_2O_4 + 4H^+$	1.25	1.0	80%	(I.39)

Furthermore, the dissolution of HNO_2 and NO in concentrated H_2SO_4 was proposed to result in production of NO^+ as described by Equations I.42 and I.43. The electrochemistry

$$HNO_2 + 2H_2SO_4 \rightleftarrows NO^+ + H_3O^+ + 2HSO_4^- \quad (I.42)$$

$$2NO + 5H_2SO_4 \rightleftarrows 2NO^+ + SO_2 + 2H_3O^+ + 4HSO_4^- \quad (I.43)$$

of NO_2^+ and NO^+ produced by the above reactions was investigated by Topol, et al., (33) with the technique of linear sweep cyclic voltammetry at a stationary electrode. With this technique, a current peak is observed rather than a limiting-current plateau. Topol, et al., concluded that the NO_2^+ is reduced in two steps, as described by Equations I.44 and I.45, during the negative sweep of the

$$NO_2^+ + 3H^+ + 2e^- \rightleftarrows NO^+ + H_3O^+; \; E_{p,c} = 520 \text{ mV} \text{ V vs. SCE} \quad (I.44)$$

$$NO^+ + e^- \rightleftarrows NO; \quad E_{p,c} = 280\text{-}300 \text{ mV} \quad (I.45)$$

electrode potential. During the subsequent positive sweep of electrode potential, one peak was obtained for the oxidation of NO as described by Equation I.46. The authors

$$NO - e^- \rightleftarrows NO^+; \; E_{p,a} = 345\text{-}370 \text{ mV} \quad (I.46)$$

state that NO_2^+ is not necessarily reduced directly to NO^+ as described by Equation I.44. Alternately, NO_2^+ could be reduced to NO_2 which disproportionates to NO_2^+ and NO^+ as outlined in Equations I.47-I.49. Because the NO produced

$$2(N(V) + e^- \rightleftarrows N(IV)) \quad (I.47)$$

$$2N(IV) \rightleftarrows N(V) + N(III) \quad (I.48)$$

$$N(III) + e^- \rightleftarrows N(II) \quad (I.49)$$

by the reduction of NO^+ can react with H_2SO_4 according to Equation I.43 to produce more NO^+, the electrocatalytic reduction of NO^+ is possible. This electrocatalytic reduction was not observed, and the rate of the reaction in Equation I.43 was concluded by Topol, et al., (33) to be very slow. Production of NO^+ from NO also occurs as described by Equation I.50 (11). This reaction is hetero-

$$4NO + 3H_2SO_4 \rightleftarrows 2NO^+ + N_2O + H_3O^+ + 3HSO_4^- \quad (I.50)$$

geneous in nature as it was observed to depend upon the area of the liquid-gas interface.

Schmid and Neumann (34) measured the potential of the HNO_2-NO couple at a Pt electrode. The potential was determined to be dependent upon the activities of H^+, HNO_2 and NO as predicted by the Nernst Equation. The resulting relationship for the HNO_2-NO couple is given here in Equation I.52.

$$HNO_2 + H^+ + e^- \rightleftarrows NO + H_2O \quad (I.51)$$

$$E = E^\circ + 2.3 \frac{RT}{F} \log \frac{a_{HNO_2}\, a_{H^+}}{a_{NO}\, a_{H_2O}} \; ; \; E^\circ = 0.986 \text{ V vs. NHE} \quad (I.52)$$

Schmid and Lobeck (35) investigated the reduction of HNO_2 in the presence of HNO_3 at a Pt electrode in 1 M to 7 M

H_2SO_4. One anodic wave corresponding to a 2-electron process was observed, and HNO_3 was concluded to be the product. Three cathodic waves (1-,2- and 4-electron processes) were observed, and NO, N_2O and NH_2OH were concluded to be the products of the respective waves. No chemical evidence was given to confirm the identity of the products.

Savodnik, Shepelin and Zalkind (36) investigated the reduction of NO at a Pt electrode in 3.0 N H_2SO_4. Two reduction waves and two oxidation waves were observed. For the first reduction wave, NO was quantitatively reduced to N_2O as determined by gas chromatography. The authors concluded that NO was reduced as described by Equation I.53.

$$2NO + 2H^+ + 2e^- \rightleftarrows N_2O + H_2O \qquad (I.53)$$

Data was not given to evaluate the yield of the conversion. The second reduction wave was concluded to result from the formation of NH_2OH according to Equation I.54. The NH_2OH was determined by an amperometric method.

$$NO + 3H^+ + 3e^- \rightleftarrows NH_2OH \qquad (I.54)$$

Heckner and Schmid (37) studied the reduction of HNO_2 at a Pt electrode in 2 M to 9 M $HClO_4$. Nitrosonium ion was concluded to be the electroactive species formed by a prior chemical reaction as described by Equation I.55. The

$$HNO_2 + H^+ \rightleftarrows NO^+ + H_2O \qquad (I.55)$$

electrode current for 2 M to 5 M $HClO_4$ was kinetically limited, and the current for 6 M to 9 M $HClO_4$ was diffusion controlled. More complicated mechanisms were proposed to explain the effect of decomposition of the HNO_2 on the observed electrochemistry.

Dutta and Landolt (38) investigated the electrochemistry of HNO_2, NO and N_2O at a Pt electrode in 4.0 M H_2SO_4. Oxidation and reduction waves were observed for both HNO_2 and NO. Two waves for the oxidation of NO were observed, and the products were concluded to be HNO_2 and NO_2. Two reduction waves were observed for NO. Three reduction waves were observed for HNO_2. The two waves for the reduction of NO were concluded to correspond with the second and third waves for the reduction of HNO_2. However, the figures supplied in the publication were of such quality that the verification of the above statement is impossible. The authors also concluded that NO was an intermediate product of the reduction of HNO_2 to NH_2OH.

Garcia, Calandra and Arvia (39) studied the reduction of NO^+ at Pt and Au electrodes in concentrated H_2SO_4. Nitrosonium ion was reversibly reduced to NO at both Pt and Au electrodes. The state of oxidation of the Pt surface affected the reduction of NO^+ with the reduction becoming less reversible as the state of oxidation increased.

Heckner (28) investigated the reduction of HNO_2 in the presence of HNO_3 at a Pt electrode in $HClO_4$. The studies were performed to elucidate the mechanism of the reduction of HNO_3 in the dissolution of metals as shown in Equations I.56-I.60. The author concluded that nitrosonium ion oxidizes the metal producing NO according to Equation I.57. The N_2O_4, produced from the reaction of HNO_2 with HNO_3 according to Equation I.59, reacts with NO to produce more HNO_2 according to Equation I.59. The HNO_2 is then converted to NO^+ as described by Equation I.56.

$$2X(HNO_2 + H^+ \rightleftarrows NO^+ + H_2O) \qquad (I.56)$$

$$2X(NO^+ + e^- \rightleftarrows NO) \qquad (I.57)$$

$$HNO_2 + HNO_3 \rightleftarrows N_2O_4 + H_2O \qquad (I.58)$$

$$2NO + N_2O_4 + 2H_2O \rightleftarrows 4HNO_2 \qquad (I.59)$$

$$HNO_3 + 2H^+ + 2e^- \rightleftarrows HNO_2 + H_2O \qquad (I.60)$$

Gadde and Bruckenstein (40) studied the reduction of HNO_2 at a Pt electrode in 0.10 M $HClO_4$ with electrochemical mass spectrometry. The technique of electrochemical mass spectrometry was performed with a porous electrode that allowed gaseous products of an electrochemical reaction to pass into a mass spectrometer. An oxidation wave at $E > 0.80$ V vs. SCE and a reduction wave at $E < 0.30$ V were observed. Detectable amounts of NO were produced by reduction of HNO_2 at $E = 0.50$ V. Nitrous oxide (N_2O) was

produced with a high current efficiency for 0.40 V > E > 0.30 V. The production of a mixture of NH_2OH (60.7%), N_2O (18.8%) and NH_3 (21.6%) was observed at E = -0.20 V. The presence of N_2O in the mixture of products was explained on the basis of the reaction in Equation I.61.

$$NH_2OH + HNO_2 \rightleftarrows N_2O + 2H_2O \qquad (I.61)$$

The production of NH_3 was described, in a schematic fashion, as occurring according to Equation I.62. The authors were

$$4N(-1) \rightleftarrows N_2O + 2NH_4^+ \qquad (I.62)$$

hesitant to specify the nature of the nitrogen(-1) species although NH_2OH has that oxidation state.

Janssen, Pieterse and Barendrecht (41) studied the reduction of NO at a Pt electrode in 4.0 M H_2SO_4. Nitric oxide was reduced in two waves. The first wave was described as occurring at E > -30 mV vs. SCE. The second wave was described as occurring in the potential range -50 mV > E > -250 mV. The NO was reduced to N_2O in the first wave. The products for the second wave were N_2O, NH_2OH and NH_3. The current efficiency for the electrode reaction was studied in the potential range 0 > E > -400 mV. The current efficiency for the production of N_2O was 100% for E > -30 mV and decreased in the potential range 0 > E > -400 mV. The current efficiency for the formation of NH_2OH and NH_3 reached peak values of 70% and 20%,

respectively, at E = -200 mV with the current efficiency decreasing at more negative potentials because of the evolution of H_2. The data on current efficiency and other information from the literature were used by Janssen, et al., to propose the mechanism shown in Equation I.63.

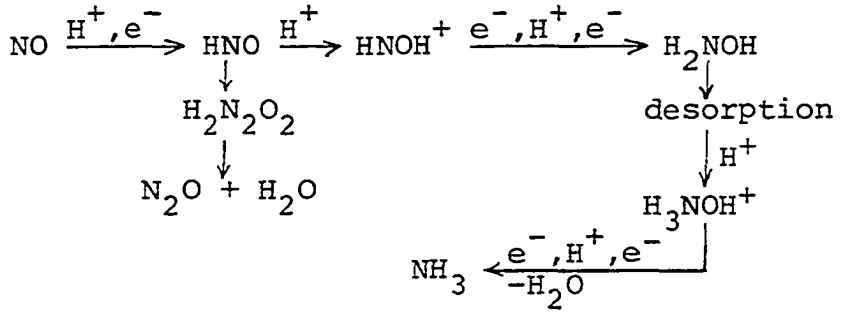

(I.63)

As an interesting coincidence, the observed efficiencies agree reasonably well with the analytical results obtained by Gadde and Bruckenstein (40) in spite of differences in the reactions proposed.

There is disagreement as to the identity of the electroactive species in the reduction of NO. Janssen, et al., (41), Savodnik, et al., (36, 42) and Dutta and Landolt (38) proposed that NO is the electroactive species. Topol, et al., (33) proposed that the electroactive species in concentrated H_2SO_4 is NO^+ produced as described by Equation I.43.

Barendrecht and van der Plas (43) investigated the reduction of HNO_2 in 7.5 M H_2SO_4 at a Pt ring-disk electrode. Three reduction waves were observed and attributed to reactions described by Equations I.64, I.65 and I.66. The

$$NO^+ + e^- \rightleftarrows NO \qquad (I.64)$$

$$2NO + 2H^+ + 2e^- \rightleftarrows 2HNO \qquad (I.65)$$

$$2HNO \rightarrow N_2O + H_2O$$

$$HNO + 3H^+ + 2e^- \rightleftarrows NH_3OH^+ \qquad (I.66)$$

HNO was proposed as the intermediate product because N_2O is a very stable compound, and solutions of N_2O were not observed to be reduced.

Direct comparison of the publications is difficult because many of the studies investigated only one electroactive species in a single electrolyte solution. However, there are several points of agreement among the proposed reactions: (i) the electroactive species for the reduction of HNO_2 in concentrated solutions of acids is NO^+. (ii) In concentrated H_2SO_4, NO^+ is the electroactive species whenever NO or HNO_2 are reduced, and NO_2^+ is the electroactive species whenever NO_2 or HNO_3 are reduced. (iii) The products of the reduction of HNO_2 are NO, N_2O, NH_2OH and NH_3. (iv) The reduction products of NO are N_2O, NH_2OH and NH_3.

Several areas remain in which further investigation is needed: (i) the nature of the electroactive species for the reduction of NO_2 and NO; (ii) the effect of halide ions on the electrochemical behavior of various nitrogen

compounds; (iii) trends in the electrochemical behavior of nitrogen compounds as a function of acid concentration; (iv) changes in the observed electrochemical reduction of HNO_2 because of slow decomposition of HNO_2 and the accumulation of decomposition products.

The results of an investigation into the electrochemical reductions of NO, HNO_2 and NO_2 at a platinum electrode in acidic solutions are reported in this thesis. Conventional electrochemical techniques were applied to deduce the nature of the electroactive species for NO and NO_2 including voltammetry at a rotating Pt-disk electrode and coulometry at a Pt flow-through electrode. Three reduction waves were observed for each of the compounds of nitrogen. The current-potential curves were virtually identical for each compound in a particular acidic solution at a given concentration of acid. This fact is concluded to result because the electroactive species for all three cases is derived from HNO_2. Nitrous acid is produced in the solutions of NO and NO_2 by disproportionation as shown in Equations I.1 and I.11. The electroactive species for the first cathodic wave in acidic solutions of HNO_2 is concluded to be NO^+ which is produced chemically at the surface of the electrode by the reaction shown in Equation I.2. Changes in the values of the half-wave potential ($E_{1/2}$) and limiting current (I_l) observed for HNO_2 as a function

of acid concentration, are ascribed to changes in the activity of H^+ and H_2O.

Addition of halide ions to solutions of 3.0 M perchloric acid containing each of the oxides of nitrogen results in the increase of the values for $E_{1/2}$ and I_l for the first cathodic wave. This catalytic activity of the halide ion is reported for the first time and is attributed to the formation of nitrosyl halides (XNO) which are also electroactive at the platinum electrode.

The effect of decomposition of the HNO_2 on the observed current-potential curves was determined. Evidence is presented to support the conclusion that the second reduction wave is the reduction of N_2O_3.

C. Experimental

1. Instrumentation and apparatus

Rotating disk electrodes (RDE) were constructed by Pine Instrument Co. of Grove City, Pennsylvania. The RDE was constructed from a disk of the electrode material soldered on the end of a stainless steel or brass shaft. A cylindrical Teflon shroud covered the electrode and shaft. The dimensions and electrode material of all disk electrodes used are given in Table I.4.

A tubular Pt electrode was constructed in the Chemistry Shop of Iowa State University. A cross-sectional diagram of the tubular Pt electrode is given in Figure I.2. The

Table I.4. Geometric parameters of rotating disk electrodes

Electrode	Material	Radius (cm)	Disk Area (cm^2)
A	platinum	0.382	0.458
B	platinum	0.237	0.177
C	gold	0.381	0.455

Pt tube was produced by drilling a hole 1 mm in diameter through the center of a 5 mm Pt rod.

A tubular Pt electrode packed with chips of Pt wire functioned as a coulometric Pt electrode. This coulometric electrode is designated Electrode C in Reference 44.

The reference electrode was a saturated calomel electrode (SCE) with a saturated solution of NaCl instead of the customary solution of KCl. The potential of this reference electrode was approximately +0.234 V vs. the normal hydrogen electrode. All experimental values of potential are given versus this reference electrode. The counter electrode was a coil of Pt wire.

The potentiostat was a Pine RDE-3 from Pine Instrument Co. Current-potential (I-E) data was recorded with an EAI Model 1130 X-Y recorder from Electronics Associates, Inc., of West Long Branch, New Jersey. Rotators for the disk electrodes were Models PIR and MSP from Pine Instrument Co. For a voltage input increasing from 0 to 10 V, the

Figure I.2. Cross-sectional diagram of a tubular platinum detector

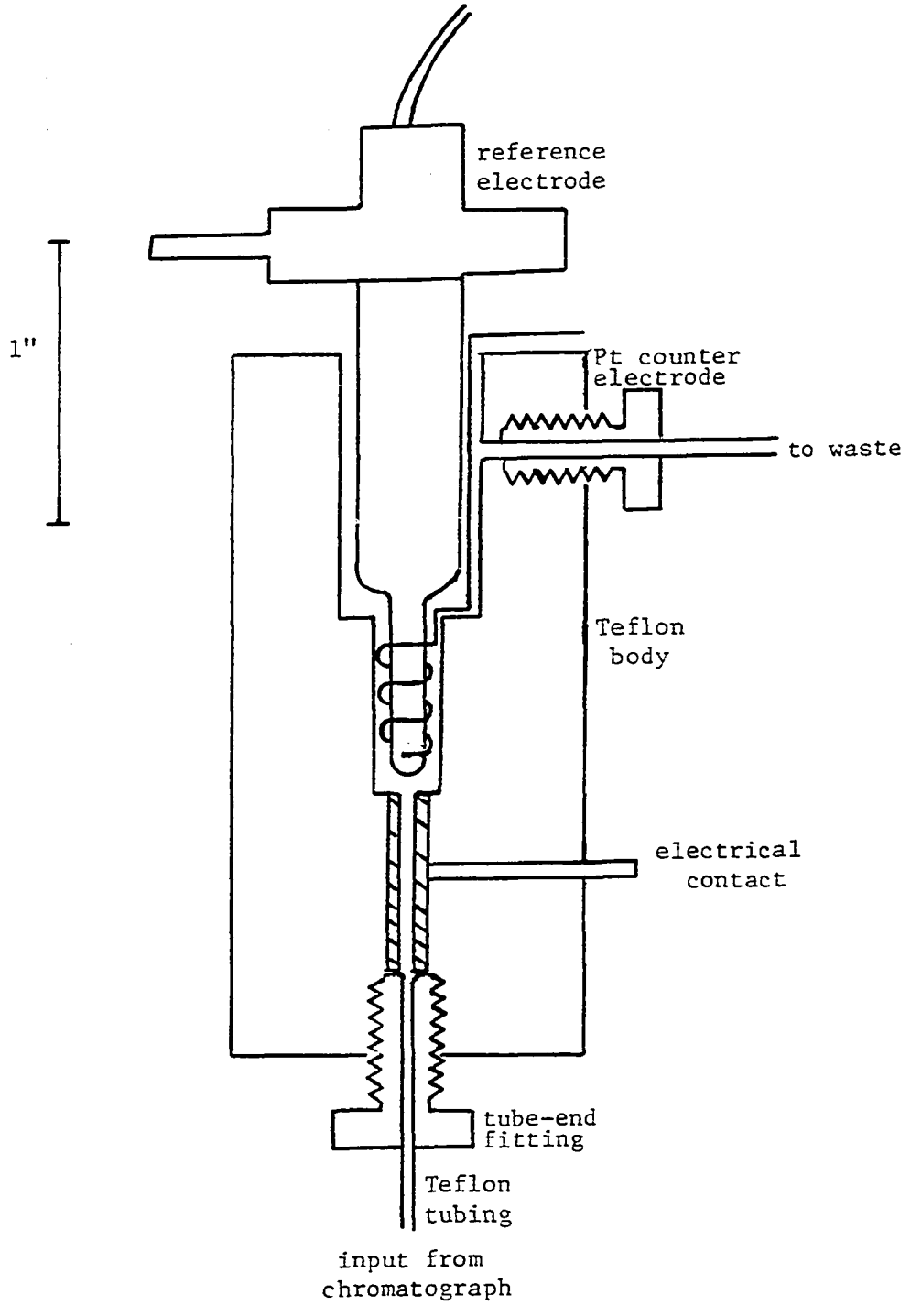
reference
electrode
1"
Pt counter
electrode
to waste
Teflon
body
electrical
contact
tube-end
fitting
Teflon
tubing
input from
chromatograph

rotation speed increased from 0 to 10,000 rev/min for the Model MSP rotator.

The electrolysis cell was constructed entirely of glass by the Chemistry Glass Shop at Iowa State University and had a capacity of 0.5 L. A double wall permitted thermostatic control of cell temperature. The auxiliary electrode was placed in a chamber isolated from the bulk of electrolyte by a glass frit with fine porosity. The reference electrode was placed in a chamber connected to a glass capillary by a ground glass stopcock. The cell was cleaned by soaking in hot H_2SO_4.

A flowanalyzer, schematically shown in Figure I.3, was constructed from Teflon tubing, Kel-F valves, glass-Teflon fittings and polypropylene fittings from Larry Bell Associates of Hopkins, Minnesota. The design of the flowanalyzer was based on the design of a liquid chromatograph given by Seymour, Sickafoose and Fritz (45) which was modified by Johnson and Larochelle (46).

Fluid flow was produced by the application of compressed He to the storage containers. The flow rate of the eluent and reagent streams was controlled with Teflon-glass valves (capillary metering type) from Roger Gilmont Instruments, Inc., of Great Neck, New York. Standard glass-Teflon connectors were attached to the valves by the Chemistry Glass Shop. Flow rates were measured with flowmeters from Roger Gilmont Instruments.

Figure I.3. Schematic diagram of the flowanalyzer

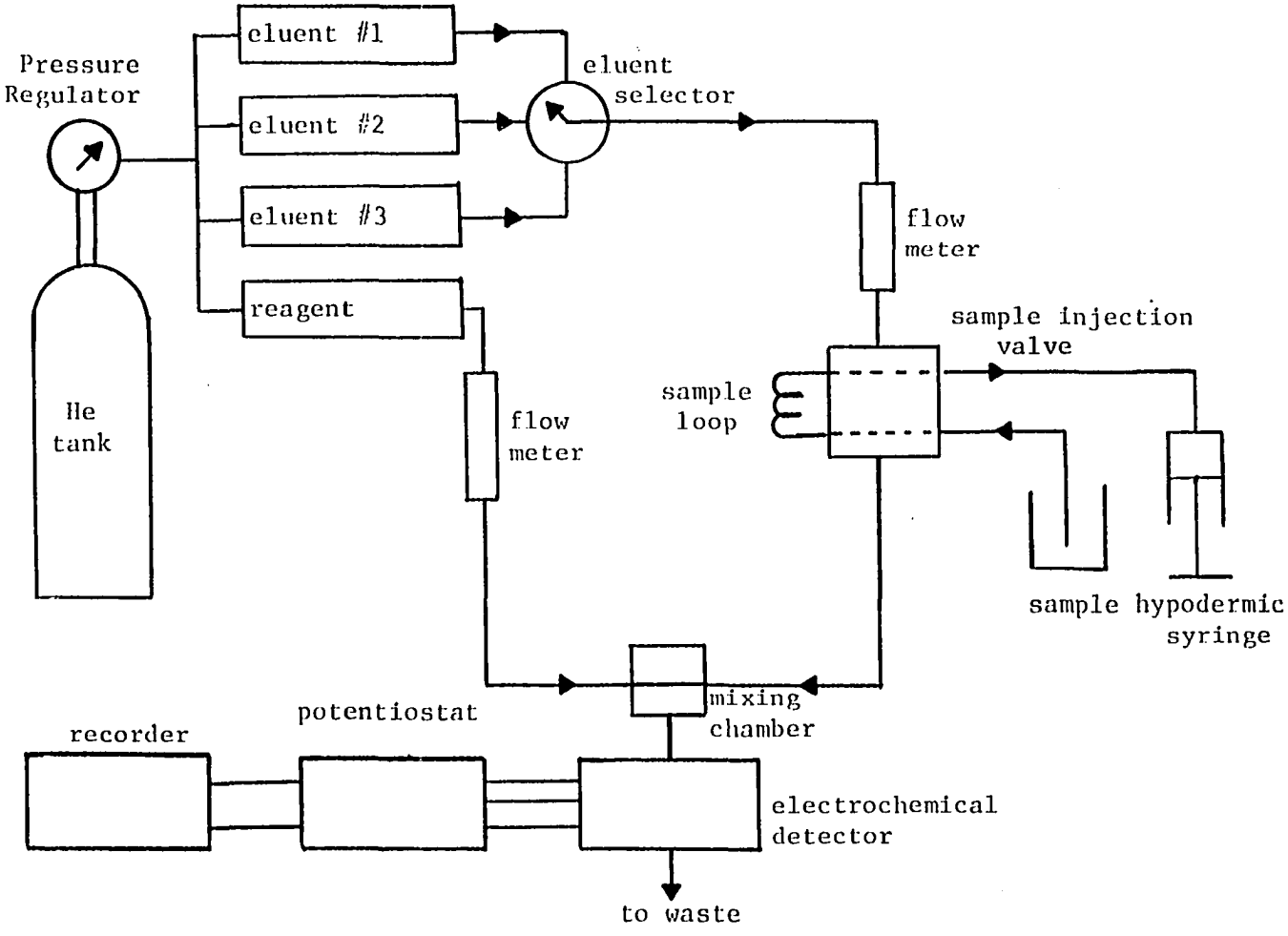
eluent #1
eluent #2
eluent #3
reagent
Pressure Regulator
He tank
eluent selector
flow meter
flow meter
sample injection valve
sample loop
sample hypodermic syringe
mixing chamber
potentiostat
recorder
electrochemical detector
to waste

The fluid flow from the sample injection valve was mixed with fluid flow from the reagent tank in a mixing chamber (Model 2MC) from Pine Instrument Co.

The procedures for calibration of sample loops, measurement of flow rates and construction of caps for the eluent reservoirs are described in Reference 44.

Prior to pressurization of containers, the solutions were deaerated with He. This procedure minimized the formation of gas bubbles in the flowanalyzer.

2. Chemicals and reagents

Solutions of supporting electrolyte were prepared from reagent grade acids from Fisher Scientific Co. of Fair Lawn, New Jersey. The water used was demineralized after distillation. A stock solution of 0.100 M $NaNO_2$ was prepared with reagent grade $NaNO_2$ from J. T. Baker Co. of Phillipsburg, New Jersey. The $NaNO_2$ was dried at 90°C for 4 hr and then stored in a desiccator. Other solutions of $NaNO_2$ were prepared by dilution of quantities of the stock solution measured with a Gilmont micrometer syringe.

The NO_2 was from Matheson Gas Products of Joliet, Illinois. Because of the large quantities of NO used in some of the experiments, the NO was chemically generated as described in Reference 47. Nitric oxide is evolved when H_2SO_4 is added to a mixture of KNO_2 and KI as shown in Equation I.67. Solutions prepared from NO produced

$$KNO_2 + KI + 2H^+ \rightleftarrows NO + 1/2\ I_2 + 2K^+ + H_2O \qquad (I.67)$$

chemically in my laboratory were indistinguishable from solutions prepared with NO obtained from Matheson Gas Products in respect to the I-E curves obtained.

Solutions of NO and NO_2 were prepared with the apparatus shown in Figure I.4. The apparatus consists of a 100-ml volumetric flask into which a Teflon plug containing two Teflon tubes was inserted. The internal diameter of the Teflon tubes was 0.031 inch, and the volume of gas retained by the Teflon tubes was small compared to the volume of gas injected into the inverted volumetric flask. A micrometer syringe with a capacity of 2.0 mL was used to deliver the gas into the volumetric flask. The second Teflon tube functioned as a vent to relieve the pressure produced by the injection of the gas. After the gas was delivered into the volumetric flask, the flask was shaken while still inverted to dissolve the gas into the electrolyte solution. A two-way Teflon valve was located between the syringe and the delivery tube to allow removal of the syringe while the flask was being shaken.

The ideal gas law, given by Equation I.68, was used to calculate the volumes of gas required to produce a solution of a given concentration.

$$PV = nRT \qquad (I.68)$$

Figure I.4. Apparatus used for preparing solutions of NO and NO_2

A Gilmont micrometer syringe

B On-off valve

C Teflon plug

D 0.031 inches I.D. Teflon tubes

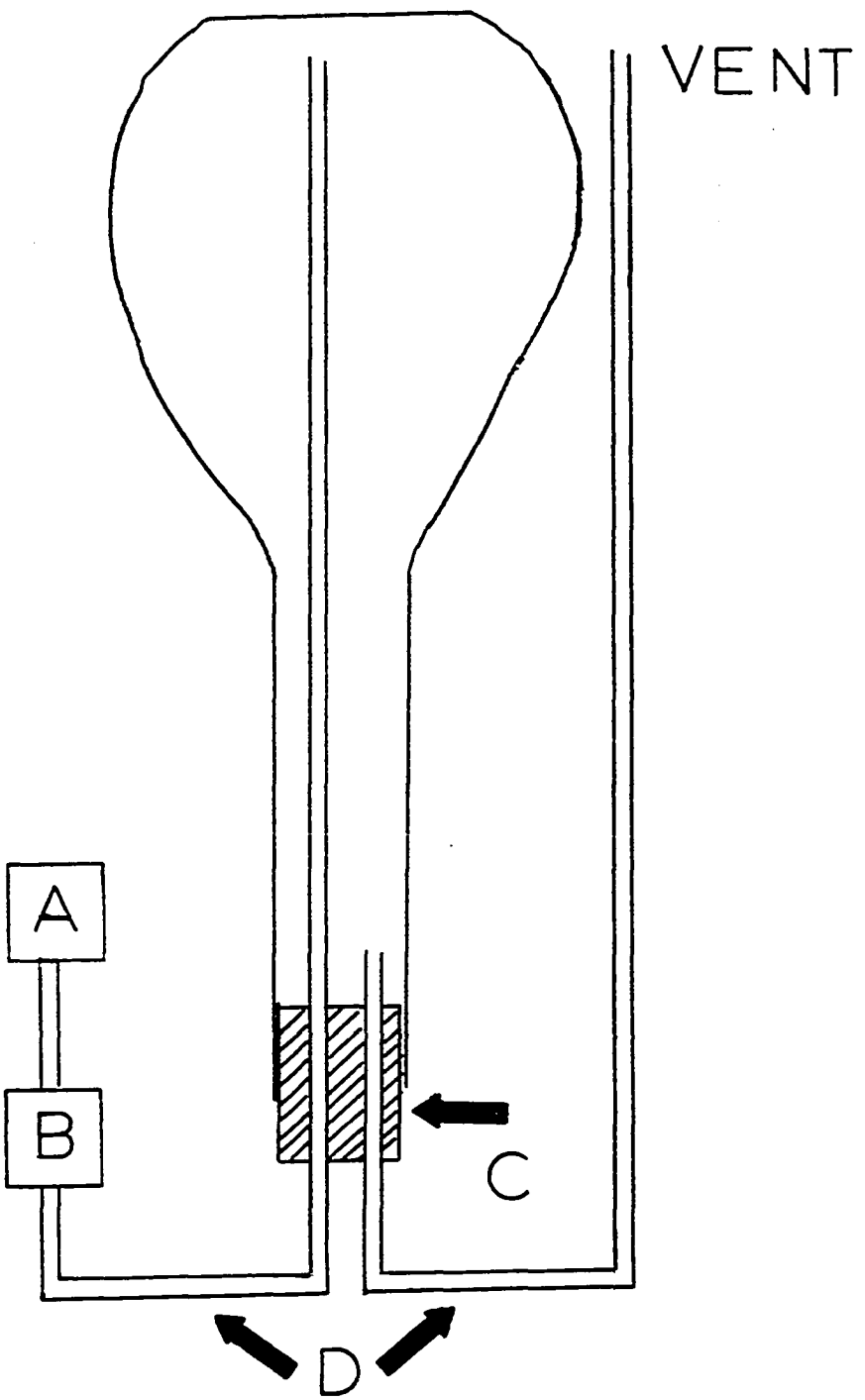
VENT
A
B
C
D

In Equation I.68: P = pressure (atm),

V = volume (L),

n = number of moles,

R = 0.0820549 (L-atm deg^{-1} $mole^{-1}$),

T = temperature (°K)

For the injection of 1.8 mL of NO into the flask containing 100 mL of liquid, a solution 7.36 x 10^{-4} M in NO was produced. The situation is more complicated for NO_2 because NO_2 is always in equilibrium with N_2O_4 as given in Equation I.10. At 25°C, the equilibrium constant for the dimerization of NO_2 is 8.8 atm^{-1} (27). The partial pressures (P) of the two species were calculated as follows:

$$P_{NO_2} + P_{N_2O_4} = 1 \qquad \text{(I.69)}$$

$$\text{let } x = P_{NO_2} \text{ then } 1 - x = P_{N_2O_4} \qquad \text{(I.70)}$$

$$K = 8.8 = P_{N_2O_4}/P^2_{NO_2} = (1 - x)/x^2 \qquad \text{(I.71)}$$

$$P_{NO_2} = x = 0.284 \qquad \text{(I.72)}$$

$$P_{N_2O_4} = 1 - x = 0.715 \qquad \text{(I.73)}$$

One liter of a gas mixture of NO_2 and N_2O_4 would be equivalent to:

$$0.284(1) + 0.715(2) = 1.72 \text{ L of pure } NO_2. \qquad \text{(I.74)}$$

3. Procedures

Data determined as a function of acid concentration were obtained by diluting the acid in the electrolysis cell with water containing the same concentration of analyte as the solution in the electrolysis cell. For electrochemical studies with NO, the solution in the electrolysis cell was maintained saturated with respect to NO. The temperature of the electrolysis cell was maintained at 22°C ± 2°C for all studies. To minimize the effect of decomposition of HNO_2 over a long time period, the data was taken 5 min after each dilution.

At the start of each series of experiments, the surface of the RDE was polished with 1 μm AB polishing alumina on a microcloth from Buchler, Ltd., of Evanston, Illinois. Water was used to lubricate the electrode during polishing and to prevent the build up of excessive heat. After polishing, the residual alumina was removed from the electrode surface with a wet cotton swab, and the electrode was rinsed with distilled water.

D. Results and Discussion

1. Voltammetry at a Pt electrode in acidic media

The current-potential (I-E) curves for NO, HNO_2 and NO_2 at a Pt electrode with $HClO_4$ as the supporting electrolyte at a concentration of 6.0 M are given in Figure I.5. Three reduction waves, denoted R^I, R^{II} and R^{III} in Figure I.5, are

Figure I.5. Current-potential curves for NO, HNO_2 and NO_2

Tubular Pt detector

1 V/min

0.80 mL/min

A 5×10^{-4} M HNO_2

B 5×10^{-4} M NO

C 5×10^{-4} M NO_2

D residual current

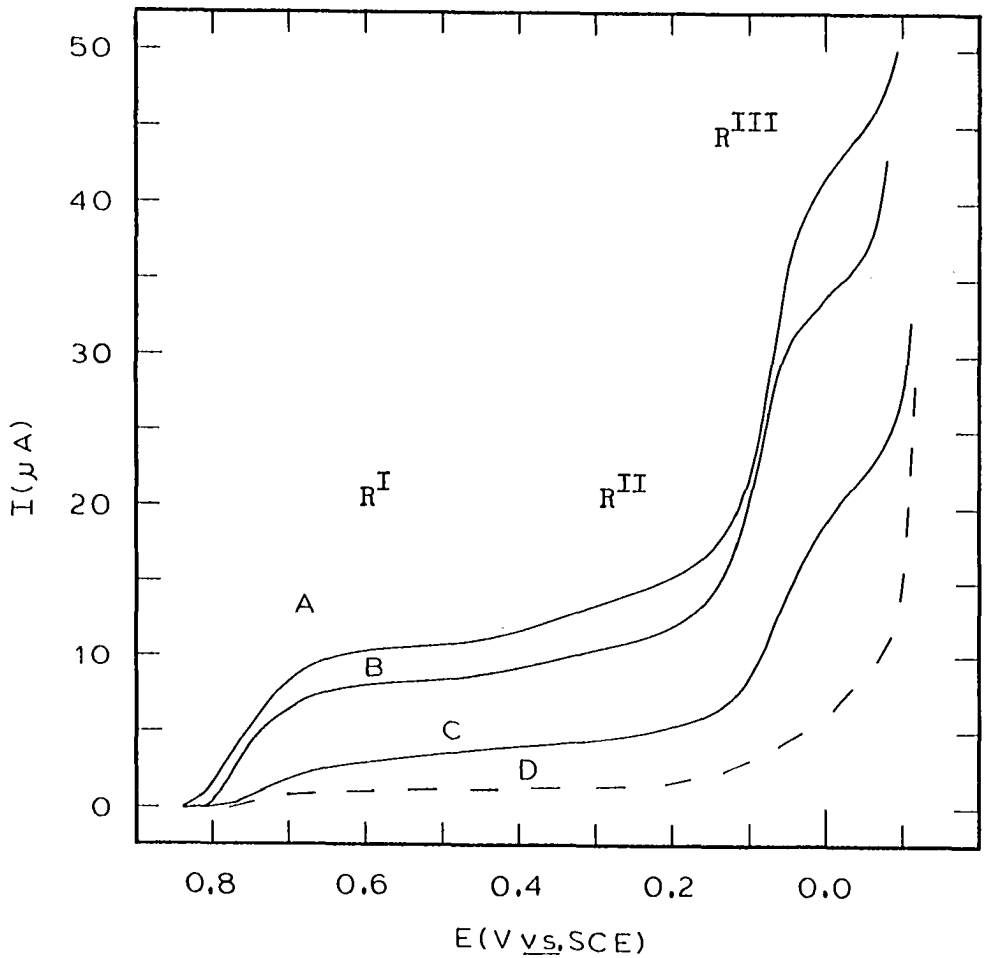
50
40
30
20
10
0
I(μA)
R^III
R^I
R^II
A
B
C
D
0.8
0.6
0.4
0.2
0.0
E(V vs. SCE)

observed for each of the three nitrogen compounds. A wave is said to be reversible in appearance if the shape of the I-E curve can be predicted from the Nernst Equation. A simple test for reversibility is given in Equation I.75 (48).

$$E_{1/3} - E_{2/3} = \frac{0.0356}{n} \qquad (I.75)$$

In Equation I.75,

$$E_{1/3} = E \text{ at } I = 1/3\ I_l$$

and

$$E_{2/3} = E \text{ at } I = 2/3\ I_l$$

where I_l is the limiting value of I. The use of Equation I.75 for wave R^I reveals that $E_{1/3} - E_{2/3}$ equals 0.0353 for each of the three nitrogen compounds. Wave R^I is concluded to be a reversible, one-electron reduction. The $E_{1/2}$ values are 760, 750 and 756 mV in 6.0 M $HClO_4$ for NO, HNO_2 and NO_2, respectively. In 6.0 M $HClO_4$, the $E_{1/2}$ for wave R^{II} is 0.32 V for each of the three compounds. Although wave R^{II} is not clearly evident in Figure I.5, wave R^{II} is clearly shown in Figure I.16. The $E_{1/2}$ for wave R^{III} in 6.0 M $HClO_4$ is approximately 0.10 V. The value of I_l for wave R^{III} is approximately four times that for R^I indicating that waves R^I and R^{III} are 1- and 4-electron reductions, respectively.

The explanation of the similarity of the I-E curves for NO, HNO_2 and NO_2 is based on the similarity of chemical

reactions prior to electron transfer. The chemical reaction of NO_2 with water to produce HNO_2 and HNO_3 and the disproportionation reaction of NO to produce HNO_2 and N_2O are discussed in Section I.B.1. These chemical reactions show that HNO_2 is present whenever NO, HNO_2 or NO_2 are dissolved in acidic media. The observation that the values of limiting current for NO_2 and NO are smaller than that of HNO_2 is consistent with the chemical reactions given by Equations I.1 and I.11. Only one-half of the NO_2 or NO can be converted to HNO_2, and the point of equilibrium is controlled by the acidity of the media. Because the reduction waves for NO, HNO_2 and NO_2 are similar, HNO_2 was concluded to be produced from chemical reactions for all three compounds, and the electroactive species was concluded to be derived from HNO_2. Additional data to support this conclusion is given in succeeding sections.

Experimental results support the conclusion that wave R^{II} is the reduction of N_2O_3. When sufficient $NaNO_2$ was added to 6.0 M $HClO_4$ so that NO and NO_2 were evolved, the solution turned blue in color indicating the presence of N_2O_3 (49). Current-potential curves, shown in Figure I.16, were recorded for such a solution. The ratio of the current for R^{II} divided by the current for R^{I} was larger in solutions in which the blue color existed. The concentration of N_2O_3 is negligible in solutions having

an analytical concentration of N(III) below 10^{-3} M (see Section I.B.1). Wave R^{II} also appeared larger, as compared to R^{I}, in solutions where significant decomposition of HNO_2 had occurred. For instance, in solutions of HNO_2 in 6.0 M $HClO_4$ which had been heated to approximately 60°C and then cooled to 20°C, wave R^{II} was larger, as compared to R^{I}, than before the heat treatment. Wave R^{II} also became larger with time as the HNO_2 was allowed to remain in concentrated acid solutions. The initial product of the decomposition of HNO_2 is N_2O_3 (see Section I.B.1). In the preceding cases where the concentration of N_2O_3 had been deliberately increased, the current for wave R^{II} had increased. Further evidence to support the conclusion that process R^{II} is the reduction of N_2O_3 is given in Section I.D.4.

The conclusion that the disproportionation of NO, according to Equation I.76, occurs in the region of the

$$4NO + 2H^+ \rightleftarrows 2NO^+ + N_2O + H_2O \qquad (I.76)$$

electrode-solution is supported by experimental results. The continuous bubbling of NO into an acidic solution should result in a continuous increase in the observed electrochemical current if the disproportionation reaction is occurring in the bulk of the solution because NO^+ and N_2O are both more soluble than NO. However, this prediction

was not observed. Studies by Topol, et al., (11) of the rate of disproportionation of NO support the conclusion that the reaction in Equation I.76 is slow and does not reach equilibrium even after several days. They also report that the reaction given by Equation I.76 is heterogeneous in nature because the rate was observed to depend upon the area of the gas-liquid interface. The observation that NO is not reduced at a Au electrode, while reversible reduction waves are obtained for HNO_2 and NO_2 at a Au electrode, has been made both in this research and by others (1, 39). A reduction wave for NO would be observed at a Au electrode if the disproportionation reaction to produce the electroactive species was occurring at a significant rate in the bulk of the solution. The disproportionation reaction might possibly occur at the electrode surface via the dimer. The dimer then reacts with H^+ as described by the reaction in Equation I.77.

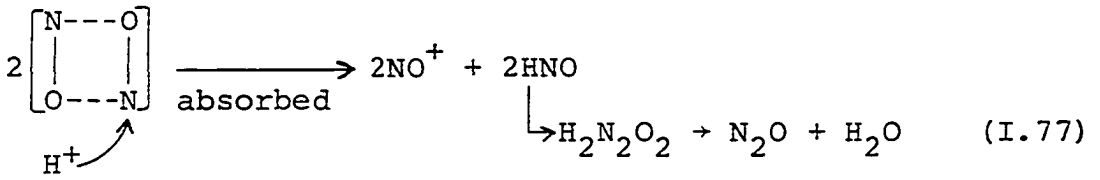

(I.77)

Perhaps, this NO dimer does not form at the Au surface, and thus, no electrochemical reduction waves are noted when Au is the working electrode.

2. Dependence of electrochemistry on concentration of acid and halide ion

The electrochemistry of nitrogen(II,III,IV) depends upon acid concentration and the presence of various anions, e.g., Cl^- and Br^-. Changes in $E_{1/2}$ and I_l values observed for changes in solution conditions can be used to deduce the nature of the electrode reactions. Mechanistic interpretations based on measurements of $E_{1/2}$ and I_l are easily made only for reversible I-E waves. Wave R^{II} is irreversible except under special conditions discussed later (Section I.D.4). Values of $E_{1/2}$ and I_l for wave R^{III} cannot be determined accurately because of the high background currents resulting from the reduction of H^+. Consequently, values of $E_{1/2}$ and I_l are given here only for wave R^I.

The limiting current (I_l) for an electroactive species is a function of the viscosity of the solution as presented in the Appendix. So that values of I_l measured under conditions resulting in extreme changes of viscosity could be compared to ascertain certain chemical dependencies, the measured values of I_l were recalculated to correspond to a solution with the viscosity of water. Details of the calculation are given in the Appendix. To further aid in the comparisons, the recalculated values were also normalized by division with the maximum value of I_l

observed for variation of a particular chemical entity. Hence, all normalized values of I_l ($I_{l,n}$) are in the range 0 to 1. Values of $I_{l,n}$ are shown in Figures I.6-I.8 as a function of acid concentration for NO, HNO_2 and NO_2 in solutions of $HClO_4$, HCl and $HClO_4$ containing 0.05 M Br^-, respectively. The average values of $I_{l,n}$ for the three nitrogen compounds are shown plotted in Figure I.9 for the sake of comparison. Values of $E_{1/2}$ for NO, HNO_2 and NO_2 were plotted in Figure I.10 as a function of acid concentration for the three cases.

The values of $I_{l,n}$ for all three nitrogen compounds in $HClO_4$ increased rapidly for increasing acid concentration in the range 4 M to 7 M. This corresponds approximately to the range of acid concentrations in which $X_{NO^+} + XNO$ becomes significant in $HClO_4$ as shown in Figure I.1. The formation constant for ClO_4NO is very small, and I conclude that NO^+ is the electroactive species for solutions of NO, HNO_2 and NO_2 in $HClO_4$. This conclusion is in agreement with the literature reviewed in Section I.B.2. The enhancement of $I_{l,n}$, resulting from increased acid activity in $HClO_4$, is the result of promotion of the chemical reactions summarized by Equations I.78-I.80 for

$$2NO \overset{+H^+}{\rightleftharpoons} NO^+ + 1/2N_2O + 1/2H_2O$$
$$\Big\downarrow +e^- \rightarrow NO \qquad \text{(I.78)}$$

Figure I.6. Values of $I_{1,n}$ for NO, HNO_2 and NO_2 in $HClO_4$

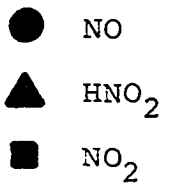

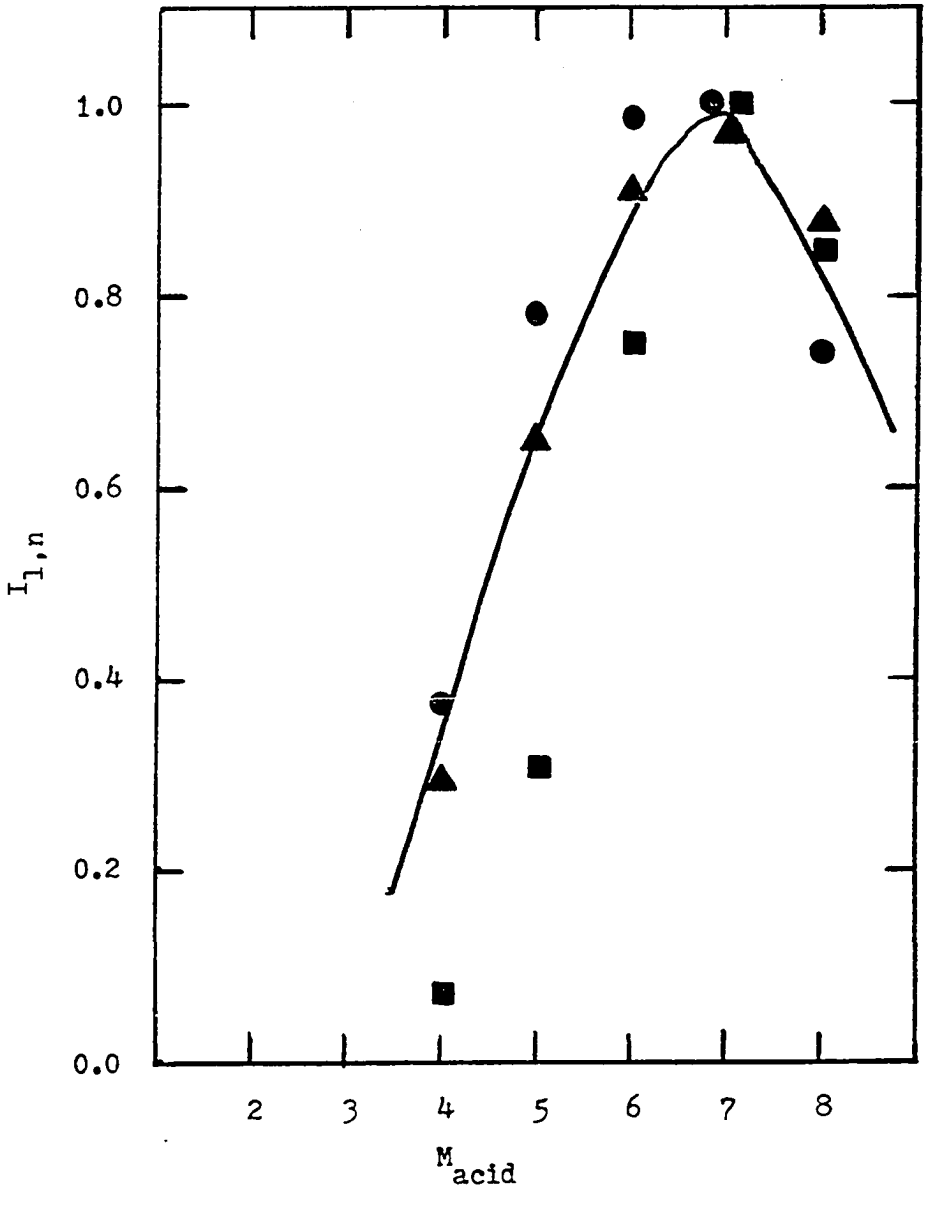
1.0
0.8
0.6
0.4
0.2
0.0
$I_{1,n}$
2
3
4
5
6
7
8
M_{acid}

Figure I.7. Values of $I_{l,n}$ for NO, HNO_2 and NO_2 in HCl

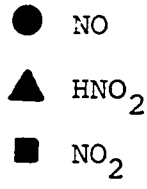

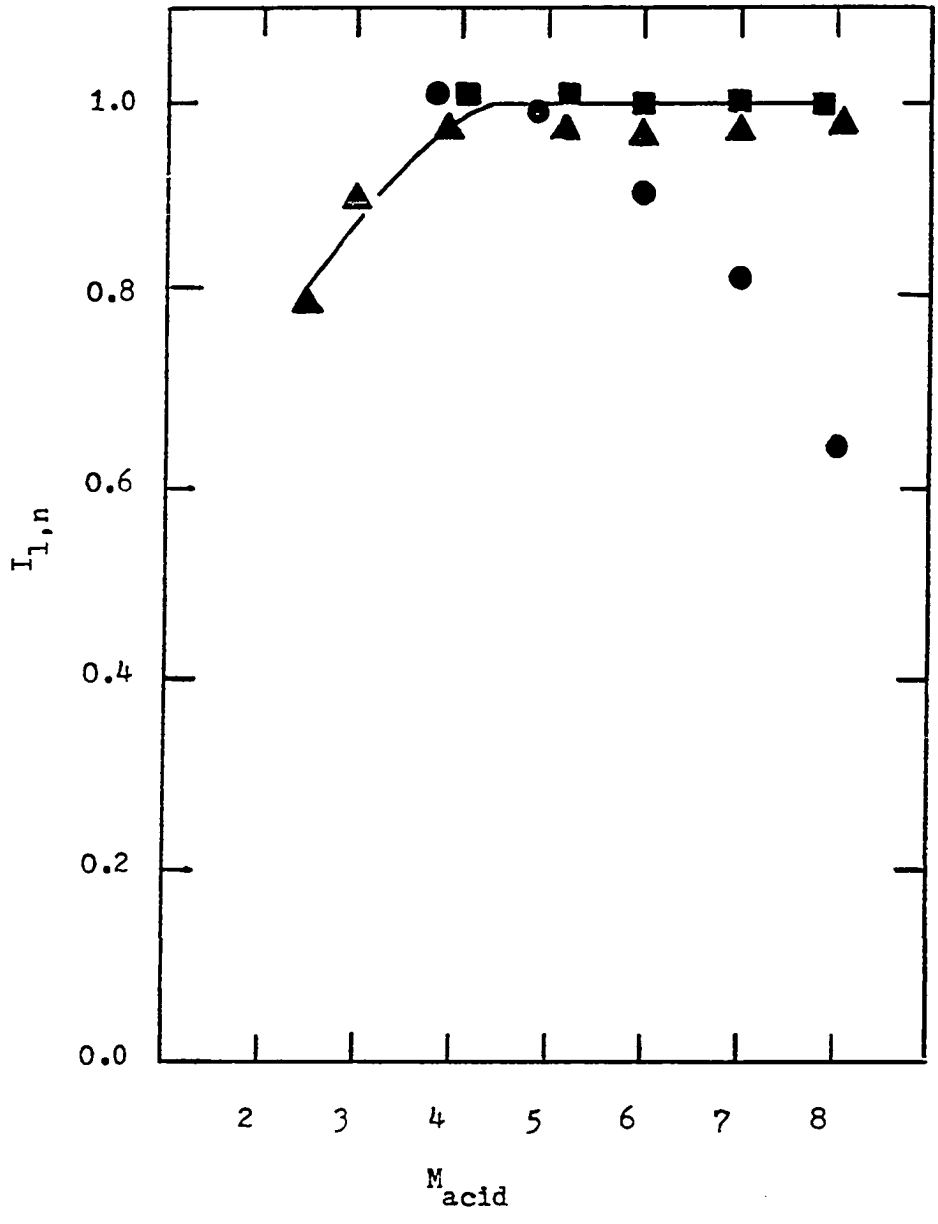
1.0
0.8
0.6
0.4
0.2
0.0
$I_{1,n}$
2
3
4
5
6
7
8
M_{acid}

Figure I.8. Values of $I_{l,n}$ for NO, HNO_2 and NO_2 in $HClO_4$ containing 0.05 M Br^-

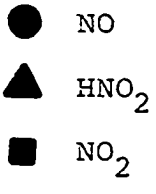

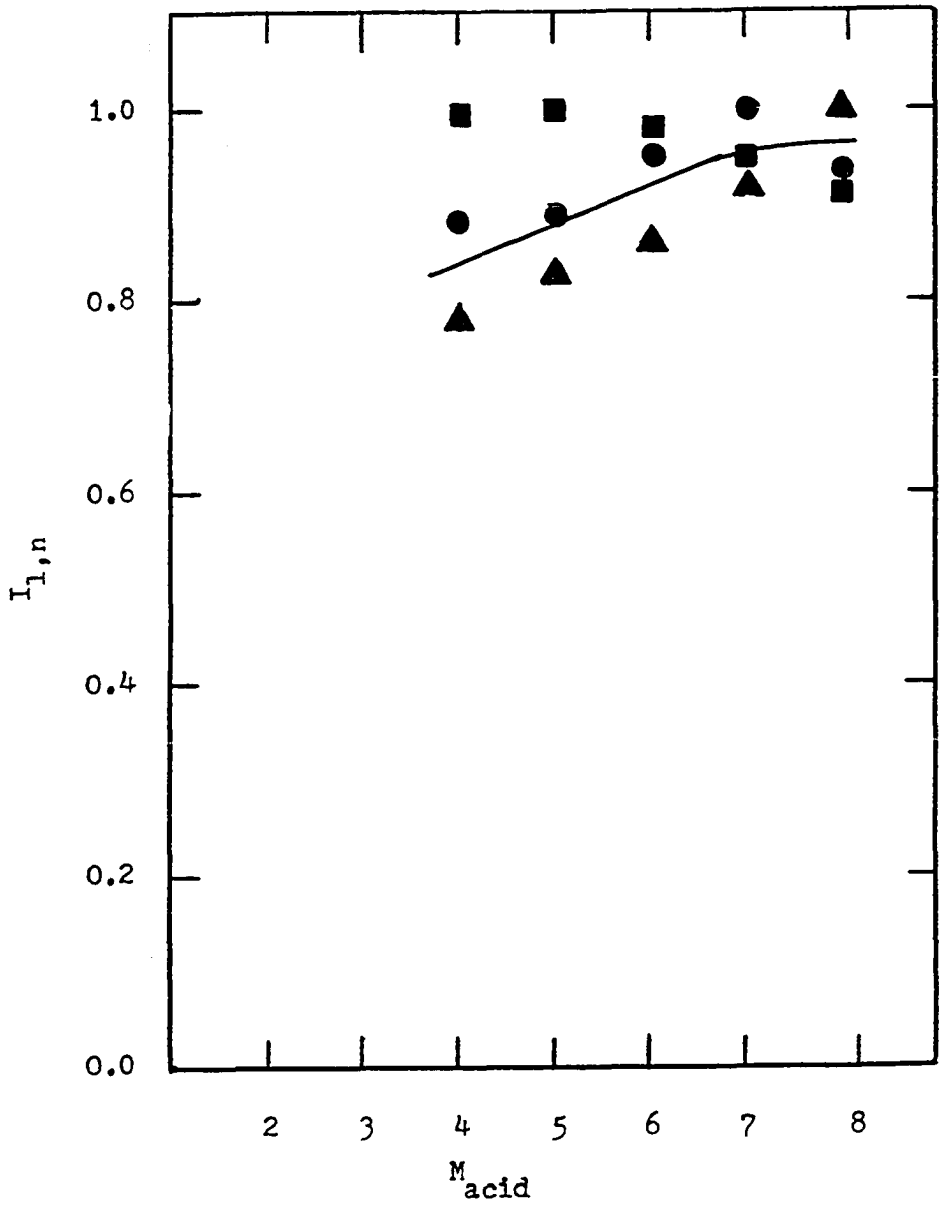
1.0
0.8
0.6
0.4
0.2
0.0
$I_{1,n}$
2
3
4
5
6
7
8
M_{acid}

Figure II.9. Comparison of $I_{l,n}$ values for $HClO_4$, $HClO_4$ containing 0.05 M Br^- and HCl

A HCl

B $HClO_4$ containing 0.05 M Br^-

C $HClO_4$

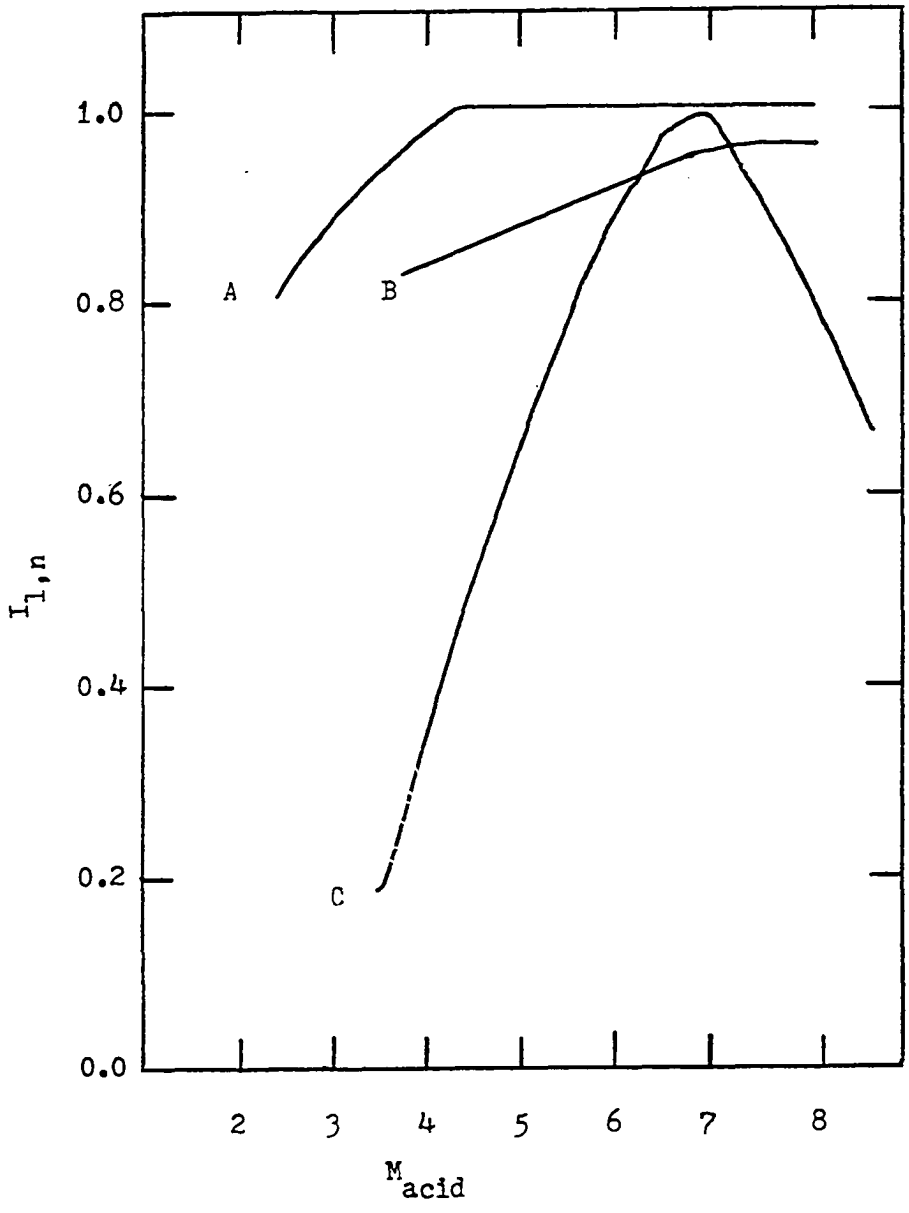
1.0
0.8
0.6
0.4
0.2
0.0
$I_{1,n}$
A
B
C
2
3
4
5
6
7
8
M_{acid}

Figure I.10. Values of $E_{1/2}$ for NO, HNO_2 and NO_2

A $HClO_4$

B HCl

C $HClO_4$ + 0.05 M Br^-

● ○ NO_2

■ □ HNO_2

▲ △ NO

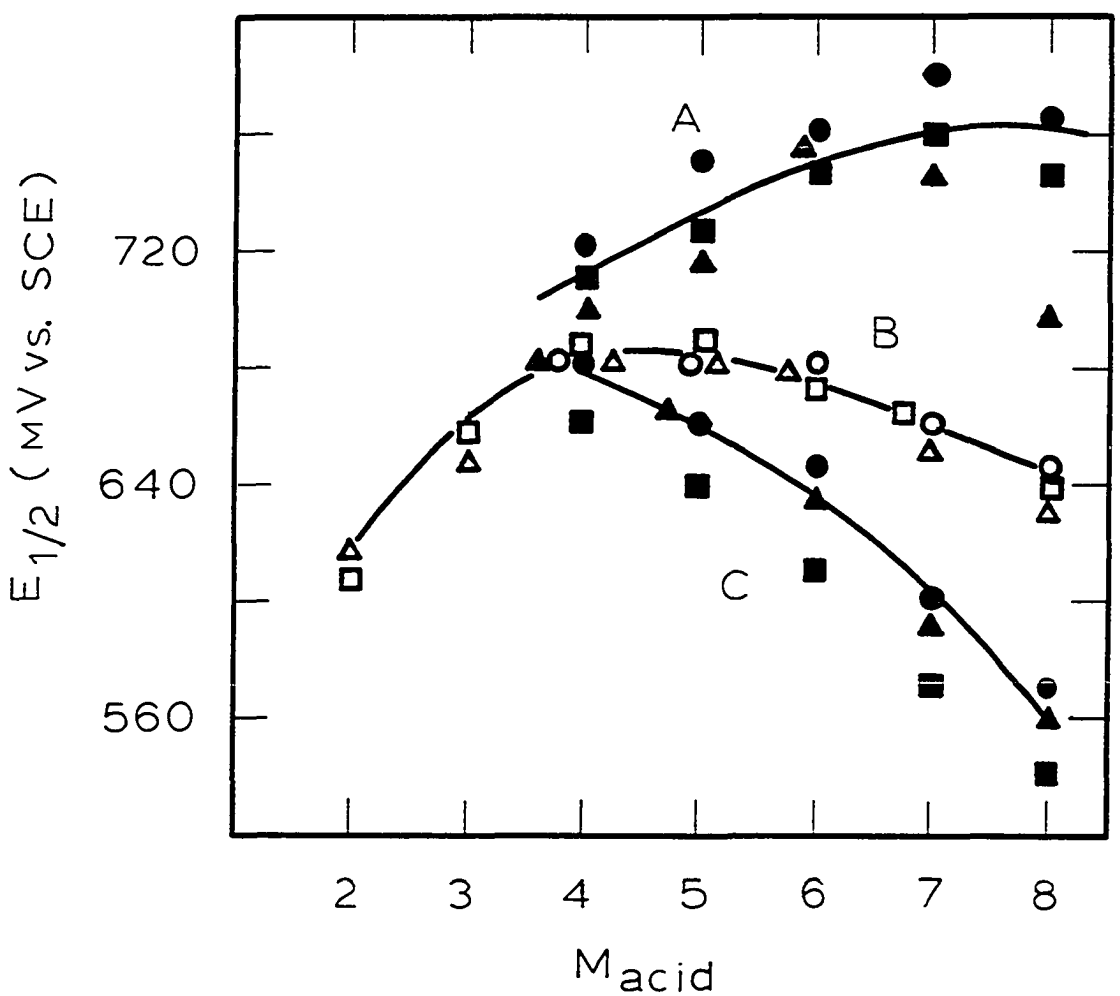
A
B
C
720
640
560
$E_{1/2}$ (MV vs. SCE)
2
3
4
5
6
7
8
M_{acid}

$$HNO_2 \overset{+H^+}{\rightleftharpoons} H_2NO_2^+ \overset{-H_2O}{\rightleftharpoons} NO^+ \overset{+e^-}{\rightleftharpoons} NO \qquad (I.79)$$

$$2NO_2 \overset{+H_2O}{\rightleftharpoons} HNO_2 + NO_3^- + H^+$$

$$HNO_2 \overset{+H^+}{\underset{-H_2O}{\rightleftharpoons}} NO^+ \overset{+e^-}{\rightleftharpoons} NO \qquad (I.80)$$

the solutions of NO, HNO_2 and NO_2. For concentrations of $HClO_4$ below 7 M, the value of $X_{NO^+} + XNO$ has not reached the maximum value; $X_{NO^+} + XNO = 1$ only for concentrations of $HClO_4$ above 8.5 M. This fact is not in conflict with the conclusion that NO^+ is the electroactive species in $HClO_4$ if the chemical reaction to produce NO^+ is sufficiently rapid so that I_1 for wave R^I is limited by the mass transport of the chemical precursor of NO^+.

The values of $I_{1,n}$ for NO, HNO_2 and NO_2 obtained in HCl increased rapidly for acid concentrations increasing in the range 2 M to 4 M. This is the concentration range in which $X_{NO^+} + XNO$ increases significantly for HCl solutions as shown in Figure I.1. The fact that $X_{NO^+} + XNO$ increases rapidly at lower values of acid concentration for HCl in comparison to $HClO_4$ reflects the larger value of the formation constant for ClNO in comparison to ClO_4NO (see Table I.1). The values of $I_{1,n}$ for NO were observed to decrease at the higher concentrations of HCl. This aspect of the reduction of NO is further discussed later in this section and in Section I.D.3.

Recognition of the large value of the formation constant for BrNO, in comparison with that for ClNO, leads to the conclusion that addition of Br^- to solutions of NO, HNO_2 and NO_2 in $HClO_4$ should enhance the values of $I_{l,n}$ for wave R^I. This prediction was verified by the experimental results. Values of $I_{l,n}$ obtained for 4 M $HClO_4$ containing 0.05 M Br^- were more than two times larger than the values of $I_{l,n}$ for 4 M $HClO_4$ without added Br^-. The XNO species is apparently electroactive in addition to NO^+.

The maximum current observed for the reduction of dissolved NO_2 and NO in the different acidic solutions was substantially different, and this data is shown in Table I.5. For the reduction of dissolved NO_2, addition of

Table I.5. Maximum values of I_l

	I(μA)		
	2×10^{-3} M NO	5×10^{-4} M HNO_2	5×10^{-4} M NO_2
$HClO_4$	205	65	15
$HClO_4$ + 0.05 M Br^-	175	56	47
HCl	133	56	21

0.05 M Br^- to $HClO_4$ resulted in the largest limiting current. From consultation of Equation I.81 for the reaction of NO_2 with H_2O, the increasing activity of H^+

$$2NO_2 + H_2O \rightleftarrows HNO_2 + NO_3^- + H^+ \quad \text{(I.81)}$$
$$\qquad\qquad\qquad\quad \downarrow HX \rightarrow XNO + H_2O$$

and the decreasing activity of water are predicted to shift the equilibrium to the left as the acid concentration is increased. The presence of halide ions shifts the equilibrium to the right by forming nitrosyl halides. Hence, the largest electrode current for NO_2 was observed in $HClO_4$ containing 0.05 M Br^-. For NO, the largest current was observed in $HClO_4$ alone. Considering Equation I.82, which describes the disproportionation reaction of

$$4NO + 2H^+ \rightleftarrows 2NO^+ + N_2O + H_2O \quad \text{(I.82)}$$

NO, the increasing activity of H^+ and decreasing activity of water shift the equilibrium toward the formation of NO^+ when acid concentration is increased. Because $HClO_4$ has the highest activity of H^+ and lowest activity of water of the three solutions, it is reasonable that the largest maximum current was observed in $HClO_4$ without added halide ion. These discussions further support the hypothesis that NO, HNO_2 and NO_2 are all reduced through species derived from HNO_2.

Increases in the values of $E_{1/2}$ in $HClO_4$ and HCl solutions, as the concentration of the acid is increased, are similar to the increases in values of $I_{l,n}$ for these solutions. The increase in the values of $E_{1/2}$ are concluded

to result from the promotion of chemical reactions given in Equations I.78-I.80.

The $E_{1/2}$ values, shown in Figure I.10, were observed to be larger in $HClO_4$ as compared to HCl or $HClO_4$ containing 0.05 M Br^-. Likewise, $E_{1/2}$ values in HCl are larger than those in $HClO_4$ containing 0.05 M Br^-. The nitrosyl compounds, in acidic solutions, are increasingly dissociated in the order $Br^- < Cl^- < ClO_4^-$ as shown in Equation I.83. As part of the mechanism of the reduction

$$HNO_2 + HX \rightleftarrows XNO + H_2O;\ K_{Br^-} > K_{Cl^-} > K_{ClO_4^-} \qquad (I.83)$$

of these species, the anion (X) must be removed in the reduction of the XNO to NO as shown in Equation I.84. The

$$O{=}N{-}X + e^- \rightleftarrows NO + X^- \qquad (I.84)$$

larger the energy required to remove the anion, the smaller the $E_{1/2}$ for the reduction of the nitrogen(III) species. Thus, the $E_{1/2}$ for solutions containing Br^- is less positive than for solutions containing only ClO_4^-.

Decreases in the values of $I_{l,n}$ and $E_{1/2}$ at high concentrations of acid cannot be easily explained. The increasing viscosity of the solutions has been eliminated as a factor by normalizing the $I_{l,n}$ values. The activity of H^+ is rapidly increasing, as the concentration of the acid is increased, in the concentration range where the decrease

in $I_{l,n}$ and $E_{1/2}$ is noted in $HClO_4$ as shown in Figures I.9 and I.10. The effect of this dramatic increase in activity of acid on the activities of other species in solution is not readily ascertained. The decline in $I_{l,n}$ and $E_{1/2}$ at high concentrations of acid is concluded to be due to the increasing activity of H^+ and the decreasing activity of H_2O.

3. Variation of rotation speed studies

Two mechanisms are responsible for transport of electroactive species to the vicinity of the surface of an electrode in a stirred solution containing an excess of supporting electrolyte: convection and diffusion. Convection is the predominant means of mass transport whenever the solution is agitated. A thin layer of solution ($\sim 10^{-2}$ cm) adheres to the surface of the electrode in which convection is negligible, and mass transport of the electroactive species across this thin layer of fluid to the electrode surface occurs by diffusion. This thin layer is called the "diffusion layer". In brief: convection is responsible for bringing electroactive species from the bulk of the solution to the outer boundary of the diffusion layer, and diffusion is responsible for transport across the diffusion layer.

The thickness of the diffusion layer, δ, for a rotating disk electrode can be calculated approximately by the

equation of Levich (50).

$$\delta = 1.62D^{2/3}\nu^{1/6}\omega^{-1/2} \qquad \text{(I.85)}$$

In Equation I.85: D = diffusion coefficient (cm^2/sec)

ν = kinematic viscosity (cm^2/sec)

ω = rotational velocity (rad/sec)

The limiting current for the electrode, I_l, is the value of the faradaic current which is controlled solely by the rate of convective-diffusional transport of the electroactive species to the electrode surface. The value of I_l is related to δ and the analytical concentration of the electroactive species in the bulk of the solution by Equation I.86.

$$I_l = \frac{nFADC^b}{\delta} = 0.62nFAD^{2/3}\omega^{1/2}\nu^{-1/6}C^b \qquad \text{(I.86)}$$

In Equation I.86: n = equivalents per mole

F = Faraday's constant (coul/equivalent)

A = area of electrode (cm^2)

C^b = bulk concentration of electroactive species (moles/L)

According to Equation I.86, I_l is directly proportional to $\omega^{1/2}$. Diagnostic evidence that a particular faradaic reaction is controlled by mass transport, as opposed to the rate of a slow chemical or electrochemical reaction at the electrode surface, is a linear plot of I vs. $\omega^{1/2}$ with zero intercept.

In experiments described here, a rotator was used for which the rotational velocity could be programmed to increase smoothly from 0 to 9000 rev/min within a time period of one minute. The signal for the rotator was a linear voltage ramp produced by analog integration of a constant.

The linearity of plots of I vs. $\omega^{1/2}$ was used to obtain diagnostic information about the effects of acid concentration and halide ion on the reduction of dissolved HNO_2 and NO. The plots are shown in this thesis only for HNO_2 and NO because the chemical reaction of NO_2 with water occurs instantaneously upon addition of NO_2 to the acidic solutions and yield plots of I vs. $\omega^{1/2}$ which are identical to those of HNO_2 except for the value of the slope. To illustrate the effects of acid concentration and halide ion, plots of I vs. $\omega^{1/2}$ were made for 3.0 M, 6.0 M and 9.0 M $HClO_4$ and with or without 0.05 M Br^- added.

The effect of increasing acid concentration on the linearity of plots of I vs. $\omega^{1/2}$ for HNO_2 and NO is seen by examining Figure I.11 and I.12, respectively. For both HNO_2 and NO, the plots are linear at low values of $\omega^{1/2}$ in 6.0 M and 9.0 M $HClO_4$. The value of I is practically zero for both HNO_2 and NO in 3.0 M $HClO_4$ because of the irreversibility of the reduction at this acid

Figure I.11. Electrode current as a function of rotation speed for HNO_2 in 3.0 M, 6.0 M and 9.0 M $HClO_4$

Electrode B

● 3.0 M

■ 6.0 M

▲ 9.0 M

5.0×10^{-4} M HNO_2

E = 0.40 V

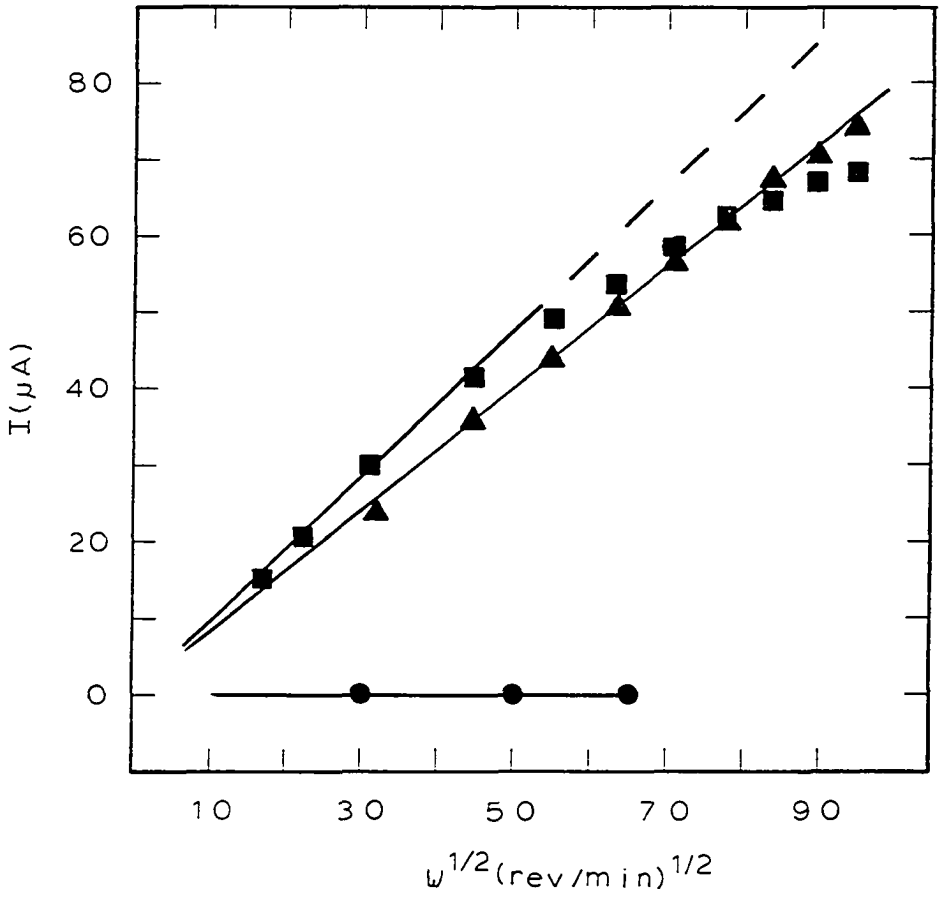
80
60
40
20
0
I(μA)
10
30
50
70
90
ω^1/2(rev/min)^1/2

Figure I.12. Electrode current as a function of rotation speed for NO in 3.0 M, 6.0 M and 9.0 M $HClO_4$

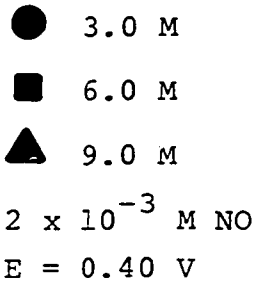

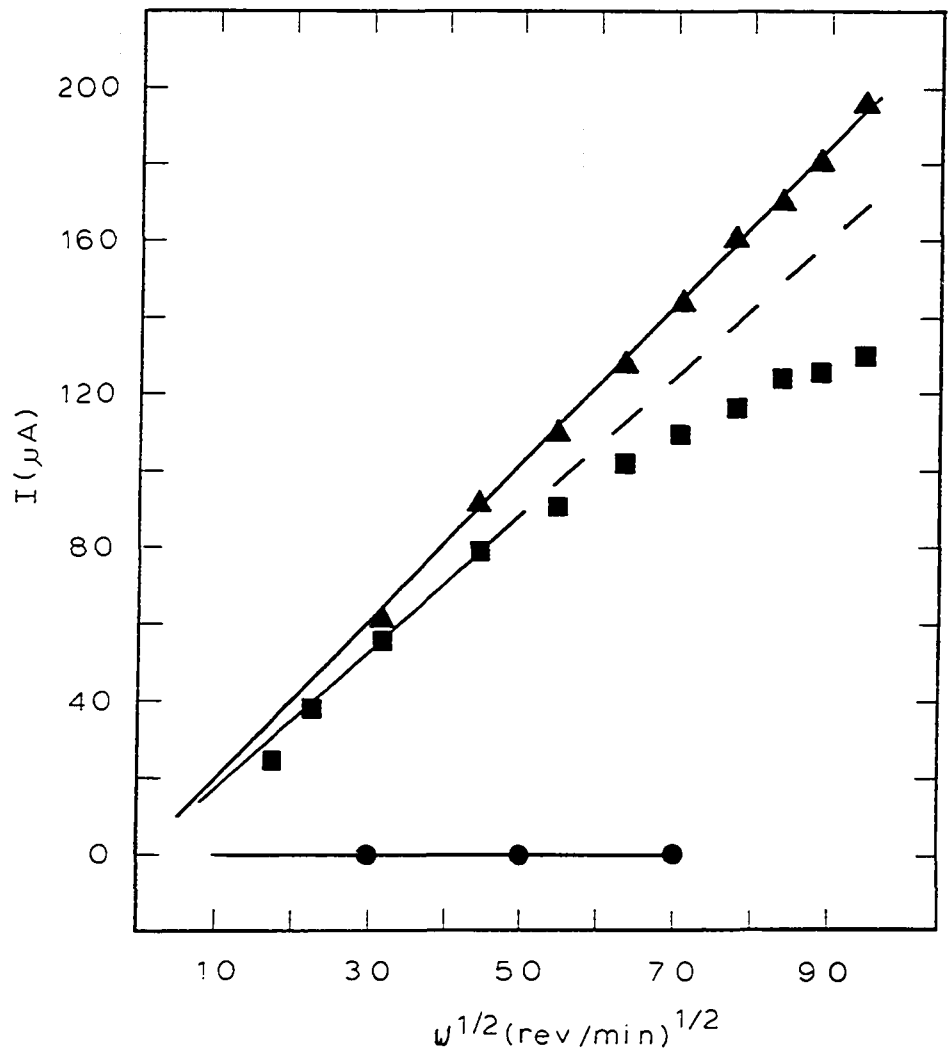
200
160
120
80
40
0
I (μA)
10
30
50
70
90
ω^1/2 (rev/min)^1/2

concentration. The plots become linear to higher values of $\omega^{1/2}$ as the concentration of the acid is increased for both HNO_2 and NO as shown in Figures I.11 and I.12. The rate of those processes that control the electrode current when the electrode current is no longer controlled by convective-diffusional mass transport are concluded to increase in rate as the acid concentration is increased.

The effect of halide ion on plots of I vs. $\omega^{1/2}$ for HNO_2 is determined by examining Figure I.13. The addition of 0.05 M Br^- to 3.0 M $HClO_4$ dramatically increased the observed electrode current, and the linearity of the plot of I vs. $\omega^{1/2}$ is essentially the same as for 9.0 M $HClO_4$ containing 0.05 M Br^-. The slopes of plots of I vs. $\omega^{1/2}$ are larger for the halide containing solutions; however, the linearity of the plots at high $\omega^{1/2}$ is better for the solution of HNO_2 in 9.0 M $HClO_4$. One interpretation of this data is that in 9.0 M $HClO_4$ the prior chemical reactions of HNO_2 do not go to completion and the addition of Br^- promotes the reaction for the production of the electroactive species. The Br^- also has the effect of decreasing the linearity of the plot of I vs. $\omega^{1/2}$, and the rate of reduction in Br^- containing solutions is concluded to be slower than in $HClO_4$ alone.

The effect of halide ion on the plots of I vs. $\omega^{1/2}$ for NO, shown in Figure I.14, is different than the effect

Figure I.13. Effect of Br^- on plots of I_l vs. $\omega^{1/2}$ for HNO_2

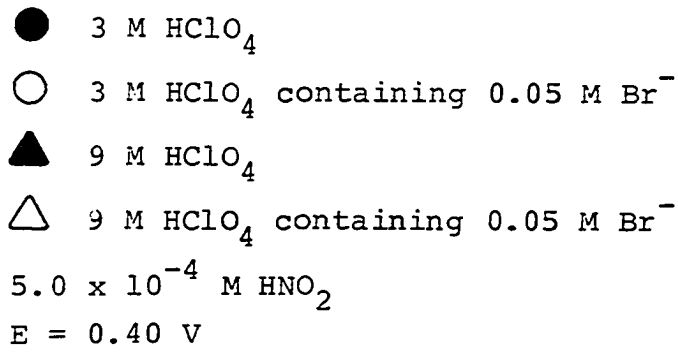

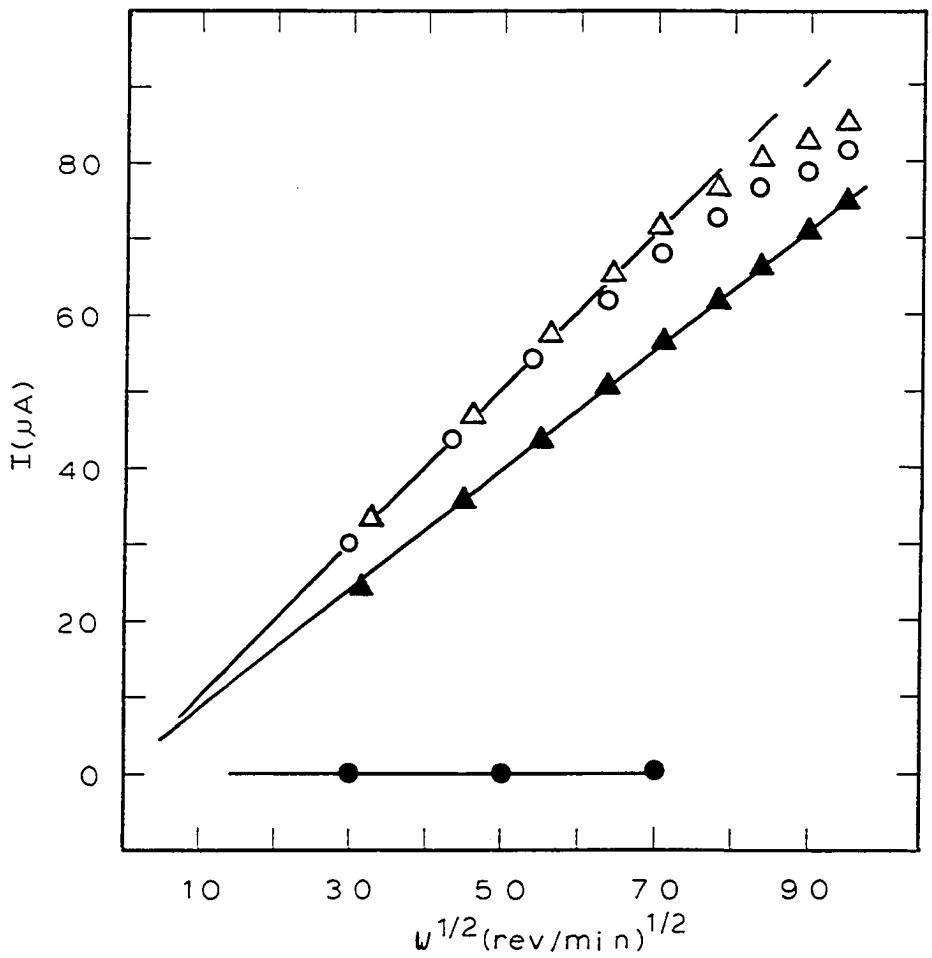
I(μA)
80
60
40
20
0
10
30
50
70
90
ω^1/2(rev/min)^1/2

Figure I.14. Effect of Br^- on plots of I_l vs. $\omega^{1/2}$ for NO

Electrode B

▲ 9.0 M $HClO_4$

△ 9.0 M $HClO_4$ containing 0.05 M Br^-

2 x 10^{-3} M NO

E = 0.40 V

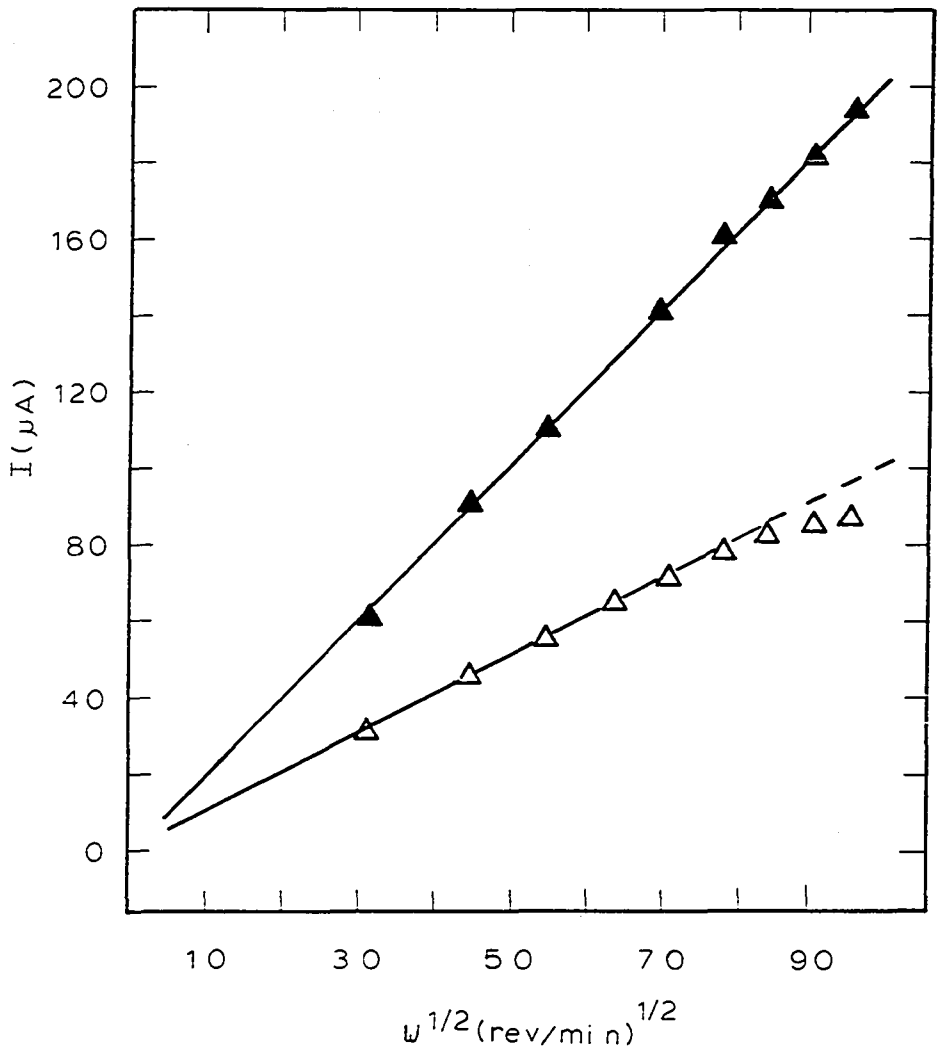
200
160
120
80
40
0
I(μA)
10
30
50
70
90
ω^1/2 (rev/min)^1/2

of Br^- on the plots of I vs. $\omega^{1/2}$ for HNO_2 shown in Figure I.13. The slope of the plot for NO is decreased in solutions containing Br^- at high concentrations of acid. The linearity of the plot is also less for solutions containing Br^- as is also seen for HNO_2 (Figure I.13). This data agrees with I_1 data for different acidic solutions shown in Table I.5. Both the data in Figure I.14 and Table I.5 show lower electrode currents for the reduction of NO in solutions containing halide ion. Halide ions adsorb at Pt electrodes (51) and are concluded to compete with NO for surface sites at which the NO disproportionates (see Section I.D.1).

4. Cyclic voltammetry at a stationary platinum electrode

Cyclic voltammetry at a stationary electrode (CVSE) is a powerful tool for the investigation of products of electrochemical reactions. Unlike the rotating electrode, the products of electrochemical reactions remain in the diffusion layer long enough to study electrochemically. In the investigation of reductions, the initial sweep of potential is in the negative direction producing cathodic peak(s) and is followed by a positive sweep resulting in anodic peaks(s) characteristic of the products of reactions occurring during the negative sweep. The potential and current corresponding to the maximum of the peak is

important because they give information about the rate at which the electroactive species is depleted in the diffusion layer. Changes in the maximum of the peaks as the scan rate is changed is indicative of irreversible behavior, and changes in the maximum can be used to evaluate kinetic parameters (52).

The cyclic voltammograms for NO, HNO_2 and NO_2 at a stationary platinum electrode are given in Figure I.15. The voltammograms for the three compounds are virtually identical except for the magnitude of the currents involved. The three waves are labeled as R^I, R^{II} and O^I in Figure I.15. R^I and R^{II} are the same waves previously discussed in Section I.D.1 for the rotating electrode. The electrode potential was not scanned sufficiently negative to initiate wave R^{III} in order to simplify the voltammograms. Wave O^I is concluded to result from the oxidation of NO which is the product of wave R^I as described in Equation I.87.

$$O^I: \quad NO \rightleftarrows NO^+ + e^- \tag{I.87}$$

If NO is the product of both processes, then the observation of only one anodic process is consistent with the proposed reactions in Equations I.88 and I.89.

$$R^I: \quad NO^+ + e^- \rightleftarrows NO \tag{I.88}$$

$$R^{II}: \quad N_2O_3 + 2H^+ + 2e^- \rightleftarrows 2NO + H_2O \tag{I.89}$$

Wave R^{II} is proposed to be the reduction of N_2O_3 in Section I.D.1. Comparing I-E curves for a rotating

Figure I.15. Current-potential curves for NO, HNO_2 and NO_2 at a stationary Pt electrode

Only the first sweep is shown

Electrode A

3.0 M HCl

5.0 V/min

A 5×10^{-4} M HNO_2

B 5×10^{-4} M NO

C 5×10^{-4} M NO_2

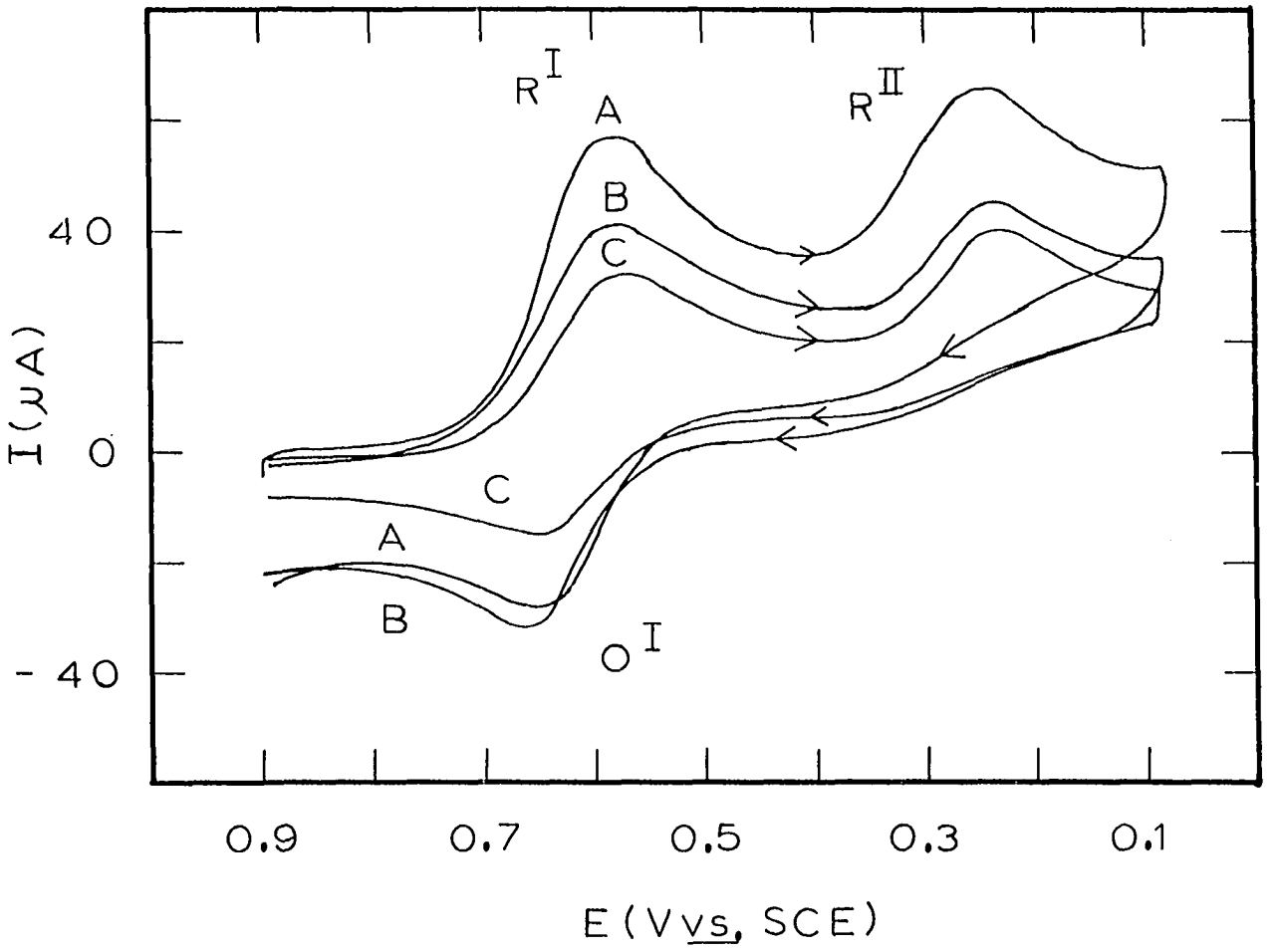
R I
A
R II
B
C
40
I(μA)
0
C
A
B
O I
- 40
0.9
0.7
0.5
0.3
0.1
E (V vs, SCE)

electrode and a stationary electrode (Figures I.17 and I.15), the current for wave R^{II} is significantly larger at the stationary electrode when compared to the current for R^{I}. That the second peak in the voltammogram at a stationary electrode corresponds to the second wave at a rotating electrode is shown in Figure I.16 where the solution used for the rotating electrode has been allowed to decompose. Dinitrogen trioxide can be produced in the diffusion layer by the reaction described in Equation I.90.

$$HNO_2 + NO^+ \rightleftarrows N_2O_3 + H^+ \qquad (I.90)$$

Once produced, the N_2O_3 slowly decomposes to nitrous acid as described by Equation I.91 (37). At a rotating

$$N_2O_3 + H_2O \rightleftarrows 2HNO_2;\ k = 50s^{-1} \qquad (I.91)$$

electrode, the N_2O_3 produced is swept into the bulk of the solution, and very little current is observed for the reduction of N_2O_3. The rate of removal of N_2O_3 is much slower at a stationary electrode, and the observed current is much higher.

5. Coulometry with flow-through platinum electrode

Coulometry can be used to determine the number of electrons involved in an electrode reaction (n) and to ascertain the stoichiometry of chemical reactions prior to the electron transfer. The value of n determined with this technique is often of dubious significance because

Figure I.16. Comparison of I-E curves obtained with stationary and rotated electrodes

A Stationary electrode
Electrode A
5×10^{-4} M HNO_2 in 6.0 M $HClO_4$
5 V/min

B Rotating electrode
Electrode A
HNO_2 in 6.0 M $HClO_4$ (enough NO_2^- added to evolve oxides of nitrogen)
1 V/min

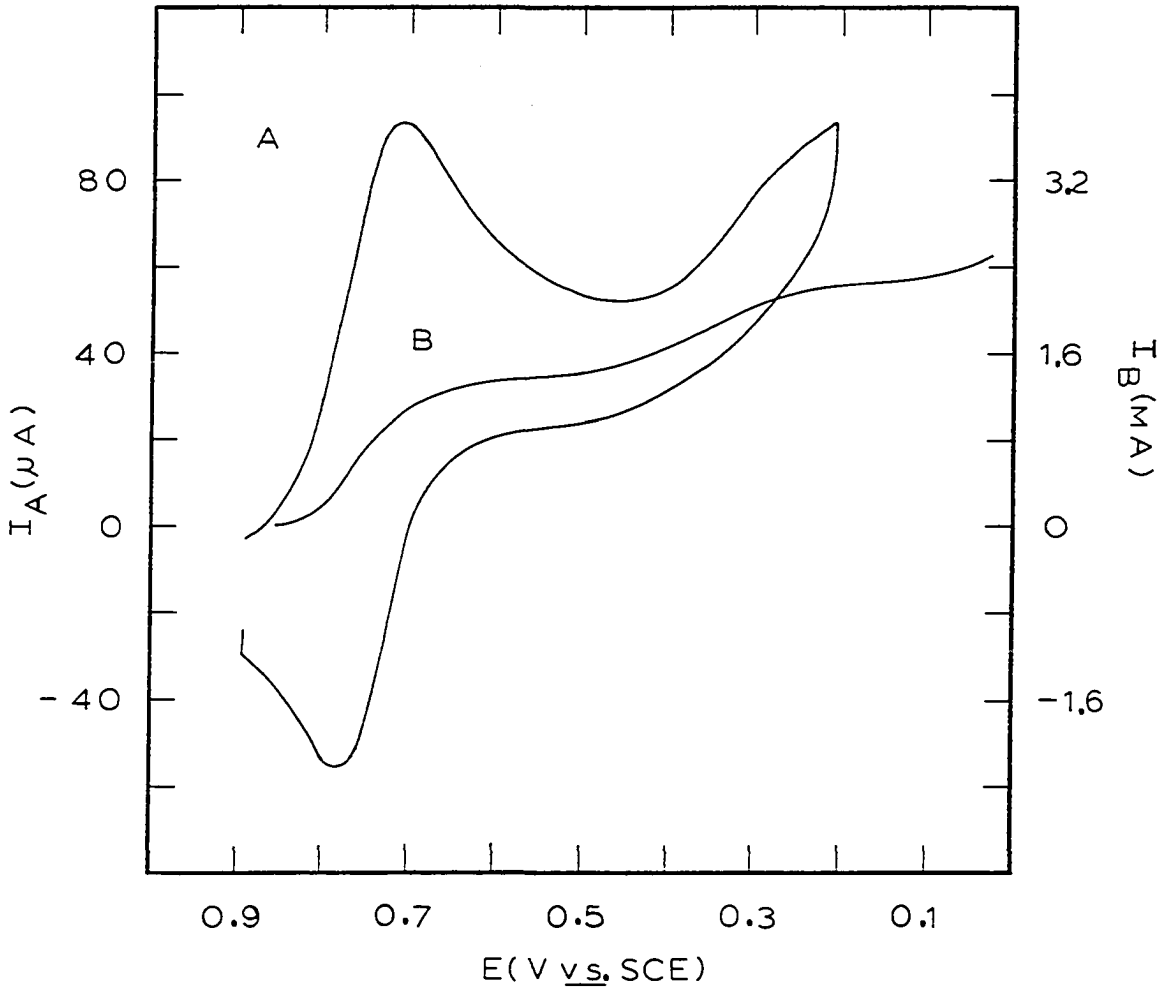
A
B
80
40
0
-40
3.2
1.6
0
-1.6
$I_A(\mu A)$
$I_B(MA)$
0.9
0.7
0.5
0.3
0.1
E(V vs. SCE)

Figure I.17. Current-potential curves for O_2 and HNO_2 in 3.0 M HCl

Electrode A

900 rev/min

0.5 V/min

A 1.0×10^{-4} M HNO_2 (deaerated)

B saturated with O_2

C deaerated residual

—— positive potential sweep

– – negative potential sweep

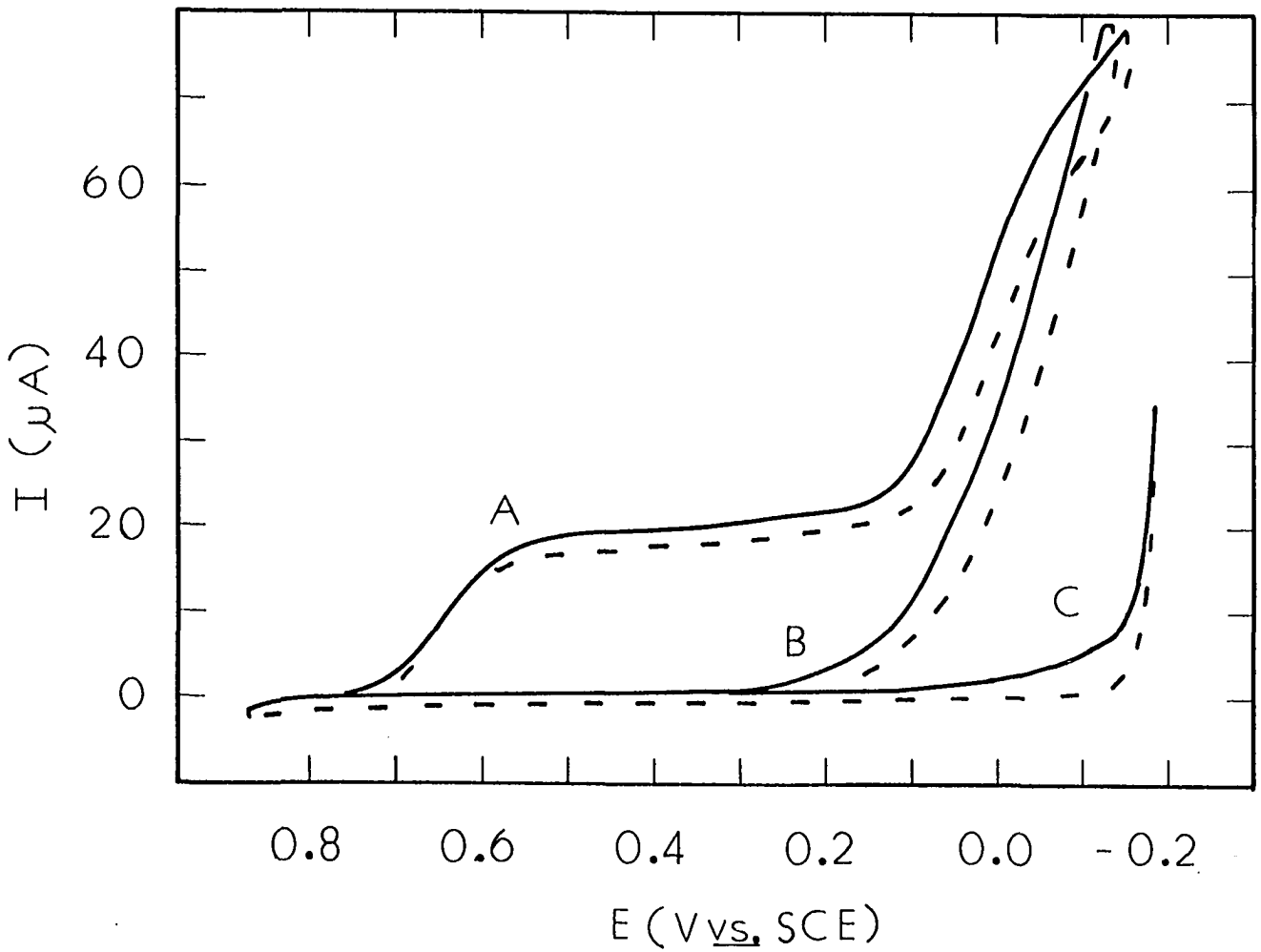
60
40
20
0
I (μA)
A
B
C
0.8
0.6
0.4
0.2
0.0
-0.2
E (V vs. SCE)

of chemical reactions occurring other than those associated with the electron transfer reaction. The decomposition of HNO_2 is an example of such a reaction. The reaction of NH_2OH, the product at potentials corresponding to R^{III}, with HNO_2 is another example of such a reaction and is given in Equation I.92 (40). The effect of such reactions

$$HNO_2 + NH_2OH \rightleftarrows N_2O + 2H_2O \qquad (I.92)$$

can be minimized by decreasing the time required for electrolysis. Coulometric reduction (100% electrolysis) of HNO_2 with a packed tubular electrode can be accomplished within a few seconds (44) which is much faster than other techniques for obtaining coulometric results.

The coulometric detector was used with a flowanalyzer such as shown in Figure I.3. The compound of interest was injected into the stream with a suitable sample injection valve. This stream composed only of water was mixed with acid of sufficient concentration to produce the desired final concentration of acid based on the relative flow rates of the two streams.

The packed tubular detector used was the same one prepared by Dr. John Larochelle and is described in Reference 44. The detector was checked for coulometric response by injecting a solution 4.00×10^{-4} M I^- into the flow stream. The electrode potential was +1.00 V, and the flow rate of the stream was 1.5 ml/min. A value of n equal to 0.99 was

obtained for the oxidation of I^- to I_2; thus, reaffirming the coulometric response of the detector.

The value of n for the reduction of HNO_2 was determined as a function of acid concentration and electrode potential. The values of n obtained for the injection of 0.197 ml aliquots of 5.00×10^{-4} M NO_2^- as a function of acid concentration are shown in Table I.6. The value of n

Table I.6. Value of n as a function of acid concentration (E = +0.500 V, 1.0 mL/min)

Concentration of HCl	n
2.0	0.45
3.0	0.74
4.0	0.91
5.0	0.96
6.0	1.01
7.0	1.05

is seen to increase as the acid concentration is increased with n being within 5% of 1.0 at acid concentrations above 5.0 M HCl. The value of n obtained for different electrode potentials is given in Table I.7. The value of n increases to 1.0 as the value of E becomes smaller. At values of E corresponding to R^{II}, the value of n is still equal to 1.0 in agreement with the conclusion that R^{II} is the reduction of the decomposition product N_2O_3

Table I.7. Value of n as a function of electrode potential (5.0 M HCl, 1.0 mL/min)

E (V vs. SCE)	n
0.700	0.07
0.600	0.66
0.500	0.91
0.400	0.91
0.300	0.94
0.200	0.97
0.100	0.95
0.000	1.31
-0.100	1.91
-0.200	1.98

(see Section I.D.1). The value of n never does approach 4.0 as would be predicted from the relative heights of R^{I} and R^{III}. One explanation is the loss of HNO_2 through the reaction given in Equation I.93. Gadde and Bruckenstein

$$HNO_2 + NH_2OH \rightleftarrows N_2O + 2H_2O \qquad (I.93)$$

proposed this reaction to explain the production of N_2O during the electrolysis of HNO_2 (40). If the reaction in Equation I.93 did go to completion, a value of n equal to 2.0 would be expected because one mole of HNO_2 would be consumed for each mole of HNO_2 reduced.

Results of coulometric experiments as a function of flow rate are given in Table I.8 for HNO_2 in 5.0 M HCl. The electrode potential corresponded to the plateau for

Table I.8. Value of n as a function of flow rate (5.0 M HCl, E = +0.500)

Flow Rate (mL/min)	n
1.0	1.01
0.75	1.01
0.50	1.03
0.40	1.20
0.30	1.35
0.25	1.55

wave R^I (see Figure I.17). The value of n is 1.0 at intermediate flow rates but increases at low flow rates. To explain this phenomenon, a diagram of the concentration profile of HNO_2 and the electrochemical reaction product NO in the interfacial region and as a function of time is given in Figure I.18. Remember that the volume of solution inside the packed detector is quite small and that NO can disproportionate to produce NO^+ (Equation I.1). As the HNO_2 is reduced to NO, the concentration of NO increases in the area outside the diffusion layer. When $t = 0.5\ \tau$ (τ = time required to completely electrolyze the HNO_2) in Figure I.18, the concentration of HNO_2 in the bulk of the solution has decreased to one-half the original value. The concentration of NO has increased from zero to one-half the original concentration of HNO_2. When $t = \tau$, the concentration of HNO_2 in the bulk has

Figure I.18. Concentration profiles of HNO_2 and NO

X distance from electrode surface

τ time required to completely electrolyze analyte

C concentration

Distance shown is approximately the diffusion layer thickness.

$$HNO_2 + H^+ + e^- = NO + H_2O$$

$$4NO + 2H^+ = 2NO^+ + N_2O + H_2O$$

大 = 0　　大 = 0.5 τ　　大 = τ

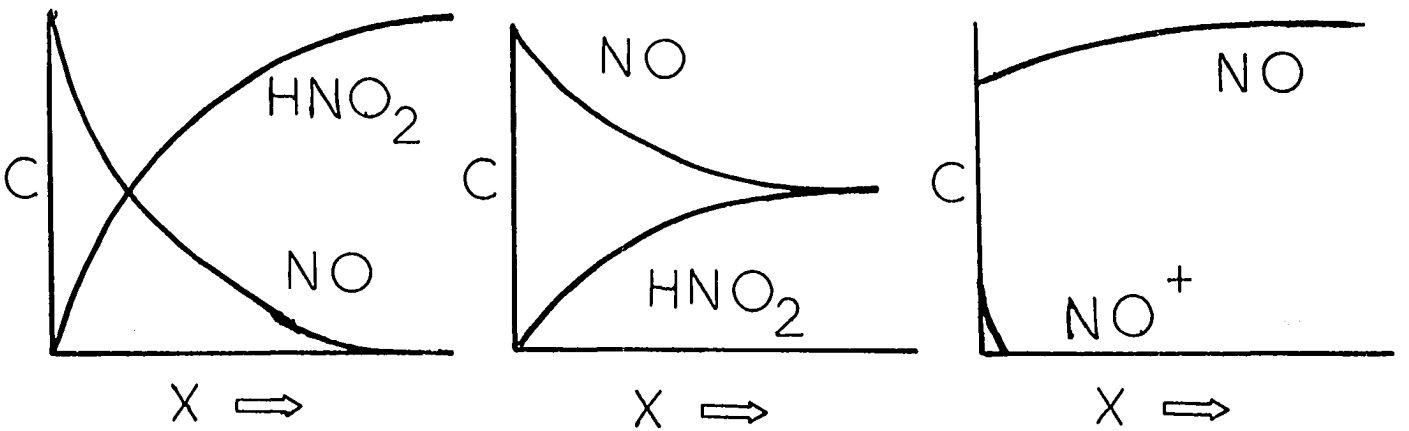

decreased to zero, and the concentration of NO has increased to the original concentration of the HNO_2. Only in the later stages of the electrolysis is the concentration of NO in the bulk of the solution larger than the concentration of NO near the electrode surface. When the above condition is met, the gradient of diffusion is toward the electrode surface, and the disproportionation of NO occurs.

Results of coulometric experiments with NO are presented in Table I.9. The lack of precision in the

Table I.9. Values of n for NO (5.0 M HCl, E = +0.400, 1.0 mL/min)

Concentration (M)	n
4.1×10^{-4}	0.52
4.1×10^{-4}	0.45
2.0×10^{-4}	0.42
2×10^{-3}	0.60
	n_{avg} = 0.49

results is because of the method of preparation of the solutions. The results are consistent with the previous premise that the electrochemistry of NO is the result of NO^+ produced, as described by Equation I.94, because only

$$4NO + 2H^+ \rightleftarrows 2NO^+ + N_2O + H_2O \qquad (I.94)$$

$$2NO^+ + 2e^- \rightleftarrows 2NO \qquad (I.95)$$

$$n = \frac{2e^-}{4NO} = 0.5e^- \text{ per NO} \qquad (I.96)$$

one-half of the NO becomes the NO^+ which is reduced. This data also agrees with the reaction order data shown in Table I.3 which was obtained by Mussini and Casarini (32).

The coulometric results with NO_2 are given in Table I.10. Again, the lack of precision in the results is due

Table I.10. Values of n for NO_2 (3.0 M $HClO_4$ + 0.1 M Br^-, E = +0.400, 1.0 mL/min)

Concentration (M)	n
5×10^{-4}	0.45
5×10^{-4}	0.52
5×10^{-4}	0.41
5×10^{-4}	0.48
	$n_{avg} = 0.46$

to the method of preparation of the solutions. The data on the limiting current as a function of acid concentration in Figure I.9 and Table I.5 was consulted in choosing the conditions under which the coulometry experiments were performed. Coulometric experiments using 3.0 M $HClO_4$ containing 0.1 M Br^- gave results consistent with the stoichiometry expressed in Equation I.97. At higher acid

$$2NO_2 + H_2O \rightleftarrows HNO_2 + NO_3^- + H^+ \qquad (I.97)$$

concentration, lower values of n were obtained. The higher activity of acid shifts the equilibrium towards the formation of NO_2 consistent with the equilibria expressed by Equation I.97.

6. Determination of NO_2^-

The results of Section I of this thesis were used to select the optimum conditions for the indirect determination of nitrosamines. As a detection limit of 1 ppb was needed for the determination of nitrosamines, a detection limit of 1 ppb NO_2^- was also needed. The selection of various experimental conditions is discussed below.

One of the most important selections is that of the acid used in the determination of the NO_2^-. The viscosity of the acid should be as low as possible to minimize the gas pressure required to obtain the flow rates needed. For instance, H_2SO_4 is unsuitable because pressures higher than the eluent bottles can safely withstand are necessary to obtain flow rates of even 0.5 ml/min. Because the acid was mixed with another stream, low viscosity acids are better because they mix easier (diffusion coefficients become smaller as the viscosity of the media becomes larger, see the Appendix). Small changes in acid concentration should not produce large changes in the observed current.

Of the common strong acids, HCl has the lowest viscosity, and the limiting current is constant over a wide range of HCl concentrations (see Figure I.8). Usually 9.0 M HCl was mixed with H_2O, and the flow rates of water and acid streams were equal resulting in a final concentration of 4.5 M HCl in the stream going to the detector.

The electrode potential should be on the limiting current plateau and be at such a value that O_2 is not reduced. Current-potential curves for 3.0 M HCl saturated with respect to O_2 and for 1.00×10^{-4} M HNO_2 are shown in Figure I.17. At potentials positive of 0.30 V, no interference from O_2 was observed. The background charging current was observed to be at a minimum at an electrode potential of 0.40 V; so, this electrode potential was used for detection of the NO_2^-.

There were no electrochemical methods available for the determination of NO_2^- at the ppb level at the start of this research. A peak resulting from the injection of 0.5 ng of NO_2^- is shown in Figure I.19. A calibration curve made without the use of a column is shown in Figure I.20, and the response is shown to be linear over five orders of magnitude. Solutions more concentrated than 10^{-3} M evolve NO and NO_2 when mixed with the acid. With the use of an anion-exchange column, lower concentrations could be

Figure I.19. Detector response for blank and low concentrations of NO_2^-

Tubular Pt electrode
Flow rate = 1.0 mL/min
Detector potential = 0.40 V
0.80 mL injection volume

A injection of 0.5 ng NO_2^-

B injection of H_2O

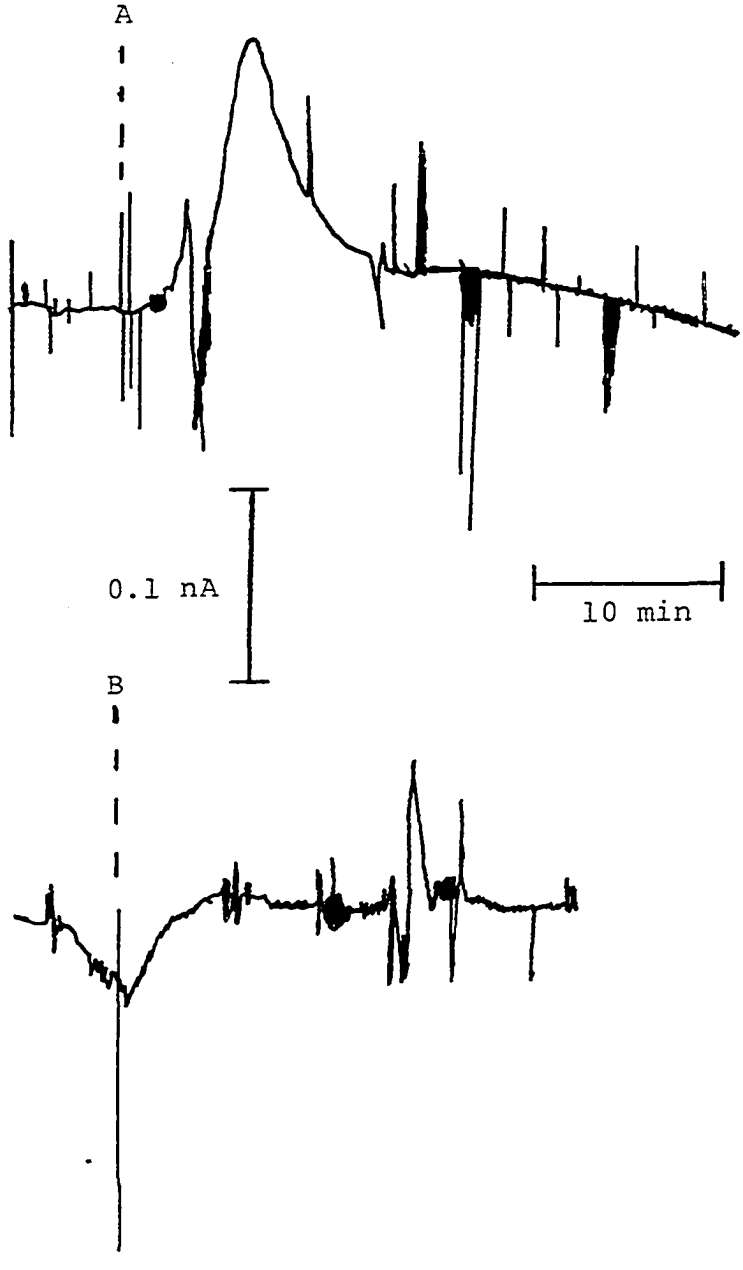
A
0.1 nA
10 min
B

Figure I.20. Calibration curve for NO_2^- at tubular Pt detector

C = Molarity

Flow rate = 1.0 ml/min

Sample injection volume = 0.80 mL

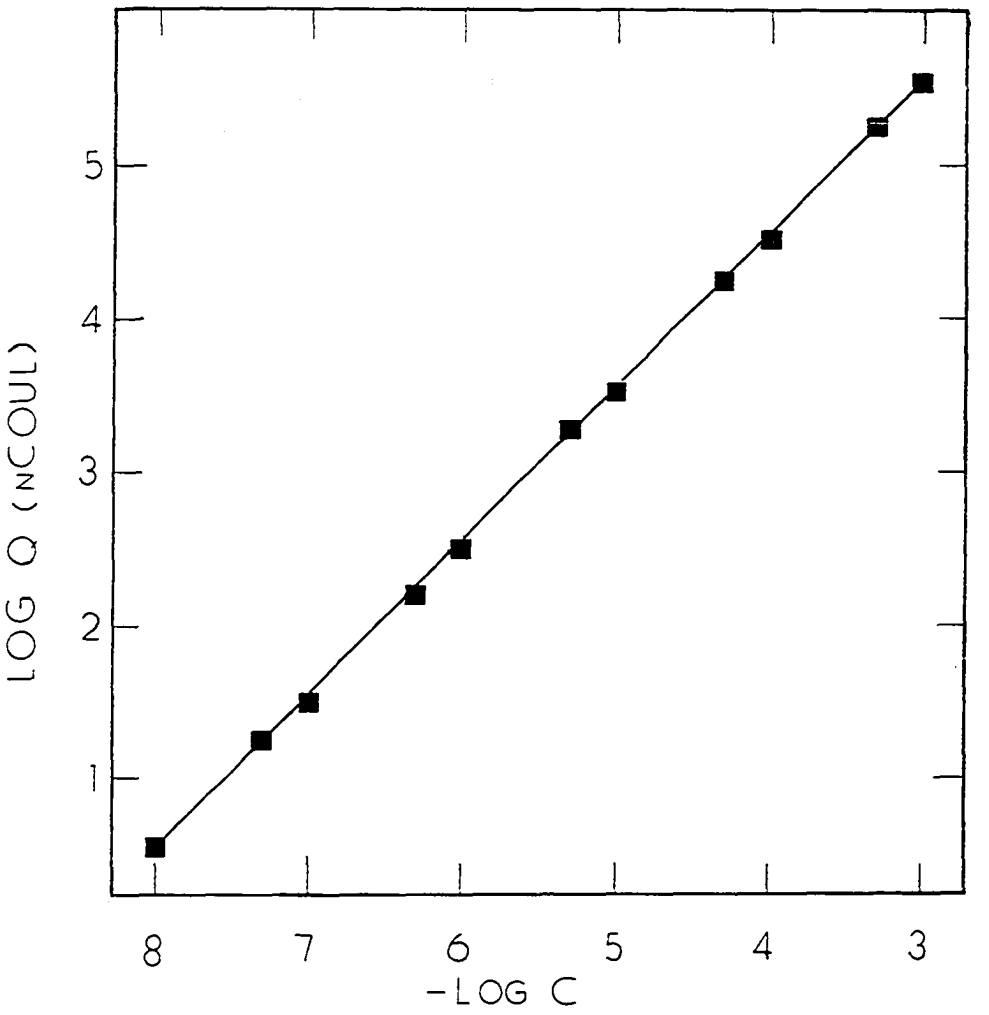
LOG Q (NCOUL)
1
2
3
4
5
8
7
6
5
4
3
-LOG C

determined by collecting the NO_2^- on the column, assuming that a low blank could be maintained.

E. Conclusions

The electrochemical reductions of NO, HNO_2 and NO_2 at a platinum electrode in acidic solutions were investigated in this thesis. The electroactive species for all three compounds was concluded to be derived from HNO_2. Nitrous acid is produced in solutions of NO and NO_2 by disproportionation as described by Equation I.98 and I.99.

$$2NO_2 + H_2O \rightleftarrows HNO_2 + NO_3^- + H^+ \qquad (I.98)$$

$$4NO + H_2O \rightleftarrows 2HNO_2 + N_2O \qquad (I.99)$$

These equations agree with reaction order data obtained by Mussini and Casarini for the reduction of NO_2 and NO in H_2SO_4 (32) and reactions proposed by Topol, _et al._, (33) for the reduction of NO_2 and NO in concentrated sulfuric acid. The reduction of NO _via_ HNO_2 conflicts with the conclusions of other researchers who concluded that NO was directly reduced to N_2O (35, 36, 38, 41, 43). Several researchers (35, 36, 38) concluded that NO was directly reduced on the basis of the production of N_2O during the reduction of NO. This production of N_2O is also predicted from the disproportionation reaction given in Equation I.99.

The electroactive species in acidic solutions which do not contain halide ion was concluded to be NO^+ produced by chemical reaction at the electrode surface according to Equation I.100. Nitrosonium ion had been previously

$$HNO_2 + H^+ \rightleftarrows H_2NO_2^+ \rightleftarrows NO^+ + H_2O \qquad \text{(I.100)}$$

proposed by many other researchers as the electroactive species (28, 32, 33, 35, 37, 38, 39, 43).

Changes in $E_{1/2}$ and I_1 observed for all three compounds as a function of acid concentration was ascribed to changes in the activity of H^+ and H_2O. The changes in I_1 were shown not to be due to the increasing viscosity of the solutions as the acid concentration was increased.

The second reduction wave was concluded to be the reduction of a decomposition product and not the reduction of NO as reported by others (35, 37, 38, 43). Evidence was presented to support the conclusion that N_2O_3 is reduced in wave R^{II}.

The reduction of all three compounds was observed to be catalyzed by halide ion. This catalytic activity of halide ion was concluded to result from the formation of nitrosyl halides. The nitrosyl halides were concluded to be electroactive at the Pt electrode.

The determination of NO_2^- at the ppb level by reduction at a Pt flow-through electrode in 4.5 M HCl was shown to be feasible.

II. DETERMINATION OF NITROSAMINES

A. Introduction

The potent carcinogenic effect of nitrosamines was first reported by Barnes and Magee in 1956 (53). Later studies have revealed that over 65 different nitrosamines are carcinogenic and dimethylnitrosamine is the most potent carcinogen of the group.

The abbreviations used in this thesis in reference to various nitrosamines are listed in Table II.1

Nitrosamines are produced from the reaction of nitrous acid with secondary amines as described by Equation II.1. Mirvish (54) proposed the reactions in

$$R_2NH + HNO_2 \rightleftarrows R_2N\text{-}N{=}O + H_2O \qquad \text{(II.1)}$$

Equations II.2 and II.3 to explain the observed rate law

$$2HNO_2 \rightleftarrows N_2O_3 + H_2O \qquad \text{(II.2)}$$

$$R_2NH + N_2O_3 \rightleftarrows R_2N\text{-}NO + HNO_2 \qquad \text{(II.3)}$$

given by Equation II.4. The observation that the rate

$$\text{Rate} = k[R_2NH][HNO_2]^2 \qquad \text{(II.4)}$$

was dependent upon pH was the basis for concluding that the species actually reacting are N_2O_3 and R_2NH. As the pH decreases, the concentration of R_2NH decreases, as the secondary amine is converted to an amine salt, and the concentration of N_2O_3 increases. For the case of

Table II.1. Abbreviations for common nitrosamines

Compound	Structure	Abbreviation
N-Nitrosodimethylamine	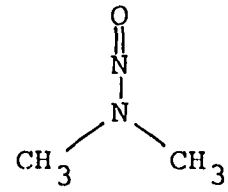	DMN
N-Nitrosodiethylamine	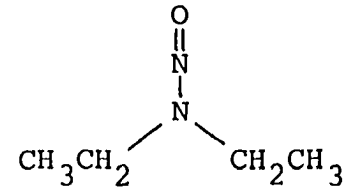	DEN
N-Nitrosodi-n-propylamine	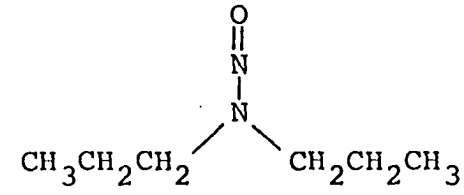	DPrN
N-Nitrosodiphenylamine	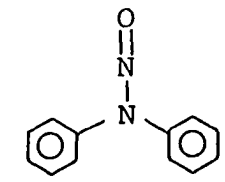	DPhN
N-Nitrosodi-n-butylamine	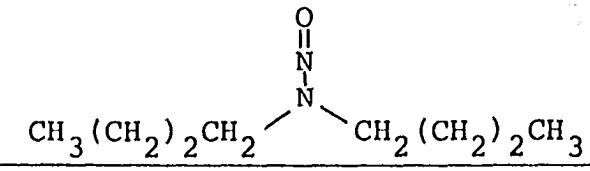	DBuN

dimethylamine, the rate of the formation of DMN reached a maximum at pH equal to 3.5. The ubiquitous nature of amines and nitrite in nature ensures a wide variety of situations where nitrosamines can be formed.

Several foods contain the necessary amines and nitrite appropriate for production of nitrosamines (55). Nitrite is often added to foods to preserve color, enhance flavor and protect against botulism. Nitrite can also be produced from nitrate by microbial reduction (56, 57). Concentrations of nitrosamine determined in food, such as meat, have typically been approximately 5 ppb (58). In some cases, the nitrosamines are produced predominantly during the cooking of the food. Fazio, et al., (59) found N-nitrosopyrrolidine in fried but not raw bacon at levels of 10 ppb to 108 ppb. The concentration of N-nitrosopyrrolidine remaining in the bacon grease was 45 ppb to 207 ppb. A more complete discussion of nitrosamines in foods is given elsewhere (55, 60).

One of the major concerns about nitrosamines is that they can be formed inside the body after ingestion of foods containing either secondary amines or nitrite. Sen, et al., (61) demonstrated that nitrosamines could be formed in gastric juices, and others have found saliva contains NO_2^- at concentrations of 1 ppm to 10 ppm (55). Hawksworth and Hill (62) determined that strains of

Escherichia coli from the human intestine can enzymatically produce nitrosamines from nitrate and secondary amines at neutral values of pH. Strains of lactobacilli, group D streptococci, clostridia, bacteroides and bifidobacteries were found to produce nitrosamines from secondary amines and nitrite at neutral values of pH.

Nitrosamines can also be produced from the burning of tobacco (55). Tobacco contains several secondary amines, and oxides of nitrogen at concentrations as much as 1000 ppm are produced when tobacco is burned. For example, 680 ng of DMN was found in the sidestream smoke of a common nonfilter cigarette. The sidestream smoke was found to contain nitrosamines at levels ten times higher than that inhaled by the smoker (63)!

Certain formulations of herbicides have been found to contain large amounts of nitrosamines. One major product was determined to contain 154,000 ppm of nitrosamines (64). The nitrosamine was produced in the herbicide as a result of the reaction during formulation of secondary amines with nitrite added as a corrosion preventative.

There are numerous theories concerning the induction of cancer by nitrosamines. One possible explanation is that nitrosamine is metabolized to a diazoalkane ($N\equiv\overset{+}{N}-\overset{-}{C}H-R$) which alkylates nucleic acids, thereby changing the genetic code (55).

Little doubt exists about the hazard of nitrosamines. There remain unanswered, important questions as to the significance of nitrosamines present at the ppb level in foods. Analytical methods for detecting the presence of all nitrosamines would be of great benefit in screening foods for the presence of nitrosamines.

The original intent of this research was the development of a method for the determination of nitrosamines using photolysis as a confirmational tool. An electrochemical detector was desired which was compatible with liquid chromatography such that the nitrosamines could be separated from interferences in one analytical operation. The reduction of nitrosamines requires H^+, as depicted in Equation II.5a, and electrodes at which the background

$$R_2N\text{-}NO + 2H^+ + 2e^- \rightleftarrows R\text{-}N{=}N\text{-}R + H_2O \qquad \text{(II.5a)}$$

current for the reduction of H^+ is low at the potentials necessary to reduce nitrosamines were needed. The values of $E_{1/2}$ for the reduction of nitrosamines at Hg in a solution of pH 1 range from -0.5 to -1.0 V vs. SCE (65). Several choices for the electrode appeared suitable at the outset: cadmium (Cd), mercury-coated Cd (Hg-Cd), mercury-coated platinum (Hg-Pt) and mercury-coated gold (Hg-Au). Two important problems arose in the application of these electrode materials to the determination of nitrosamines. Oxygen is reduced at these electrodes, and changes in the

concentration of O_2, because of diffusion of O_2 through the Teflon tubing used for the construction of the analytical apparatus, caused large shifts in the background current. Hydrogen ion is reduced at the potentials necessary for the detection of DMN at these electrodes, and the high background current severely limited the detection limit. As a result of these problems, the direct determination of nitrosamines was no longer attempted.

A screening method based on the electrochemical determination of NO_2^- produced during the photochemical decomposition of nitrosamines is described in this thesis. The conditions for the electrochemical detection of NO_2^- is described in Section I of this thesis. The analytical methods developed were applied to the analysis of tuna and fried bacon.

B. Literature Review

1. Isolation of nitrosamines

Nitrosamines have widely different physical properties depending on the character of the secondary amine from which the nitrosamine was produced. For example, dimethylnitrosamine is an oily liquid that boils at 150°C; whereas, diphenylnitrosamine is a solid with a melting point of 56°C. Fine, et al., (66) has placed nitrosamines into three classifications: (i) volatile nitrosamines; nitrosamines removed from a food matrix by distillation, i. e.,

DMN, DEN, DPrN and DBuN; (ii) nonionic, nonvolatile nitrosamines; nitrosamines not removed by distillation, i. e., DPhN, and (iii) ionic, nonvolatile nitrosamines; nitrosamines not amenable to extraction with nonaqueous solvents because of their large solubility in water. By taking advantage of differences in physical properties, different classes of nitrosamines can be separated.

The dialkylnitrosamines tend to be the most carcinogenic, and much effort has been devoted to the development of methods for determining these nitrosamines. Dialkylnitrosamines are quite volatile and were removed from foods by distillation at reduced pressures (55, 60, 67-70). In some cases, mineral oil added to the food matrix aided in removal of nitrosamines from the food by extracting the nitrosamines from the food matrix (67). The distillate was collected in cold fingers chilled by liquid nitrogen (67). Extraction of the distillate with methylene chloride removed the nitrosamines from the aqueous distillate (67-70). Some interferences were removed from methylene chloride by back extractions with 0.1 M NaOH and then 0.1 M HCl (69). For greater sensitivity, the volume of the methylene chloride was reduced by evaporation in a Kuderna-Danish apparatus (68, 69). More extensive clean-up procedures have been described using alumina, Celite and ion-exchange columns (68, 69, 71).

Nonionic, nonvolatile nitrosamines were extracted by Fine, et al., (66) with the use of liquid nitrogen and methylene chloride. Samples were blended in a liquid nitrogen slurry, and the fine powder remaining after the liquid nitrogen had evaporated was extracted with methylene chloride. Oily residues were extracted with acetonitrile. According to Fine, et al., (66), both the acetonitrile and methylene chloride can be removed from the sample under a stream of nitrogen. The residue was then dissolved in the solvent used for liquid chromatography.

2. Determination of nitrosamines

An early method for the determination of nitrosamines was based on thin-layer chromatography. After separation, the TLC plate was exposed to UV light, and the nitrosamines were photolytically decomposed (72). The nitrite was visualized by use of color-forming reagents. This method has the disadvantage that the color-forming reagents can also react with fatty acids, tocopherols, pigments and other compounds to give false positives (55).

Gas chromatography with various detectors has also been used (68, 69, 73), but the nonspecificity of most detectors limits their usefulness. The most commonly accepted method of detection for the determinations based on gas chromatography is mass spectrometry (55, 68). In at least one case however, an ion peak for a silicon

compound was unresolved from the parent ion peak for DMN even with a resolution of 10,000 (74, 75). Confirmation of the presence of nitrosamines was difficult for concentrations of nitrosamines in food below 10 ppb (68).

One detector which was developed in the last few years was applied successively for the determination of nitrosamines based on gas chromatography (76, 77). This is the Thermal-Energy Analyzer (TEA). The TEA was constructed from a $WO_3/W_{20}O_{58}$ catalyst which was maintained at a temperature of 300°C to produce controlled pyrolysis of the nitrosamines. A nitrosyl radical, NO, is produced by the pyrolysis. The radical is oxidized by O_3 to electronically excited nitrogen dioxide (NO_2*). The NO_2* decays to the ground state with simultaneous emission of infrared radiation. This IR radiation was detected by a photomultiplier tube. The TEA was used with GC and LC in the analysis of food samples for nitrosamines (66, 78). Although this detector was claimed to be specific for nitrosamines, interferences were observed for several nonnitrosamines (77). For instance, 5-nitrouracil gave a response which was approximately two per cent of the response for nitrosamines. A similar approach involved denitrosation in 1,3-dichloroethane with HBr (79). The NO produced was determined in the same manner as with the TEA. No application of this technique was reported in the chemical literature.

Polarography has been used for the determination of nitrosamines (80-82), but the method suffers from interferences by pyrazines which are very common in foods (56, 60). Differential pulse polarography has been investigated for the determination of nitrosamines (83, 84) but suffers from interferences caused by reduction of O_2 and NO_2^- (83). Although the technique had a detection limit in the ppb region, no application of this technique was reported.

3. Photochemistry of various nitrogen compounds

Two absorption bands were observed by Layne, et al., in the UV-VIS spectra for nitrosamines in aqueous solutions (85). The more intense absorption band had a maximum at approximately 220 nm and a molar absorptivity of 7,000 (M^{-1} cm^{-1}). This absorption band was identified as resulting from a $\pi \rightarrow \pi^*$ transition. A less intense band at approximately 360 nm had a molar absorptivity of about 100 (M^{-1} cm^{-1}). This band was concluded to correspond to a $n \rightarrow \pi^*$ transition. The absorption spectrum was essentially the same for all solutions with a pH > 1. The intensity of the $n \rightarrow \pi^*$ band decreased rapidly in more acidic solutions and was absent in concentrated sulfuric acid (86).

Daiber and Preussmann (87) developed a method for the determination of nitrosamines based on the photochemical

decomposition of nitrosamines, and the method described in this thesis was based on their work. Nitrosamines were photolyzed with light from a Hg lamp for 15 min. The organic products of the photolysis reaction were not determined. The photolysis solvent was 0.1% Na_2CO_3 in one method and phosphate buffer at pH 6.5 in another. The nitrite produced was then visualized with Greiss reagent. The chemical reactions occurring in this colorimetric procedure are given in Equation I.5b. Absorbance of the azo

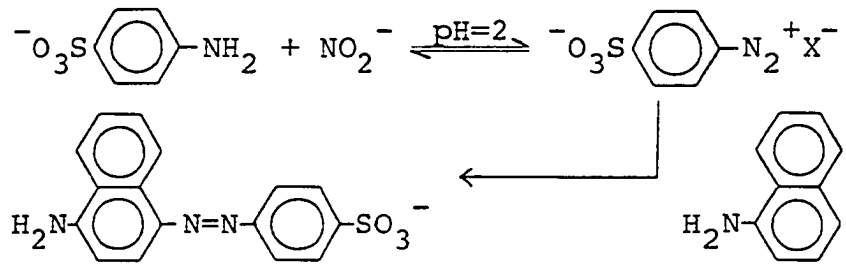

(II.5b)

compound produced by the Greiss reagent was directly proportional to the molar concentration of six different nitrosamines whose structures are given in Table II.2 All the nitrosamines were photolyzed at efficiencies greater than 95% for the concentration range 2×10^{-5} M to 2×10^{-4} M (2 μg to 20 μg). The detection limit of the method was 1 μg of DPrN in the extract. Several interferences are expected as discussed in Reference 55.

Walters, Johnson and Ray (82) used photolysis to confirm the presence of nitrosamines. Derivative polarograms of nitrosamines in 0.2 N HCl were recorded before and after

Table II.2. Nitrosamines determined by Daiber and Preussmann (87)

Compound	Structure
N-Nitrosodimethylamine	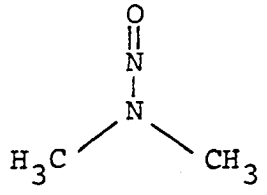
N-Nitroso-di-n-propylamine	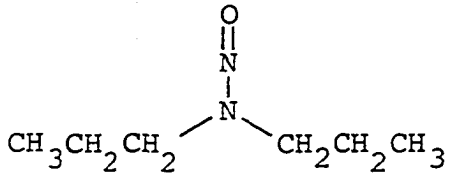
N-Nitroso-ethyl-t-butylamine	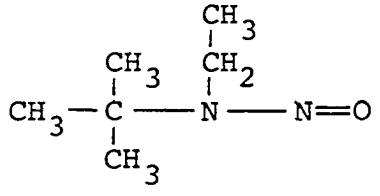
N-nitroso-4-picolyl-methylamine	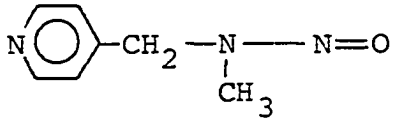
N-nitroso-methyl-allylamine	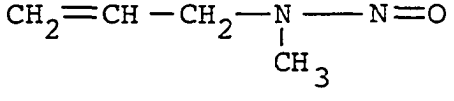
N-Nitroso-trimethylhydrazine	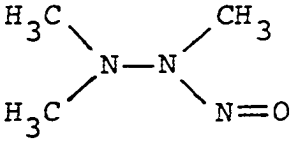

photolysis. The disappearance of a peak in the derivative polarogram after photolysis was the basis for concluding that the polarographic peak resulted from the reduction of a nitrosamine. The production of nitrite by photolysis of several compounds in alkaline solutions was investigated. Compounds that were reported to photolyze to produce nitrite in alkaline media are listed in Table II.3.

Burns and Alliston (88) studied the rate of photolysis of various nitrosamines in different solutions. A 15-watt ultraviolet lamp (254 nm) designed for use in chromatographic detectors was used to measure the half-lives of photolytic decomposition. Half-lives for nitrosamines were shorter at lower values of pH, i. e., 2.2 hr for pH = 4 and 3.5 hr for pH = 9.2 for DMN. The half-life for DBuN was 1.5 hr for a pH of 9.2. For DMN, the half-lives varied from 1.3 hr to 7.3 hr depending on the solvent.

Daniels, et al., (89) investigated the photolysis of NO_3^- in aqueous solutions. The reactions in Equations II.6 through II.8 were proposed to explain the observed rate of production of NO_2^-.

$$NO_3^- \xrightarrow{h\nu} NO_2^- + O \qquad \text{(II.6)}$$

$$O + NO_3^- \xrightarrow{k_1} O_2 + NO_2^- \qquad \text{(II.7)}$$

$$O + NO_2^- \xrightarrow{k_2} NO_3^-; \text{ at 300 nm } k_2/k_1 = 2 \times 10^4 \qquad \text{(II.8)}$$

Table II.3. Compounds which photolyze to produce nitrite in alkaline media

Compound	Structure
N-Nitroso-N-methylurea (N-Nitrosoamide)	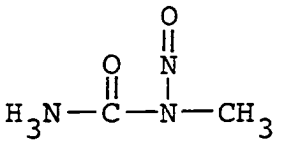
N-Nitrodimethylamine (N-Nitramine)	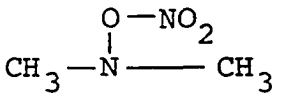
Nitromethane (C-Nitrocompound)	$CH_3—NO_2$
Pentylnitrite (alkylnitrite)	$CH_3(CH_2)_3—CH_2—ONO$
Ethylnitrate (alkylnitrate)	$CH_3CH_2ONO_2$

Fan and Tannenbaum (90) modified the procedure introduced by Daiber and Preussmann. Parts from a Technicon Autoanalyzer I were used to automate the procedure. To eliminate interference from nitrate (91), a long-wavelength irradiator (∿ 350 nm) consisting of a General Electric germicidal lamp was used. A residence time of 30 min was required to photolyze 50% of the nitrosamine. The method gave linear response for concentrations of nitrosamine less than 1 ppm. The detection limit was 30 ng of nitrosamine calculated as DPrN. Interferences noted by Walters, et al., (82) (see Table II.3) were acknowledged but the extent of the interferences was not determined for this procedure. Sander (91) indicated that photolysis at 350 nm is more specific for compounds having the N-NO structure than photolysis at 250 nm. A more extensive review of the photolysis of NO_3^- is given in Reference 92.

Doerr and Fiddler (93) have proposed the use of photolysis in the confirmation of peaks resulting from the use of TEA. Seven different nitrosamines were completely photolyzed in methylene chloride, hexane, methanol and water by exposure to radiation at 366 nm for 1 hr. With this technique, extract solutions were analyzed before and after photolysis using GC with detection by TEA. Peaks obtained prior to photolysis which disappeared after photolysis were presumed to correspond to nitrosamines.

Nitro compounds give a weak response (77), but the extent of photolysis of nitro-compounds under the conditions employed was not determined.

C. Experimental

1. Instrumentation and apparatus

Two different potentiostats were used in this work. A simple two-electrode potentiostat, diagrammed in Figure II.1, was used where the electrode currents were less than 50 nA. The magnitude of IR_2 was maintained at less than 50 mV by using different values of R_2. At higher currents, a potentiostat (Model RDE-3) from Pine Instrument Co. was used. Current-time curves were recorded with a strip-chart recorder (Model SR-255B) from Heath-Schlumberger Co. of Benton Harbor, Michigan. Potential measurements were made with an integrating digital multimeter (Model 7050) from Systron-Donner, Inc., of Culver City, California. Integration of peaks was made with a Keuffel-Esser Dual Compensating Planimeter. All construction of glass apparatus was made by the Chemistry Glass Shop at Iowa State University.

A photoanalyzer (PA), shown in Figure II.2, was used for all experiments in this section. This PA was essentially the flowanalyzer of Section I.C.1 with added anion-exchange columns and photolysis apparatus. The construction of

Figure II.1. Two-electrode potentiostat

R_1 = 10 K, 10-turn potentiometer

R_2 = 10 M ohm for currents less than 5 nA

R_2 = 1 M ohm for currents less than 50 nA

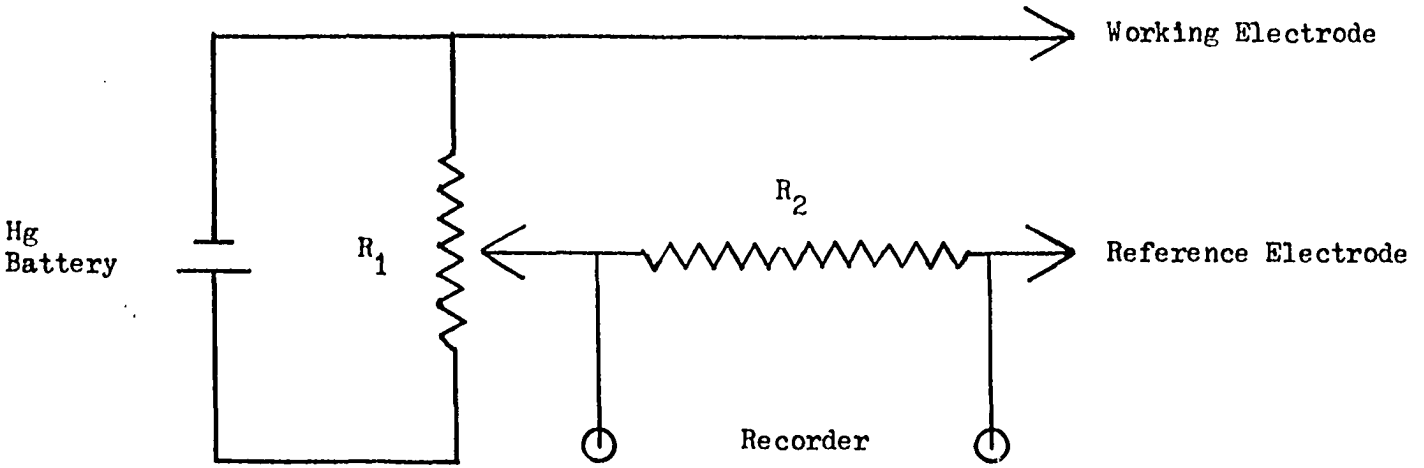
Working Electrode
Hg
Battery
R1
R2
Reference Electrode
Recorder

Figure II.2. Schematic diagram of photoanalyzer

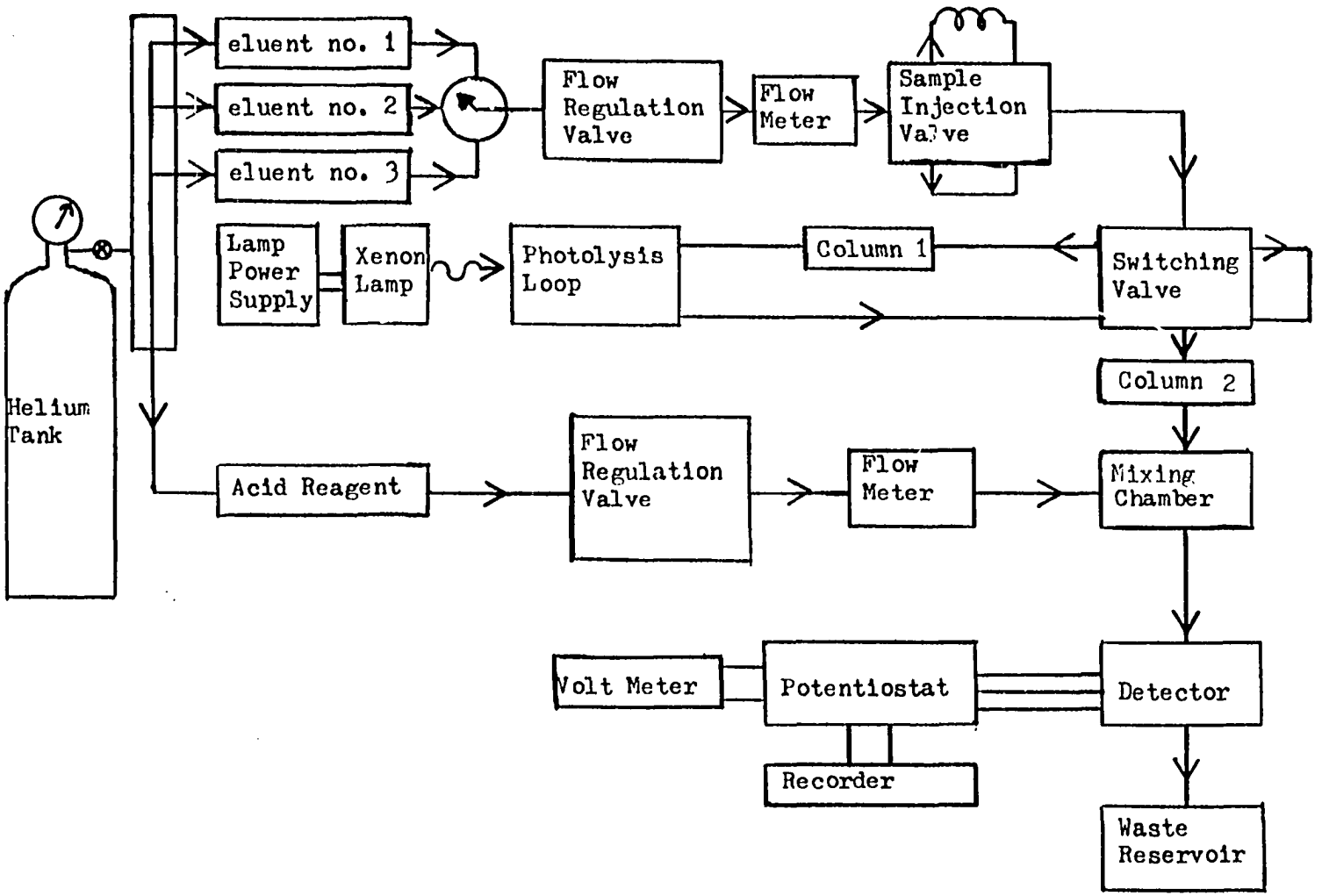
eluent no. 1
eluent no. 2
eluent no. 3
Flow Regulation Valve
Flow Meter
Sample Injection Valve
Lamp Power Supply
Xenon Lamp
Photolysis Loop
Column 1
Switching Valve
Column 2
Helium Tank
Acid Reagent
Flow Regulation Valve
Flow Meter
Mixing Chamber
Volt Meter
Potentiostat
Detector
Recorder
Waste Reservoir

all parts, except the photolysis apparatus and anion-exchange columns, is discussed in Section I.C.1.

The photolysis apparatus consists of a coil of quartz tubing (1 mm I. D. and 2 mm O. D.), a 500-watt Xenon lamp and a lamp power supply. The coil of quartz tubing, referred to as the "photolysis loop," is shown in Figure II.3. To make connections between the photolysis loop and the rest of the PA, the ends of the photolysis loop were inserted into Pyrex tubing (1 cm long, 3 mm I. D. and 5 mm O. D.) and were sealed into this tubing with Epoxy resin. The Pyrex tubing had been previously fused to the ends of standard glass-Teflon connectors. The photolysis loop was irradiated with a 500-watt, high-pressure Xenon arc (Model 959C-98) from Hanovia, Inc., of Newark, New Jersey. The power supply was Model LPS-255 from Schoeffel Instrument Corp. of Westwood, New Jersey. The lamp housing and lens system are described in Reference 94. Studies of the dependence of the photolysis upon wavelength were made with a high-energy grating monochromator (Model GM250) from Schoeffel Instrument Corp. Slits of 12 mm were used for an estimated bandwidth of 22 nm. For routine work, the photolysis loop was irradiated from the side port of the lamp housing.

Chromatographic columns were packed with Amberlite IRA-900 anion-exchange resin from Rohm and Haas of Philadelphia, Pennsylvania. The mesh size of the resin

Figure II.3. Photolysis loop

Diameter = $1\frac{1}{2}$ inches

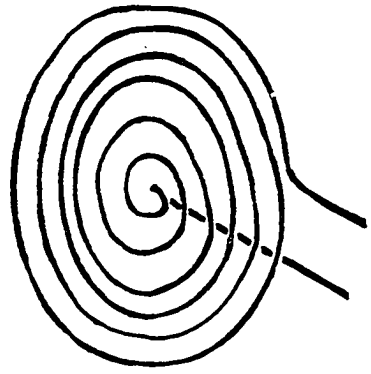

was -60 - +100. The columns were made from Pyrex glass with an internal diameter of 1.5 mm and were 10 cm long. The columns were packed to about 5 cm with the resin. Plugs of glass wool were inserted into the ends of the column to retain the resin. The columns were not used in some experiments and were replaced with the appropriate lengths of Teflon tubing.

Two flow-through Pt detectors were used. A tubular Pt electrode, shown in Figure I.3, was used for all initial work. All of the work at the lower concentrations was performed with a Pt-wire detector designed by R. Koile. A cross-sectional diagram of this electrode is given in Figure II.4. The detection limit was observed to be better when the Pt-wire detector was used.

An ultraviolet photometric detector, operating at a wavelength of 254 nm, from Chromatronix, Inc., (now Spectra-Physics of Santa Clara, California) was used for the detection of nitrosamines in some experiments.

The apparatus used to isolate volatile nitrosamines by distillation is schematically represented in Figure II.5. The Kuderna-Danish apparatus is available from Ace Glass of Vineland, New Jersey, and is shown in Figure II.6. The Snyder column used with this apparatus had 6 glass bubbles.

Figure II.4. Cross-sectional diagram of Pt-wire detector

Si-Teflon body

A Input from chromatograph

B Connection to Pt-wire working electrode

C Tube-end fitting to hold Pt wire in place

D Compartment for reference electrode

E To waste reservoir

F Connection to Pt-wire counter electrode

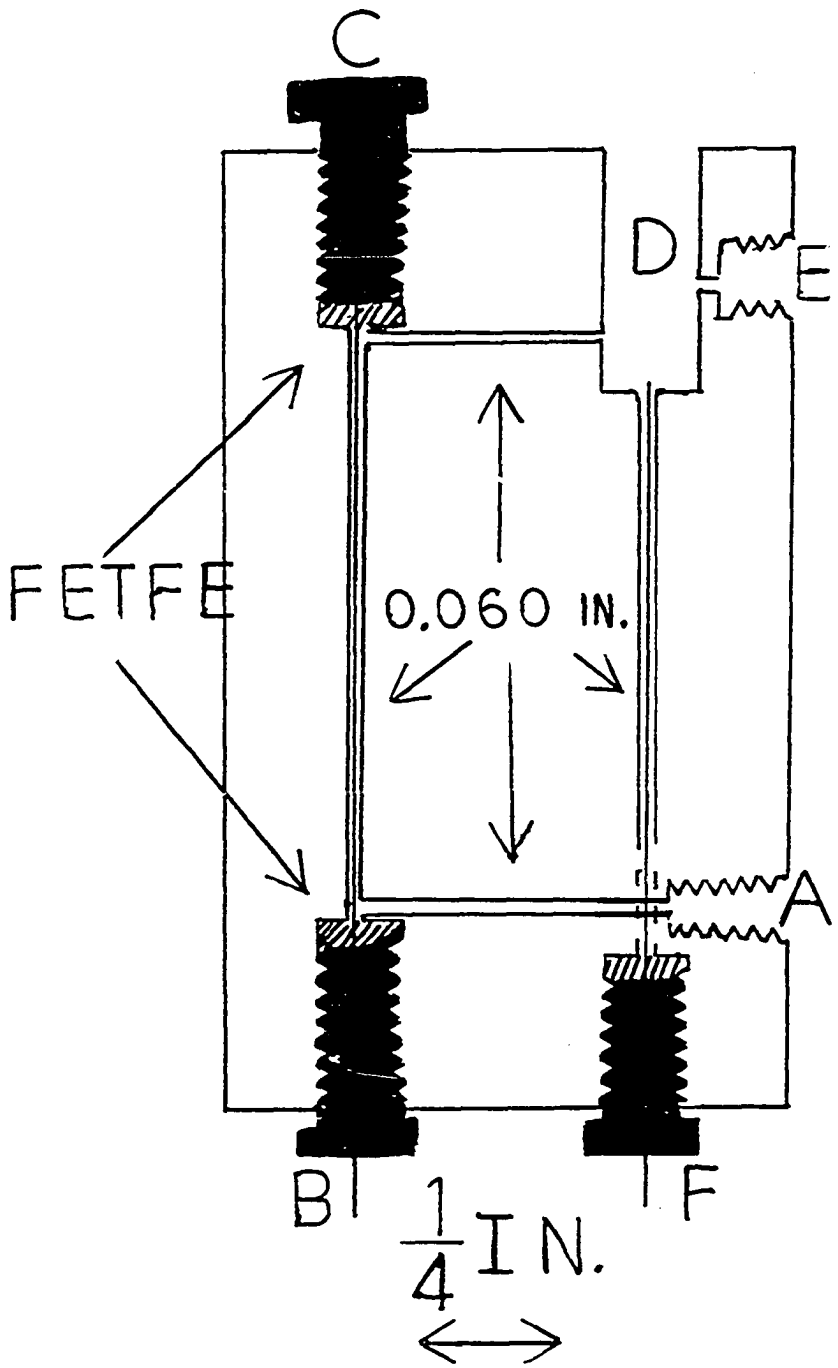
C
D
E
FETFE
0.060 IN.
A
B
F
1/4 IN.

Figure II.5. Distillation apparatus

A 500 mL RB flask

B Thermometer

C Cold traps

D Connection to vacuum pump

E 200 mL RB flask

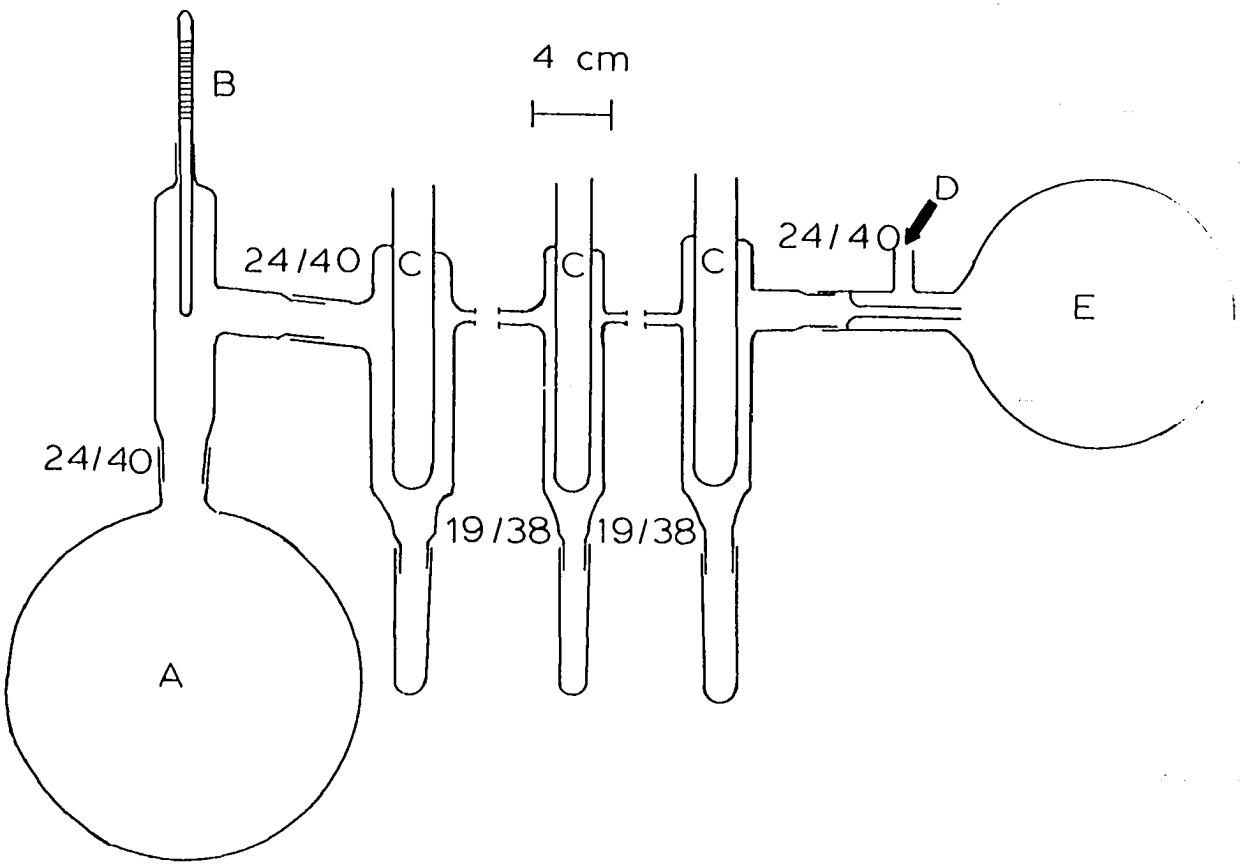
4 cm
B
24/40
C
C
C
24/40
D
E
24/40
19/38
19/38
A

Figure II.6. Kuderna-Danish evaporator

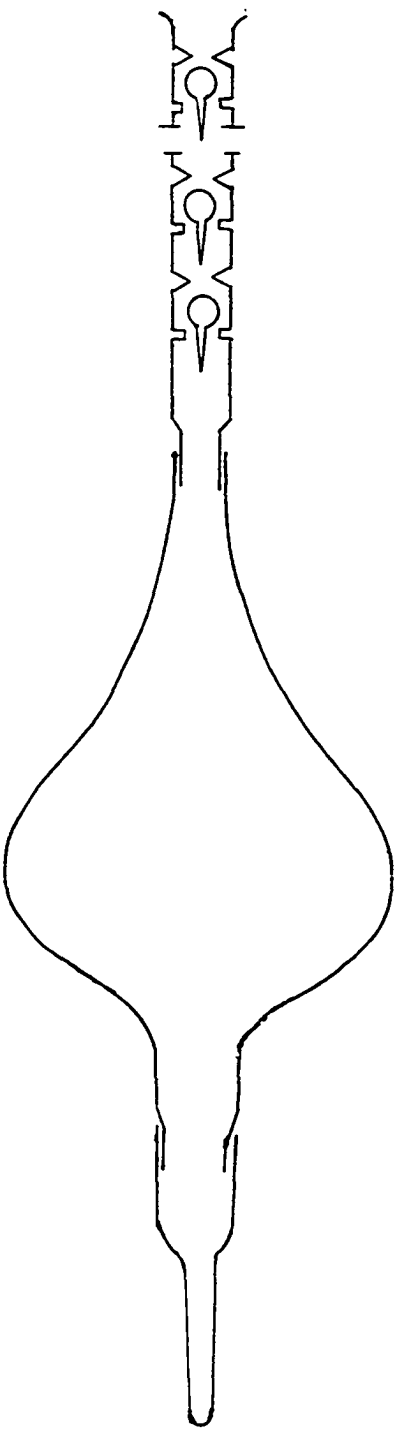

2. Chemicals and reagents

The nitrosamines that were used in this thesis were obtained from one of the following sources: Aldrich Chemical Co. of Milwaukee, Wisconsin; Eastman Organic Chemical of Rochester, New York; Matheson, Coleman and Bell of Cincinnati, Ohio. Solutions of supporting electrolyte were prepared from reagent grade acids from Fisher Scientific Co. of Fair Lawn, New Jersey. The water used was demineralized after distillation. Solutions of $NaNO_2$ were prepared as described in Section I.C.2.

3. Procedures

At the start of each working day, or after any significant decrease in sensitivity, the following procedure was used to assure reproducibility of sensitivity: (i) 0.01 M $HClO_4$ was caused to flow through the electrode, (ii) the electrode potential was scanned between +2.0 V and -2.0 V for 15 min, (iii) after completion of a negative potential sweep, the electrode potential was set to 0.10 V, (iv) 1 ml of 10^{-2} M NaI was injected into the stream flowing through the electrode and (v) the electrode potential was set to 0.40 V.

The following instrumental settings were established for the analysis of a sample: (i) eluent selection valve was switched to 5 mM NaOH, (ii) sample injection valve was switched to allow sample to be drawn into sample loop and

(iii) switching valve was set to allow flow through column 2. Flow rate of both flow streams were adjusted to 0.5 mL per min and after 5 minutes the sample was injected. After 5 more minutes (iv) turn the eluent selection valve to 0.01 M $HClO_4$, (v) set switching valve to by-pass column 1 and photolysis loop and (vi) switch sample injection valve such that flow was through the smaller by-pass loop. After NO_2^- was eluted, the settings were returned to those described in i, ii and iii.

D. Results and Discussion

1. Photolysis of nitrosamines

A method of analysis based on the determination of a photoproduct must take into account those factors affecting the production of the photoproduct. Factors which affect the determination of nitrosamine as nitrite include the following: (i) wavelength of the irradiating light, (ii) pH of the photolysis media, (iii) length of time for irradiation, (iv) concentration of the analyte, (v) the effect of different substituents on the rate of photolysis of the nitroso group and (vi) effect of photoproducts other than nitrite on the detection.

Nitrosamines have two absorption bands. One absorption band is at approximately 230 nm with the molar absorptivity equal to 7,000 (M^{-1} cm^{-1}), and the other absorption band is at approximately 350 nm with the molar absorptivity

equal to 100 (M^{-1} cm^{-1}) (85). The relative photolysis efficiencies, as determined with the PA for different wavelengths of irradiating light, are shown in Table II.4.

Table II.4. Photolysis efficiency of DPrN as a function of wavelength of irradiating light[a]

λ, nm	% Photolysis pH = 9.2	1.0 M HCl
200	13	12
235	68	19
250	40	12
280	0	
310	0	
360	0	6.7

[a]% Photolysis determined with Chromatronix UV detector.

The bandwidth of the irradiating light was 20 nm. Examination of the data clearly shows that photolysis at 230 nm is much more efficient than photolysis at 350 nm. Although the extent of photolysis at 350 nm in alkaline solutions was too low to measure with my apparatus, others have photolyzed nitrosamines at 350 nm (90, 91, 93).

The pH of the photolysis media is another factor that determines the efficiency of production of nitrite. The effect of pH on the photolysis of DPrN is clearly shown in Figure II.7. The mixing of the different buffers with the HCl produces electrolyte solutions in which the

Figure II.7. Photolysis efficiency of DPrN as a function of pH

Buffers for pH 3 through 9 were Clark and Lubs Buffers. Buffer for pH equal to 11 was a Bates and Bower Buffer.

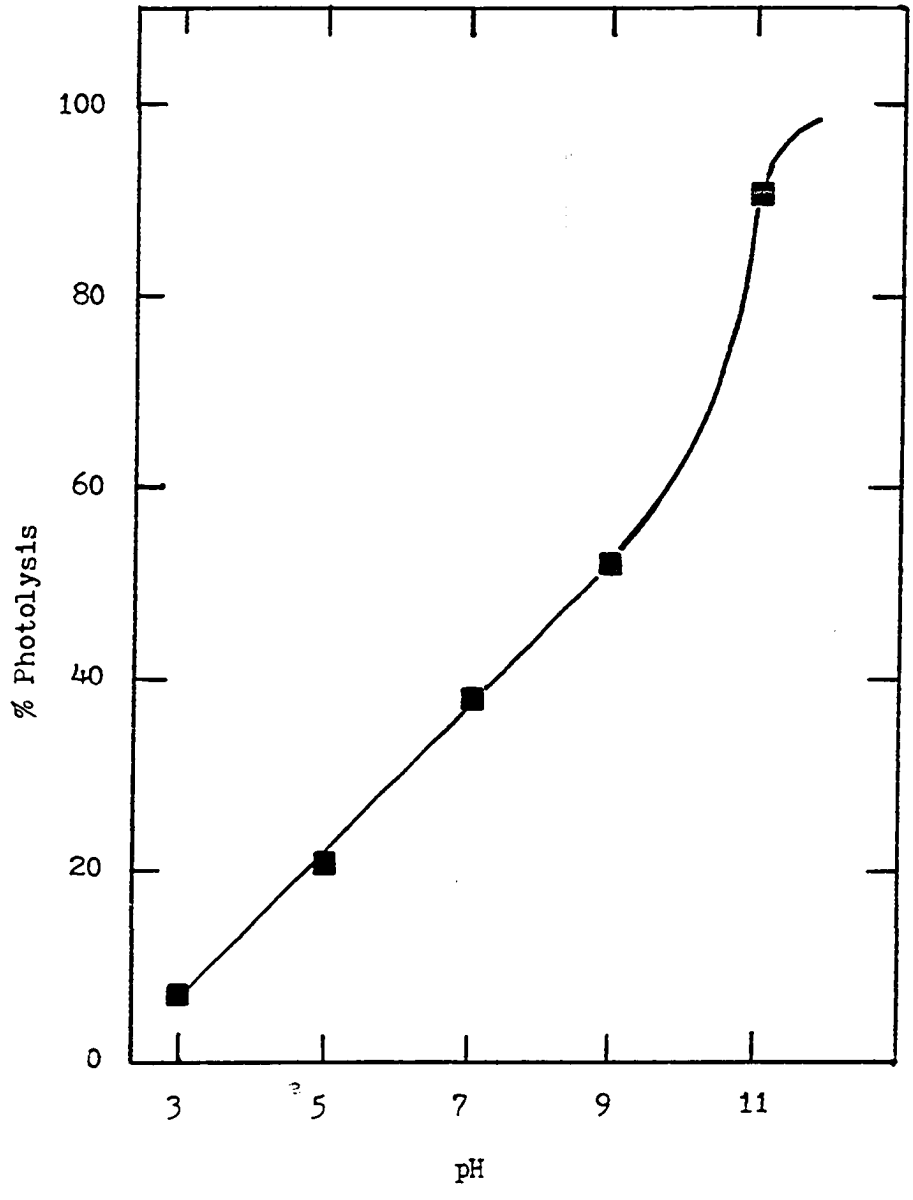
100
80
60
40
20
0
% Photolysis
3
5
7
9
11
pH

response of the detector to NO_2^- are different. To normalize the data for photolysis efficiency, the area of peaks resulting from the photolysis of DPrN was divided by the area of peaks from the injection of NO_2^-. Although the efficiency approaches 100% at high values of pH, NO_2^- is not retained on the anion-exchange columns in buffer solutions of high pH, and 5 mM NaOH was used to photolyze the nitrosamine.

The length of time that the nitrosamine was photolyzed was established by the flow rate of the eluent. This length of time is referred to as the "residence time" and was approximately 30 sec for a flow rate of 0.5 ml/min through the photolysis loop. The efficiency of the photolysis is expected to increase as the flow rate is decreased. The efficiency of photolysis for DPrN in 5 nM NaOH is shown in Table II.5. This solution was the one

Table II.5. Photolysis efficiency of DPrN[a] as a function of flow rate

Flow Rate (mL/min)	% Photolysis
0.3	97
0.4	76
0.5	65
0.8	54

[a]For injection of 0.5 µg of DPrN.

used in the analytical determination, and the reasons for the use of this solution are discussed in Section II.D.5.

Clearly, 100% photolysis was attainable at the lower flow rates. To decrease analysis time, 0.5 ml/min was commonly used for which the photolysis efficiency was approximately 65%. Although 100% photolysis efficiency is certainly desirable, complete photolysis was attainable only at the expense of increased analysis time and lower overall detection limit because of broader peaks. The photolysis efficiency was reproducible to ± 2% if the flow rate was regulated to ± 5% and was high enough that little error was introduced by small fluctuations in the photolysis efficiency.

The dependence of photolysis efficiency on concentration is certainly an important variable. A linear calibration curve is evidence that the photolysis efficiency is constant. A plot of the area of peaks resulting from photolysis of DPrN *vs.* concentration of DPrN is shown in Figure II.8. The area is linear with concentration from 5×10^{-8} M to 4.0×10^{-5} M, and this range encompasses the concentrations that would normally be encountered in the determination of nitrosamines. Because of this constant photolysis efficiency, NO_2^- can be used as the standard once the photolysis efficiency has been established. This is particularly important in the analysis of hazardous materials such as nitrosamines.

Figure II.8. Calibration curve for DPrN

Flow rate = 0.5 mL/min through photolysis loop

Pt wire electrode

Injection volume = 0.80 mL

C = Molarity

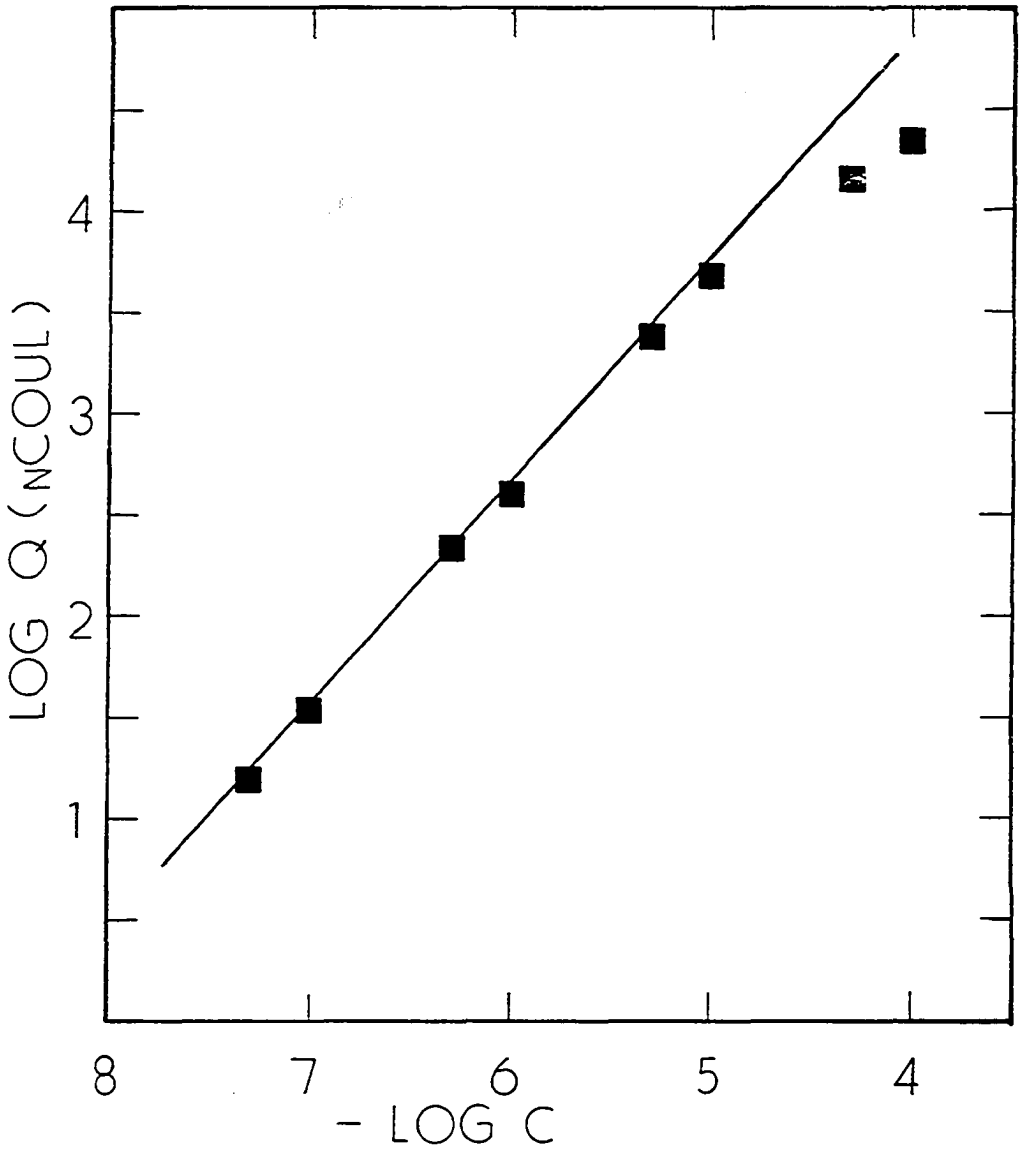
LOG Q (NCOUL)
1
2
3
4
8
7
6
5
4
- LOG C

The linearity of response has also been verified with DMN although the data is not shown here.

The rate of photolysis of a nitrosamine compound depends upon the nature of the organic substituents (88). During the photolysis, all nitrosamines should be efficiently photolyzed to ensure that they are detected. Daiber and Preussmann (87) have already shown that a large number of nitrosamines are efficiently photolyzed to nitrite (see Table II.2). To verify that the procedure developed in this thesis for the use of the PA was capable of determining all these nitrosamines, DMN, DPrN and DPhN were used as test compounds. The photolysis efficiency of these three compounds under identical conditions is shown in Table II.6. The photolysis efficiencies were large

Table II.6. Photolysis efficiencies of DMN, DPrN and DPhN (5 mM NaOH, 0.5 mL/min through photolysis loop)

Nitrosamine	% Photolysis
DMN	71
DPrN	83
DPhN	89

enough that no serious error would be incurred in a screening method.

The sensitivity of the detector for NO_2^- was observed to decrease when applied for the photo-electrochemical detection of nitrosamines. The decrease was not

observed when the nitrosamines were not photolyzed, and the decrease in sensitivity was concluded to result from the adsorption at the Pt surface of organic products of photolysis. The effect of this phenomenon is shown in Figure II.9 where DPrN was continuously passed through the detector and the shutter on the lamp was alternately opened and closed. A decrease in the faradaic current was observed as the Pt electrode was exposed to the products of photolysis. When the shutter was closed, the current decayed to the background value. The decrease in faradaic current was relatively slow after the initial decline in the current, and the changes in current were because of a decrease in the background current. The effect of adsorbing iodide on the Pt surface is also shown in Figure II.9 and shows that reproducible electrode currents were obtained when iodide was adsorbed on the electrode. Hence, iodide was adsorbed on the Pt for all experiments involving the determination of nitrosamines.

2. Isolation of nitrosamines

The goal of this research was the determination of volatile nitrosamines. The isolation procedures used were based on those reported by Fine, et al., (67) with modifications in the extraction stage and the subsequent removal of the petroleum ether. The procedure used is

Figure II.9. Effect of photoproducts on electrode current for Pt and PtI electrodes

A Pt

B PtI

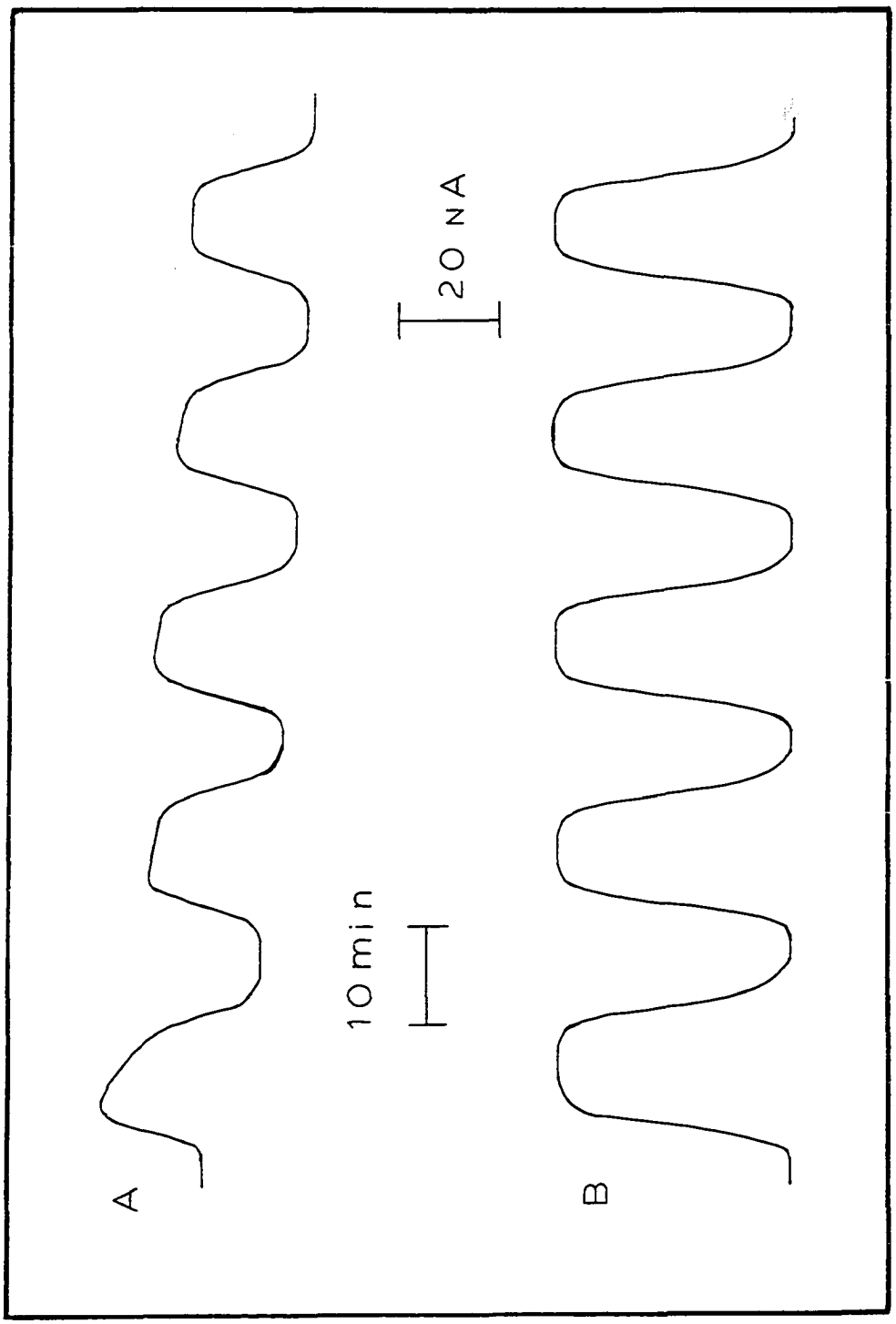
A
B
20 nA
10 min

as follows: (i) 100 g of sample was minced with a Waring Blender and placed in a 500-mL round-bottom flask; (ii) 20 mL of 0.1 M NaOH was added; (iii) 100 mL of mineral oil was added; (iv) the contents of the flask were heated under reduced pressure (1 mm Hg) at a rate such that the distillate temperature was 110°C after 45 minutes; (v) distillate was collected with a series of three cold fingers filled with liquid nitrogen; (vi) distillate was extracted three times with a volume of petroleum ether equal to that of the distillate and washings; (vii) petroleum ether was removed with a Kuderna-Danish evaporator over a steam-bath, and the nitrosamines were left in the water (2 mL) added to the Kuderna-Danish evaporator before addition of the petroleum ether; (viii) any oily residues left after removal of the petroleum ether were extracted three times with an equal volume of acetonitrile, and the acetonitrile was removed in the same way the petroleum ether was removed; (ix) water and washings were transferred to a 10-mL volumetric flask; (x) the solution was made 5 mM in NaOH by addition of 0.1 mL of 0.10 M NaOH to the contents of the volumetric flask and (xi) the contents of the volumetric flask were diluted to volume with water.

Revision of the procedure described by Fine, et al., (67) was necessary for several reasons. In the procedure

of Fine, et al., the nitrosamines remained in methylene chloride (CH_2Cl_2); whereas, only an aqueous solution can be injected into PA. The injection of water saturated with methylene chloride was observed to give a peak corresponding to 10^{-6} M DPrN when the solution was photolyzed. The substance responsible for the peak was observed to be retained by the anion-exchange column and was concluded to be OCl^- produced from the photolysis of CH_2Cl_2. The CH_2Cl_2 is soluble in water to the extent of 2% and was observed to be present in the aqueous solution from step vii of the procedure when CH_2Cl_2 was used to extract the nitrosamines. Injection of aqueous solutions of CH_2Cl_2 into the PA was observed to cause retention of the nitrosamines on column 1. The CH_2Cl_2 was concluded to adsorb onto the polystyrene resin and cause partitioning of the nitrosamines onto the anion-exchange resin. Therefore, CH_2Cl_2 was not used to extract the nitrosamines, and the use of petroleum ether for the extractant was investigated.

Because petroleum ether had not been used previously for the extraction of nitrosamines, some additional elaboration was required. Values of extraction coefficients determined experimentally are given in Table II.7 for various nitrosamines. The recovery for three extractions with equal volumes of water and petroleum ether is predicted

Table II.7. Extraction coefficients and recoveries for extraction step

Compound	E_A	R^a (%)	R^b (%)
DPrN	2.3	97.2	95[c], 80[d]
DMN	0.8	82.8	---
DPhN	20	99.9	---

[a]Calculated from Equation II.9.

[b]Experimentally determined, includes step involving removal of petroleum ether.

[c]Concentration of DPrN = 10^{-5} M.

[d]Concentration of DPrN = 10^{-7} M.

by Equation II.9.

$$R_{A,\%} = 100\{1 - [1/(E_A + 1)]^3\} \qquad \text{(II.9)}$$

where E_A = extraction coefficient and $R_{A,\%}$ = percent recovery. For DPrN at the ppm level, the experimentally determined recovery was 95% as compared to the calculated value of 97.2%. The recovery values given in Table II.7 are acceptable for a screening method.

The recovery of nitrosamines from the food matrix was determined by spiking tuna with DPrN and then analyzing the spiked tuna as previously described. The recovery obtained for different concentrations of DPrN is given in Table II.8. These recoveries are similar to those obtained by Fine, et al., (67) if the additional loss of nitrosamines in the removal of the petroleum ether is taken into account (Table II.7).

Table II.8. Recovery of DPrN from tuna

ppb of DPrN in tuna	% Recovery
32.5	80 ± 2
6.5	50 ± 5

3. Design of photoanalyzer

The photoanalyzer shown in Figure II.2, was designed to minimize interferences. The sequence of events occurring in the analysis of a sample were: (i) sample was injected into a stream of 5 mM NaOH; (ii) nitrosamine passed through column 1 and entered the photolysis loop where the nitrosamine was photolyzed to nitrite; (iii) nitrite from photolysis was retained on column 2; (iv) eluent was switched to 0.01 M $HClO_4$, and column 1 was switched out of the flow stream and (v) NO_2^- was eluted from column 2 and was detected by a Pt-electrode detector. To interfere a species must: (i) elute through column 1 with 5 mM NaOH, (ii) photolyze to produce some species retained by column 2, (iii) produce a photoproduct that is eluted from column 2 with 0.01 M $HClO_4$, and (iv) produce a photoproduct that is electroactive under the conditions used.

Essentially, only those compounds that photolyze to produce anions that are electroactive will interfere. Some interferences do exist and are discussed in Section II.D.4.

4. Interferences

A large number of compounds can exist in extracts from food samples. Several organic nitrogen compounds yield nitrite as an inorganic product of photolysis (see Table II.3). Other compounds could interfere by having electroactive anions as photoproducts. Compounds which were tested for their interference are listed in Table II.9 along with the reason that they do or do not interfere. To check for interference, solutions of the compounds of a concentration of at least 0.01 M (or saturated) were injected, and the sensitivity of the detector was such that 10^{-6} M nitrosamine could be easily detected. The compounds that do interfere are listed in Table II.10, and a Response Ratio (RR) defined by Equation II.10 is given for each interfering compound.

$$RR = \frac{\text{(ncoul/nmole) for interfering species}}{\text{(ncoul/nmole) for DPrN}} \qquad \text{(II.10)}$$

Of the interfering compounds, nitro-compounds represent the most serious interference. Both aliphatic and aromatic nitro-compounds are photolyzed, and this procedure could be modified for the determination of all nitro-compounds. The interference by CH_2Cl_2 is not serious but does prevent the use of CH_2Cl_2 as an extractant for this procedure.

Nitro-compounds are not likely to be present in foods because of the harsh conditions under which nitro-compounds

Table II.9. Compounds checked for interference

Compound	Compound Electroactive/ Photoproduct Electroactive	Interferes in Procedure
NO_3^-	no/yes	no[a]
NH_3	no/yes	no[b]
$Cr_2O_7^{2-}$	yes/--	no[a]
MnO_4^-	yes/--	no[a]
IO_3^-	yes/--	no[a]
NH_2OH	no/--	no
benzaldehyde Ø-CHO	no/--	no
glutamic acid $HO_2CCH_2CH_2CH(NH_2)CO_2H$	no/--	no
cysteine $HSCH_2CH(NH_2)COOH$	yes/--	no[c]
cystine $HO_2CCH(NH_2)CH_2SSCH_2CHCNH_2$	yes/yes	no[c]
citric acid $HOOCC(CH_2COOH)_2OH$	yes/--	no[c]
glycine NH_2CH_2COOH	no/--	no
pyrazine $C_4H_4N_2$	no/--	no
nitromethane CH_3NO_2	no/yes	yes[d]

[a] Retained on column 1.

[b] Eliminated by deaeration.

[c] Not retained on column 2.

[d] Photoproduct retained on column 2 and eluted with acid.

Table II.9. continued

Compound	Compound Electroactive/ Photoproduct Electroactive	Interferes in Procedure
nitrobenzene $\emptyset-NO_2$	no/yes	yes[d]
methylene chloride CH_2Cl_2	no/yes	yes[d]
amyl nitrite $CH_3CH_2CH_2CH_2CH_2ONO$	no/yes	no[a]
propyl nitrate $CH_3CH_2CH_2ONO_2$	no/yes	no[a]

Table II.10. Response Ratio for interfering compounds[a]

Compound	RR
CH_3NO_2	1.2
$\emptyset-NO_2$	0.28
CH_2Cl_2	4×10^{-6}
NH_3[b]	0.96

[a]Determined at the 10^{-6} M level for all except $MeCl_2$, photolysis media was 5 mM NaOH.

[b]Does not normally interfere because of non-aqueous extraction and deaeration procedures.

are produced (95). If nitro-compounds are present, it is likely that their presence would represent a serious health hazard because of their toxicity (96).

The photolysis efficiency as a function of pH is given for some of the interfering compounds in Figure II.10. All the compounds showed an increase in photolysis efficiency as the pH was increased. Under acidic conditions, N_2O is produced in the photolysis of nitrosamines as described by Equation II.11 (97-99). Perhaps under alkaline

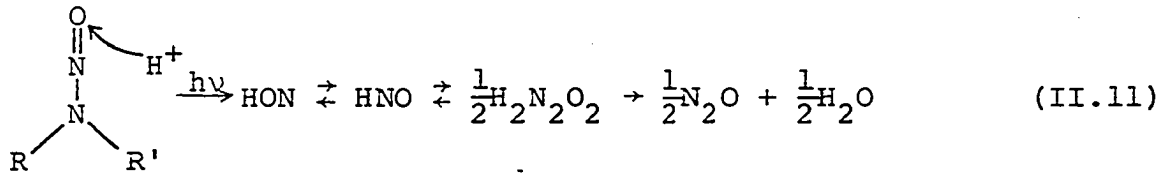

(II.11)

conditions, the reaction described by Equation II.12 occurs.

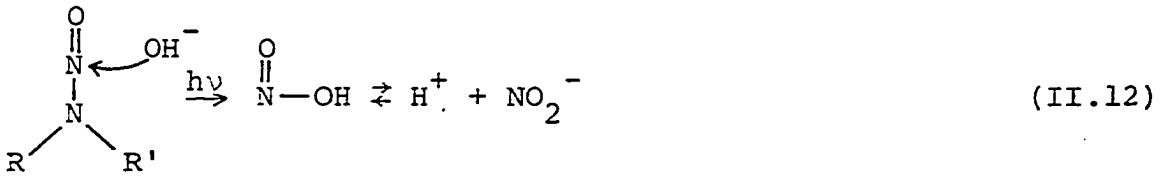

(II.12)

The RR would be slightly larger for CH_3NO_2 and $\emptyset$-NO_2 if the photolysis were performed in a solution with a pH equal to 5, but the analytical sensitivity would be less. The RR for these nitro-compounds could also be increased with the use of light of a wavelength of 350 nm for the photolysis (91).

The most unusual interference observed was that of NH_3. Most research on the photolysis of NH_3 reported in

Figure II.10. Photolysis efficiencies for interfering compounds as a function of pH

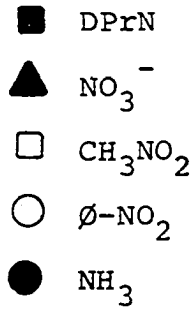

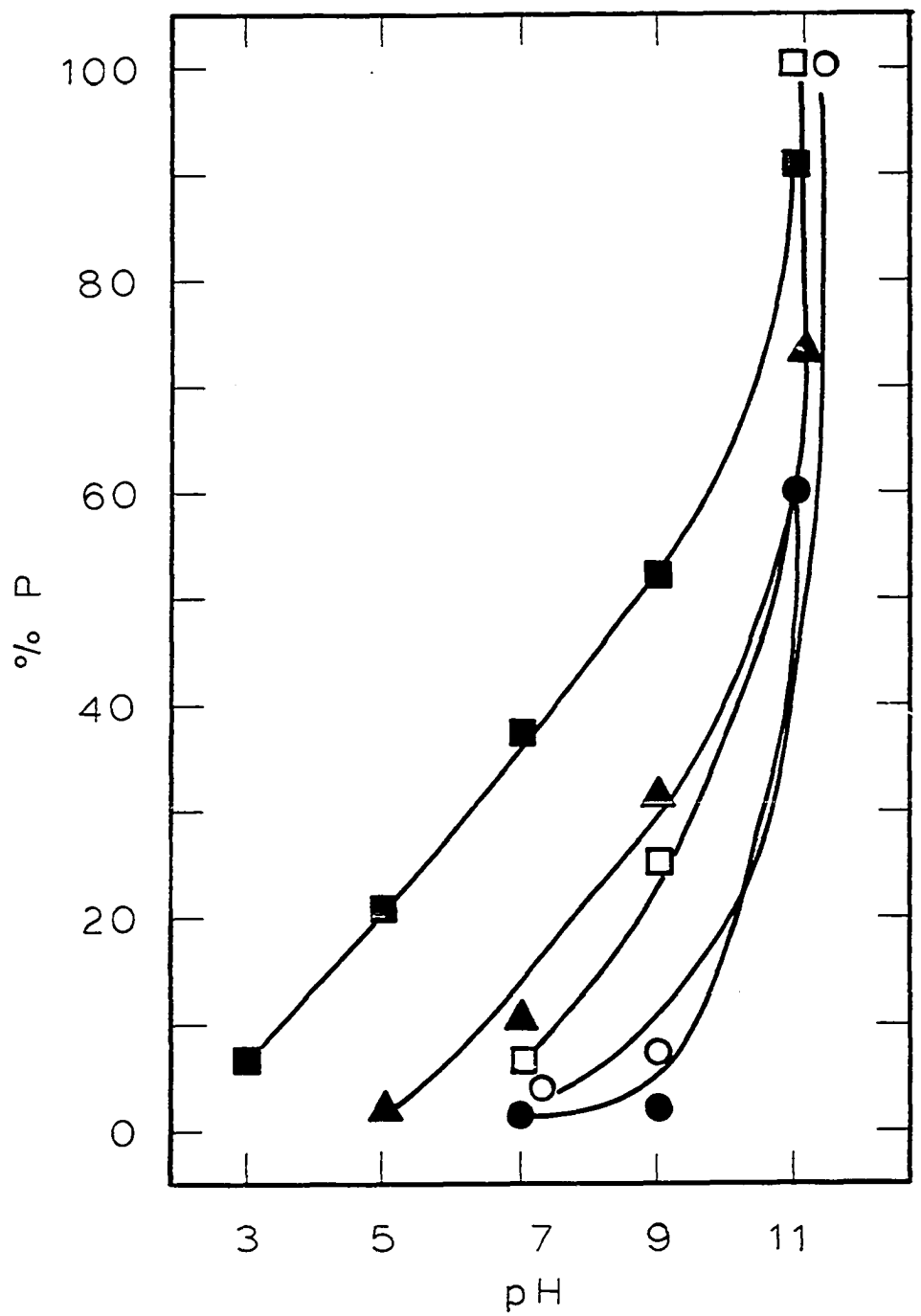
100
80
60
40
20
0
% P
3
5
7
9
11
pH

the chemical literature refers to the vacuum-ultraviolet photolysis of NH_3 in which H_2 is a product (100). If H_2 is also produced in the photolysis conditions used here, a photolysis reaction is given in Equation II.13 which is consistent with observations given here.

$$NH_3 + 2H_2O \xrightarrow{h\nu} HNO_2 + 3H_2 \qquad \text{(II.13)}$$

5. Determination of volatile nitrosamines in food samples

Several factors entered into the selection of conditions for the analytical determination described in this thesis. Low detection limit, a reasonable analysis time and freedom from interferences were factors that were considered.

To make the detection limit as low as possible, the nitrosamines should be completely photolyzed. This can only be done by either performing the photolysis at a high pH (Figure II.7) or by operating at a low flow rate (Talbe II.5). With the use of an anion-exchange column, the use of high concentrations of NaOH or buffers eluted the NO_2^-, and the separation scheme outlined in Section II.D.3 did not work. The use of low flow rates made the time required for analysis of a sample excessively long. Even with a flow rate of 0.5 ml/min through the photolysis loop, 30 min was required for the analysis of a sample. Thus, a compromise had to be made. The photolysis media

was made as alkaline as possible without the elution of the NO_2^- occurring before the nonretained species have had time to pass through the system. A solution 5 mM in NaOH was found to meet these requirements. For an anion-exchange column of different characteristics, a different concentration of NaOH would be optimum. A flow rate of 0.5 ml/min was used because relatively high photolysis efficiencies were obtained at this flow rate, the change in photolysis efficiency with change in flow rate was smaller than at lower flow rates (see Table II.5), an acceptable analysis time was obtained using this flow rate and reasonably sharp peaks for the elution of NO_2^- were obtained at this flow rate.

The selection of a solution for the elution of NO_2^- from the anion-exchange column was dependent on two factors: (i) concentration of the eluent should be kept as small as possible to minimize charging currents and (ii) for optimum analytical sensitivity, the NO_2^- should be eluted from the column in as narrow a band as possible. Obviously, these two factors are in direct conflict because the band-width of the eluting peak is narrower for concentrated eluent solutions. The use of an eluent that strongly interacts with the anion-exchange resin helps minimize the need for concentrated eluent solutions. Such an eluent is $HClO_4$. The ClO_4^- strongly interacts with

the anion-exchange resin (101), and the decreased pH produces HNO_2 (pK_a = 3.4) which is not retained. For 5 mM NaOH as a photolysis media, 0.01 M $HClO_4$ eluted the NO_2^- from the anion-exchange column in a band 1-2 min wide at a flow rate of 0.5 mL/min without giving excessive charging peaks.

The isolation procedure described in Section II.D.2 was used to analyze samples of tuna, fried bacon and bacon grease. In the procedure of Section II.D.2, 100 g of sample is used and the final volume is 10 mL after all stages of the isolation procedure are completed. This increases the concentration of the nitrosamines by a factor of ten. Further reduction of the sample volume would be of no benefit because large volumes are easily injected into the PA, and the NO_2^- is concentrated on the anion-exchange column. The presence of 1 ppb DPrN in a food sample would result in the isolation of 100 ng of DPrN. The injection of 0.80 mL of the sample extract would represent the injection of 8 ng of DPrN. This 8 ng would correspond to the injection of a solution of 7.7×10^{-8} M DPrN. The isolation procedure was also performed without the addition of any food to determine the reagent blank. The reagent blank was found to be < 0.2 ppb. The results of the determination of food materials is shown in Table II.11. The amounts of nitrosamines found are really quite

Table II.11. Results of the analysis of fried bacon, bacon grease and tuna for volatile nitrosamines

Material	Concentration of nitrosamine[a] (ppb)
fried bacon	1.3
bacon grease	3.0
tuna	0.5

[a]Calculated as DPrN.

low considering that all volatile nitrosamines are determined by this procedure. The low concentrations of nitrosamines found also indicates the absence of large quantities of nitro-compounds.

Chromatograms for the injection of the sample extract resulting from the isolation of nitrosamines from bacon grease, the injection of 10^{-7} M DPrN and the injection of 5 mM NaOH are shown in Figure II.11. The peak for the analysis of bacon grease corresponds to 3 ppb DPrN. The injection of this sample with the shutter closed on the Xenon lamp resulted in the same background as for the injection of 5 mM NaOH demonstrating that the peak is the result of some photoproduct. For all these peaks, the steady-state noise was negligible. The steady-state noise for this Pt-wire detector was much less than for the tubular Pt detector as can be seen by comparing Figure II.11 and

Figure II.11. Chromatograms for low levels of nitrosamines

A Injection of 10^{-7} M DPrN
0.5 nA/in

B Injection of 5×10^{-3} M NaOH
0.5 nA/in

C Injection of extract for bacon grease
1.0 nA/in

1 Injection of sample

2 Switch eluent from 5 mM NaOH to 0.01 M $HClO_4$; by-pass column 1 and the photolysis loop

3 Allow eluent to flow through column 1 and the photolysis loop

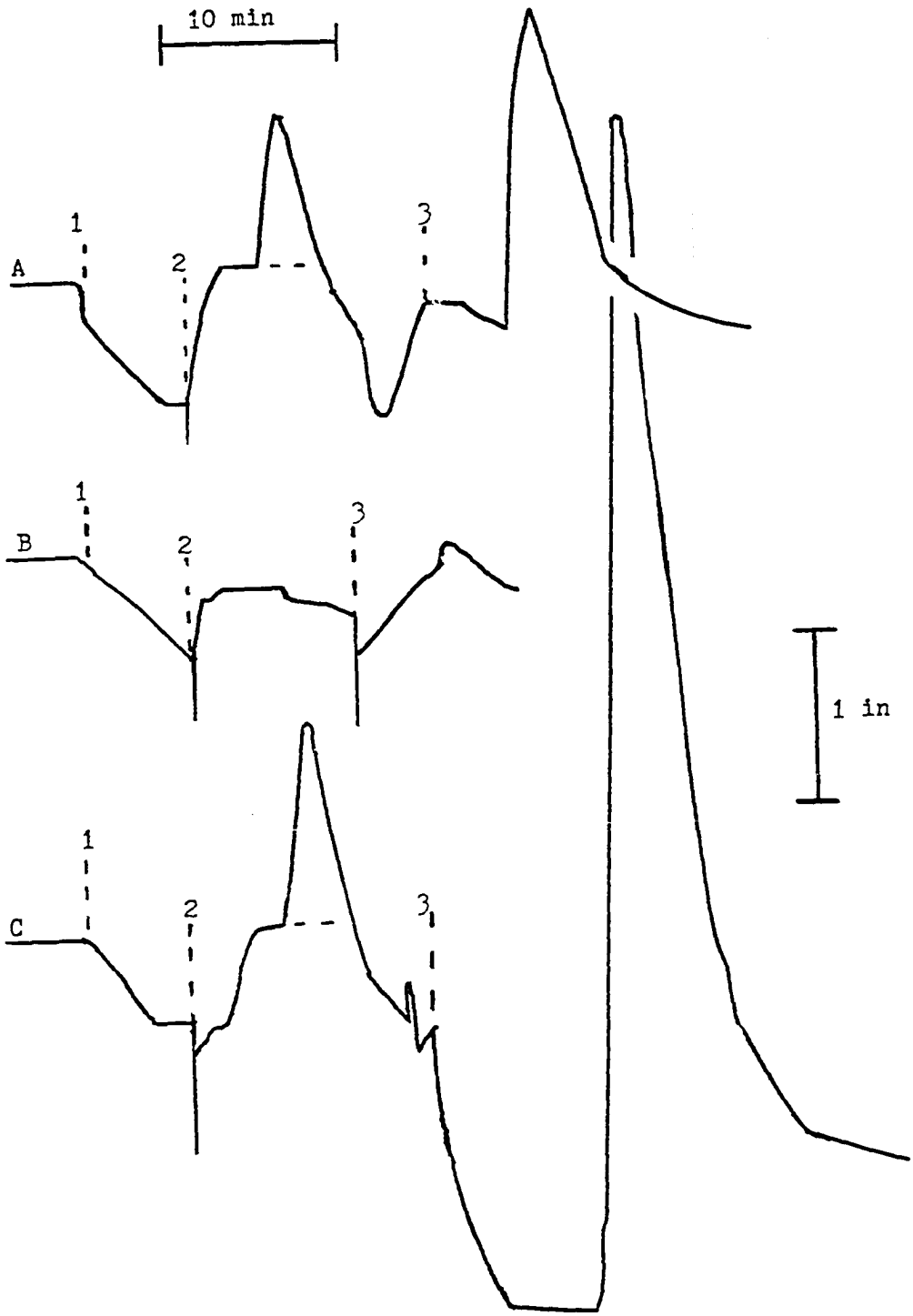
10 min
A
B
C
1
2
3
1 in

I.20. However, the short-term drifts in the background current because of changes in the composition of the eluent stream limited the detection limit. The precision of the determination at the ppb level was determined from the injection of extracts from the analysis of bacon. The relative standard deviation for the injection of three aliquots of this extract was 15 pph. Thus, the bacon was determined to contain 1.3 ± 0.2 ppb nitrosamine calculated as DPrN.

The blank shown in Figure II.11 was essentially zero, although this was not always the case. The preparation of new eluent solutions, the deaeration of the eluent solutions or the deaeration of the solutions injected usually solved any blank problem.

Another problem was the adsorption of nitrosamines by the first column after several injections (more than 10) of sample extract had been made. There was always a small amount of oily material (0.5 ml) left at the top of the volumetric flask after all the sample pretreatment steps were performed. Perhaps, a small part of that oily material was injected into the PA and adsorbed on the first column. The nitrosamine was then partitioned between the aqueous phase and the oily material adsorbed on the ion-exchange resin. This problem was detected by comparing the peak height for the injection of standards

with those obtained previously. The easiest solution to the problem was to simply replace the column packing. The use of chemibonded ion-exchange resins, where there are no aromatic parts of the resin for adsorption to occur, could solve the problem.

Another occasional problem was the appearance of a large anodic peak prior to the elution of the NO_2^-. The peak was so large that the current did not return to the background value before the NO_2^- was eluted off by the 5 mM NaOH. The problem was solved by allowing only the minimum amount of time for the nitrosamine to pass through the photolysis loop before switching column 1 and the photolysis loop out of the flow stream. Another solution was to use water as the photolysis media. A small sacrifice in photolysis efficiency resulted.

E. Conclusions

A screening method for the determination of nitrosamines by a photo-electrochemical method was developed in this thesis. A procedure is described for the analysis of food samples for volatile nitrosamines. The analytical procedure was applied to the analysis of fried bacon. The bacon was determined to contain 1.3 ppb nitrosamine calculated as N-nitrosodipropylamine. The relative standard deviation for the analysis of the aqueous solution

resulting from the removal of nitrosamines from the bacon was 15 pph. The detection limit was determined to be 0.2 ppb for N-nitrosodipropylamine. The recovery for 6.5 ppb N-nitrosodipropylamine was 50%.

The method was free from interferences, such as O_2, H^+, NO_2^- and NO_3^-, that have interfered in other procedures based either on photolysis of nitrosamines or electrochemical detection of nitrosamines. Nitro-compounds were determined to be the only serious interferences in the analytical method.

III. SUGGESTIONS FOR FUTURE WORK

The detection limit for the determination of nitrosamines was limited by changes in the background current because of charging currents associated with changes in the eluent composition. A lower concentration of eluent would be required for the low-capacity anion-exchange columns developed by Dionex, Inc., and smaller changes in the background current would be observed. The use of gradient elution would also help minimize these charging currents.

The use of a Au electrode would also lower the detection limit. The reduction of HNO_2 at a Au electrode is a 4-electron process. Thus, a four-fold increase in the faradaic current over that obtained with a Pt electrode is obtained.

Greater specificity for nitrosamines could be obtained by photolysis at 350 nm. A source with a high output of light in the 350 nm range would be required to offset the decreased absorption in this wavelength region.

Methods for the determination of nitro-compounds, NO_3^- and NH_3 at the ppb level can be developed based on information given in this thesis. The feasibility of determining other classes of compounds by photolysis to some common species should be investigated. The use of

high-output sources could make many inefficient photolytic processes amenable to this type of analysis. In-stream, gas-phase photolysis followed by GC or GC/MS could be useful in the characterization of complex molecules.

The screening method described in this thesis could be adapted to a colorimetric procedure for the determination of nitrosamines. The reagents necessary for the procedure could be mixed with the eluent from the anion-exchange column in much the same way that the acid is mixed with the eluent in this procedure. Many procedures exist for the colorimetric determination of nitrosamines (102), and several should be suitable for an automated procedure such as that developed by Fan and Tannenbaum (90). Such a method would have the advantages of concentration of the NO_2^- on an anion-exchange column and greater freedom from interferences as compared to other colorimetric procedures. Detection limits comparable to those obtained electrochemically are obtainable based on a molar absorptivity of 38,000 (M^{-1} cm^{-1}) and a path-length of 1 cm.

A differential method for the determination of NO and NO_2 in air based on the detection of NO and NO_2 at a Pt electrode and NO_2 at a Au electrode could be developed. The two electrodes could be incorporated into the same detector, and the concentrations of NO and NO_2 would be determined simultaneously.

IV. BIBLIOGRAPHY

1. J. M. Sedlak and K. F. Blurton, J. Electrochem. Soc., 123, 1476 (1976).

2. W. L. Jolly, Inorganic Chemistry of Nitrogen (W. A. Benjamin, Inc., New York, 1964), p. vii.

3. C. B. Colubrn, Developments in Inorganic Nitrogen Chemistry (Elsevier Scientific Publishing Co., New York, 1973), Volume I and II.

4. W. L. Jolly, Inorganic Chemistry of Nitrogen (W. A. Benjamin, Inc., New York, 1964).

5. J. R. Partington, A Text-Book of Inorganic Chemistry (Macmillan & Co., New York, 1957), Sixth ed., pp. 506-562.

6. F. A. Cotton and G. Wilkinson, Advanced Inorganic Chemistry (Interscience Publishers, New York, 1966), Second ed., pp. 323-358.

7. W. M. Latimer, Oxidation Potentials (Prentice-Hall, Englewood Cliffs, New Jersey, 1952), Second ed., pp. 90-104.

8. W. L. Jolly, Inorganic Chemistry of Nitrogen (W. A. Benjamin, New York, 1964), p. 75.

9. J. Masek, Fresenius Z. Anal. Chem., 224, 99 (1967).

10. W. M. Latimer, Oxidation Potentials (Prentice-Hall, Englewood Cliffs, New Jersey, 1952), Second ed., p. 101.

11. L. E. Topol, K. B. Oldham and R. G. Alder, J. Inorg. Nucl. Chem., 30, 2977 (1968).

12. C. Chien-Chung and J. H. Lunsford, J. Am. Chem. Soc., 93, 6794 (1971).

13. P. H. Kasai and R. J. Bishop, J. Am. Chem. Soc., 94, 5560 (1972).

14. W. E. Swartz and M. Youssefi, J. Electron. Spectrosc. Relat. Phenom., 8, 61 (1976).

15. G. Stedman, J. Chem. Soc. (Lond.), 2949 (1959).

16. N. S. Bayliss, R. Dingle, D. W. Watts and R. J. Wilkie, Aust. J. Chem., 16, 933 (1963).

17. C. A. Bunton and G. Stedman, J. Chem. Soc. (Lond.), 2440 (1958).

18. W. R. Angus and A. H. Leckie, Proc. R. Soc. Lond., 2576 (1950).

19. D. J. Millen, J. Chem. Soc. (Lond.), 2600 (1950).

20. T. A. Turney and G. A. Wright, Chem. Rev., 59, 497 (1959).

21. R. A. Robinson and R. H. Stokes, Electrolyte Solutions (Academic Press, Inc., 1955), pp. 491, 504.

22. J. F. Bunnett, J. Am. Chem. Soc., 83, 4956 (1961).

23. N. S. Bayliss and D. W. Watts, Aust. J. Chem., 9, 319 (1956).

24. H. Kobayaski, N. Nobutsune, K. Hara, T. Niki and K. Kitano, Nippon Kagaku Kaishi, 3, 383 (1976).

25. N. S. Bayliss and D. W. Watts, Aust. J. Chem., 16, 927 (1963).

26. T. A. Turney and G. A. Wright, J. Chem. Soc. (Lond.), 2415 (1958).

27. W. L. Jolly, Inorganic Chemistry of Nitrogen (W. A. Benjamin, Inc., New York, 1964), p. 80.

28. H. N. Heckner, J. Electroanal. Chem., 44, 9 (1973).

29. Handbook of Chemistry and Physics, edited by R. C. Weast, (Chemical Rubber Co., Cleveland, Ohio, 1969), Fiftieth ed., p. D-112.

30. F. A. Cotton and G. Wilkinson, Advanced Inorganic Chemistry (Interscience Publishers, New York, 1966), Second ed., p. 347.

31. G. Bianchi, T. Mussini and C. Traini, Chim. Ind. (Milan), 45, 1333 (1963).

32. T. Mussini and G. Casarini, Chim. Ind. (Milan), 47, 600 (1965).

33. L. E. Topol, R. A. Osteryoung and J. H. Christie, J. Electrochem. Soc., 112, 861 (1965).

34. G. Schmid and U. Neumann, Z. Phys. Chem. (Leipz.), 54, 150 (1967).

35. G. Schmid and M. A. Lobeck, Ber. Bunsenges. Phys. Chem., 73, 189 (1969).

36. N. N. Savodnik, V. A. Shepelin and Ts. I. Zalkind, Sov. Electrochem., 7, 408 (1971).

37. H. N. Heckner and G. Schmid, Electrochim. Acta, 16, 131 (1971).

38. D. Dutta and D. Landolt, J. Electrochem. Soc., 119, 1320 (1972).

39. C. T. Garcia, A. J. Calandra and A. J. Arvía, Electrochim. Acta, 17, 2184 (1972).

40. R. G. Gadde and S. Bruckenstein, J. Electroanal. Chem., 50, 163 (1974).

41. L. J. J. Janssen, M. M. J. Pieterse and E. Barendrecht, Electrochim. Acta, 22, 27 (1977).

42. N. N. Savodnik, V. A. Sheplin and Ts. I. Zalkind, Sov. Electrochem., 7, 564 (1971).

43. E. Barendrecht and J. F. van der Plas, Rec. Trav. Chim. Pays-Bas, 96, 133 (1977).

44. J. H. Larochelle, Ph.D. Thesis, Iowa State University, Ames, Iowa, 1977.

45. M. D. Seymour, J. P. Sickafoose and J. S. Fritz, Anal. Chem., 43, 1734 (1971).

46. D. C. Johnson and J. H. Larochelle, Talanta, 20, 959 (1973).

47. H. L. Johnston and W. F. Giauque, J. Am. Chem. Soc., 51, 3196 (1929).

48. D. C. Johnson, Introduction to Electrochemical Methods of Analysis (University Bookstore, Ames, Iowa, 1977), p. IV-71.

49. W. L. Jolly, Inorganic Chemistry of Nitrogen (W. A. Benjamin, Inc., New York, 1964), p. 77.

50. V. G. Levich, Physiochemical Hydrodynamics (Prentice-Hall, Englewood Cliffs, New Jersey, 1962).

51. D. C. Johnson and E. W. Resnick, Anal. Chem., 49, 1918 (1977).

52. R. N. Adams, Electrochemistry at Solid Electrodes (Marcel-Dekker, Inc., New York, 1969), pp. 43-64.

53. J. M. Barnes and P. N. Magee, Brit. J. Med., 11, 167 (1954).

54. S. S. Mirvish, J. Nat. Cancer Inst., 44, 633 (1970).

55. J. G. Sebranek and R. G. Cassens, J. Milk Food Technol., 36, 76 (1973).

56. W. E. Phillips, J. Agr. Food Chem., 16, 88 (1968).

57. I. A. Wolff and A. E. Wasserman, Science, 177, 15 (1972).

58. T. Fazio, R. H. White and J. W. Howard, J. Assoc. Offic. Anal. Chem., 54, 1157 (1971).

59. T. Fazio, L. R. Dusold and J. W. Howard, J. Assoc. Offic. Anal. Chem., 56, 919 (1973).

60. W. Fiddler, Toxicol. Appl. Pharmacol., 31, 352 (1975).

61. N. P. Sen, D. C. Smith and L. Schwinghamer, Food Cosmet. Toxicol., 7, 301 (1969).

62. G. Hawksworth and M. J. Hill, J. Biochem. (Tokyo), 122, 28P (1971).

63. Chem. Eng. News, 55, 18 (1977).

64. Chem. Eng. News, 54, 33 (1976).

65. R. B. Martin and M. O. Tashdjian, J. Phys. Chem., 60, 1028 (1956).

66. D. H. Fine, R. Ross, D. P. Rounbehler, A. Silvergleid and L. Song, J. Agr. Food Chem., 24, 1069 (1976).

67. D. H. Fine, D. P. Rounbehler and P. E. Oettinger, Anal. Chim. Acta, 78, 383 (1975).

68. T. Fazio, J. N. Damico, J. W. Howard, R. H. White and J. O. Watts, J. Agr. Food Chem., 19, 250 (1971).

69. D. H. Fine, D. P. Rounbehler and N. P. Sen, J. Agr. Food Chem., 24, 980 (1976).

70. G. B. Cox, J. Chromatogr., 83, 471 (1973).

71. N. P. Sen, D. C. Smith and L. Schwinghamer, J. Can. Inst. Food Technol., 3, 66 (1970).

72. R. Preussmann, D. Daiber and H. Hengy, Nature, 201, 502 (1964).

73. T. A. Gough and K. Sugden, J. Chromatogr., 109, 265 (1975).

74. C. J. Dooley, A. E. Wasserman and S. Osman, J. Food Sci., 38, 1096 (1973).

75. T. A. Gough and K. S. Webb, J. Chromatogr., 79, 57 (1973).

76. D. H. Fine, D. Lieb and F. Rufeh, J. Chromatogr., 107, 351 (1975).

77. D. H. Fine, F. Rufeh, D. Lieb and D. P. Rounbehler, Anal. Chem., 47, 1188 (1975).

78. D. H. Fine and D. P. Rounbehler, J. Chromatogr., 109, 271 (1975).

79. M. J. Downes, M. W. Edwards, T. S. Elsey and C. L. Walters, Analyst, 101, 742 (1976).

80. N. D. McGlashan, C. L. Walters and A. E. McLean, Lancet, 2, 1017 (1968).

81. N. D. McGlashan, R. L. Patterson and A. A. Williams, Lancet, 2, 1138 (1970).

82. C. L. Walters, E. M. Johnson and N. Ray, Analyst, 95, 485 (1970).

83. S. K. Chang and G. W. Harrington, Anal. Chem., 47, 1857 (1975).

84. K. Hasebe and J. Osteryoung, Anal. Chem., 47, 2412 (1975).

85. W. S. Layne, J. H. Jaffé and H. Zimmer, J. Am. Chem. Soc., 85, 435 (1962).

86. W. S. Layne, H. H. Jaffé and H. Zimmer, J. Am. Chem. Soc., 85, 1816 (1962).

87. D. Daiber and R. Preussmann, Z. Anal. Chem., 206, 344 (1964).

88. D. T. Burns and G. V. Alliston, J. Food Technol., 6, 433 (1971).

89. M. Daniels, R. V. Meyers and E. V. Belardo, J. Phys. Chem., 72, 389 (1968).

90. T. Y. Fan and S. R. Tannenbaum, J. Agr. Food Chem., 19, 1267 (1971).

91. J. Sander, Z. Physiol. Chem., 348 (1967).

92. M. F. Fox, Quart. Rev. (Lond.), 24, 565 (1970).

93. R. C. Doerr and W. Fiddler, J. Chromatogr., 140, 284 (1977).

94. D. C. Johnson and E. W. Resnick, Anal. Chem., 44, 637 (1972).

95. W. M. Weaver in The Chemistry of the Nitro and Nitroso Groups, edited by H. Feuer, (Interscience Publishers, New York, 1970), Part 2, Chapter 1.

96. R. E. Gosselin, H. C. Hodge, R. P. Smith and M. N. Gleason, Clinical Toxicology of Commercial Products (The Williams and Wilkins Co., Baltimore, Maryland, 1976), Fourth ed., pp. 249-255.

97. Y. L. Chow, Can. J. Chem., 45, 53 (1967).

98. M. P. Lau, A. J. Cessna, Y. L. Chow and R. W. Yip, J. Am. Chem. Soc., 93, 3808 (1971).

99. T. Axenrod and G. W. Milne, Tetrahedron, 24, 5775 (1968).

100. J. G. Calvert and J. N. Pitts, Photochemistry (John Wiley and Sons, 1966), p. 203.

101. S. Peterson, Ann. N. Y. Acad. Sci., 57, 148 (1953).

102. E. Sawicki, T. W. Stanley and J. Praff, Talanta, 10, 641 (1963).

103. J. O'M. Bockris and A. K. N. Reddy, Modern Electrochemistry (Plenum Publishing Corp., New York, 1970), p. 380.

104. Lange's Handbook of Chemistry, edited by J. A. Dean, (McGraw-Hill Co., New York, 1973), Eleventh ed., pp. 10-97, 10-132.

V. ACKNOWLEDGEMENTS

I would like to sincerely thank Dr. Dennis C. Johnson for his support and criticism during the course of my graduate career. Credit goes to Dr. John Larochelle for bringing to my attention the reduction of HNO_2 at Pt in 3.0 M HCl. Special thanks go to the members of Dr. Johnson's research group for their many discussions both useful and otherwise.

The financial support through grant GP-40646X from the National Science Foundation is gratefully acknowledged.

A special note of appreciation goes to my wife, Ronda, for her assistance during the completion of this work.

VI. APPENDIX

The limiting current observed at a RDE depends on the viscosity (η) of the media. The Levich Equation describes the limiting current obtained for a RDE (see Section I.D.3). The kinematic viscosity (ν) and the

$$I = \eta FAD^{2/3}\nu^{-1/6}\omega^{1/2}C^{b} \qquad \text{(VI.1)}$$

diffusion coefficient (D) both change as the viscosity of the media changes. Changes in D can be calculated from the Stokes-Einstein Equation (103) given in Equation VI.2

$$D = kT/6\pi Rn = k'/\eta \qquad \text{(VI.2)}$$

where k = Boltzmann's constant,

T = temperature,

R = radius of diffusing species and

η = viscosity coefficient.

The kinematic viscosity is defined as the viscosity divided by the density of the media. To simplify normalization of the diffusion coefficient k, T and R are all assumed to be constant, and D is then assumed to be inversely proportional to η. If η is substituted into the appropriate places in Equation VI.1, Equation VI.3

$$I = \eta FA(k'/\eta)^{2/3}(\eta/d)^{-1/6}\omega^{1/2}C^{b} \qquad \text{(VI.3)}$$

$$\frac{I\eta^{2/3}d^{-1/6}}{\eta^{-1/6}} = k''\eta FA\omega^{1/2}C^{b} = \frac{I\eta^{2/3}}{\nu^{-1/6}} \qquad \text{(VI.4)}$$

results. To normalize changes in viscosity, all limiting current data is multiplied by $\eta^{2/3}/\nu^{-1/6}$.

The viscosity coefficient data was obtained from Reference 37 for $HClO_4$ and was measured with a Cannon-Fenske (Size 100) Viscometer for HCl. The density data was obtained from Reference 104. The viscosity coefficient, density, and the factor $\eta^{2/3}/\nu^{-1/6}$ for $HClO_4$ and HCl between the concentrations of 4 M and 8 M are given in Table VI.1.

Table VI.1. Normalization factors for I_1

Molarity	η	d	$\eta^{2/3}/\nu^{-1/6}$
		$HClO_4$	
8	2.02	1.47	1.67
7	1.66	1.41	1.43
6	1.39	1.35	1.24
5	1.20	1.29	1.11
4	1.07	1.23	1.01
		HCl	
8	1.39	1.129	1.29
7	1.32	1.113	1.23
6	1.25	1.098	1.18
5	1.17	1.082	1.12
4	1.09	1.067	1.06